2024

Virulence And Transmission Of An Emergent Salmonid Virus After A Host Jump

Malina Loeher
College of William and Mary - Virginia Institute of Marine Science, mloeher@gmail.com

Virulence and Transmission of an Emergent Salmonid Virus after a Host Jump

---

A Dissertation

Presented to

The Faculty of the School of Marine Science

The College of William and Mary in Virginia

In Partial Fulfillment

of the Requirements for the Degree of

Doctor of Philosophy

---

by

Malina Mariko Loeher

August 2024

APPROVAL PAGE

This dissertation is submitted in partial fulfillment of

the requirements for the degree of

Doctor of Philosophy

Malina Mariko Loeher

Approved by the Committee, August 2024

Andrew R. Wargo, Ph.D.
Committee Chair / Advisor

Kimberly S. Reece, Ph.D

Ryan B. Carnegie, Ph.D.

Jan R. McDowell, Ph.D.

Gael Kurath, Ph.D.
USGS Western Fisheries Research Center
Seattle, WA, USA

This PhD is dedicated to the 11,536 salmonids whose life stories are told by this dissertation, and to the compassionate, fish-loving spirit of Kendra Moore Chan.

TABLE OF CONTENTS

ACKNOWLEDGEMENTS

This dissertation is the product of five years of my life through a pandemic, personal loss, grief, depression, and anxiety, in addition to the typical strains of academia. I would not have made it to the finish line without my incredible support network.

I thank my advisor, Andrew Wargo, for his compassion, patience, guidance, and support throughout my graduate journey.

I thank the amazing Academic Studies team members Linda Schaffner, Jen Hay, and Cathy Cake for their unending knowledge and assistance navigating various VIMS-isms.

I thank my wonderful Wargo Lab group, Barb Rutan, Hannah Brown, Aman Kohli, Meredith Seeley, and Isabelle Danforth for their encouragement, cheer, and tutelage.

I thank my committee, Kim Reece, Ryan Carnegie, Jan McDowell, and especially Gael Kurath, for their energy, mentorship, and foundational teachings.

I thank my Virulution team, including but not limited to Dave Kennedy, Bill Batts, Joanne Salzer, and Rachel Breyta, for their constancy, vision, and conversation.

I thank Mary Fabrizio, Challen Hyman, Shannon Smith, Kaitlyn O'Brien, and Alex Marquardt for their dedication to sound statistics and willingness to share their wizard skills.

I thank my parents, Grace and Larry, for giving me the colorful, abundantly resourced, loving start that has propelled through my academic career.

I thank my friends: princess chat, the Funky Bunch, the Lunch Bunch, and associates, for celebrating, commiserating, and holding me with love.

I thank my partner, Andrew Németh, for his unwavering trust, endless affection, and for driving us across the continent while I typed much of this dissertation.

I thank Adele, Sia's 'Everyday is Christmas' album, and the immortal Stevie Nicks for keeping me company through countless bench hours.

And to Kiva, more hikes are on the horizon.

ABSTRACT

In recent years, significant progress has been made toward understanding the complex interplay of viral traits that comprise overall viral fitness. In the wake of the COVID-19 pandemic, special attention has been paid to phenotypes correlated to viral genetics. Emergence of new pathogens and their genetic strains is frequently marked by changes in virulence, or morbidity and mortality inflicted upon the host organism. Virulence is theorized to be a possible fitness benefit to the pathogen if it positively correlates with transmission via pathogen shedding, but the consistency and strength of this relationship are unknown. Gaining a holistic understanding of fitness and its relationships with quantifiable viral traits is critical to the field of epidemiology as emergent pathogens and zoonoses are documented at increasingly rapid rates across the globe. Due to the globally expanding aquaculture sector, which includes aquatic plants, invertebrates, and finfishes destined for human consumption, understanding the possible drivers of viral virulence and shedding is critical to mitigate disease risk and subsequent damage in managed populations. Few empirical studies of emergent aquatic pathogens exist, underscoring the urgent need for data in this discipline. Existing studies are frequently limited in the genetic resources needed to determine whether virulence and transmission phenotypes are traits upon which natural selection acts. This dissertation uses infectious hematopoietic necrosis virus and salmonid hosts to investigate how virulence has evolved since emergence in a novel host species (Chapter 1); how shedding phenotypes have evolved in the novel host (Chapter 2); whether virulence and shedding relationships with time are consistent across viral genetic subgroups (Chapter 3); and if shedding fitness translates to transmission fitness (Chapter 4).

Virulence and Transmission of an Emergent Salmonid Virus after a Host Jump

INTRODUCTION

Emergent diseases constitute enormous threats to our ecosystems and economies. Pathogens imperil the tenuous balance of insectivores and pollinators in terrestrial systems, keystone species in rocky intertidal marine systems, and ecosystem engineers in coral reef systems. Diseases that affect multiple species have created waves of initial panic and prolonged discord among human populations across the globe multiple times in the last decade (1–8). Response to the ongoing COVID-19 pandemic demonstrates both a culmination of advances in the biological and medical sciences, and a prevailing need to expand the study of disease emergence and the evolutionary forces driving it. Specifically, an improved ability to predict the trajectory of pathogen severity (i.e. virulence) after emergence is desperately needed. This is particularly true in aquaculture, where studies of disease emergence and evolution have lagged compared to the pace of the industry.

To develop sustainable and comprehensive disease management plans for aquatic species, especially within commercial realms such as aquaculture, we must cultivate a holistic understanding of pathogens and how they are likely to change in the future. Questions of evolutionary theory are difficult to study in condensed time, but it is possible given the right resources. An ideal study system for this is infectious hematopoietic necrosis virus (IHNV), which jumped from one salmonid species to another. IHNV-salmonid interactions have evolved in the mesocosm world of aquaculture and are subject to a different set of environmental factors than wild populations. This unique aspect of IHNV evolution begs the need for investigation of virology specifically within the rapidly expanding aquaculture industry. Additionally, because of the commercial, ecological, and cultural importance attached to salmonid species, the IHNV-salmonid system is a vital system in which to ask disease evolution questions. The system also has the advantages of being well-studied, with considerable resources for designing controlled empirical studies. The IHNV-salmonid system therefore provides a unique opportunity for investigation of fundamental questions regarding pathogen evolution after emergence, which

are relevant to the management of a variety of disease systems. I utilized this system to address fundamental disease emergence questions for my graduate dissertation research.

I. Virulence evolution theory

Viruses experience many of the same selective pressures as other parasitic organisms. Viral evolution is heavily influenced by within-host replication and transmission strategies, which are analogous to metabolism and reproduction in non-parasitic organisms. To replicate, viruses gain entry to a host cell, hijack the cell machinery to replicate genetic material, and construct protective capsules. New progeny virions are shed from the host cells in search of a new host (transmission). The highest rates of replication and subsequent shedding typify viral fitness (9).

Epidemiological fitness is the fitness of a pathogen (in this case a virus) at a population level and is often quantified by the basic reproductive rate, or R_0. The simplest definition of R_0 is the number of new infections theoretically produced by a single infected host in a naïve host population (10, 11). Long-term survival and fitness of the virus depends on access to a new host, due to the finite life span of infected hosts (12). Viral fitness in a host population is thus determined largely by transmission rate and transmission duration, moderated by host recovery rates and death rates (11). It is typically believed that virulence, hereafter defined as host morbidity and mortality caused by the pathogen, impacts epidemiological fitness by influencing the balance between transmission duration and transmission rates. Modern virulence evolution theory acknowledges the spectrum of different possible tradeoffs, including the possibilities of extreme virulence or avirulence, and focuses on how virulence balances associated costs with regard to transmission potential (11, 13).

It has been theorized that high virulence is positively associated with viral fitness if it begets high replication and transmission rates. The proposed mechanism for this relationship is that viruses that replicate faster cause more cellular damage and exhaust host resources (virulence), but to the effect of producing infectious progeny faster than less virulent viruses

(13). A cost of virulence is that host death limits the temporal span during which transmission may occur (i.e. shortens transmission duration) (14). In contrast, it has also been postulated that more virulent viruses have lower recovery rates (longer transmission durations) because they can better evade the host immune response (15). Thus, selection on virulence is the product of a theoretical tradeoff between infected host survival duration, transmission rate, and host recovery rate (the time required for an infected host to become non-infectious). A common conclusion is that viruses may achieve the highest fitness at intermediate levels of virulence, balancing the tradeoffs between transmission rate and transmission duration, to maximize R_0.

The virulence tradeoff theory is largely based on studies of myxoma virus in rabbits in the mid-1900s, one of the only vertebrate host-pathogen systems with empirical data addressing this topic. Decimating mortality was observed in invasive rabbit populations in Australia after the experimental introduction of myxoma virus as a population control measure. However, less than a decade after its release, less virulent strains emerged and ultimately strains of intermediate virulence became dominant in this system (14, 16–21).

The Australian myxoma example demonstrates how intermediate virulence could be the pinnacle of viral fitness. However, examples that suggest alternate trade-off relationships are becoming increasingly recognized (22–24). One possible example contrary to the idea that viruses in novel hosts will evolve decreased virulence over time is IHNV (25), which is highly lethal in trout aquaculture and remains a major fish health challenge. Ultimately, whether pathogens will evolve increased or decreased virulence after a host jump remains unpredictable. Host mortality is the most obvious and urgent consequence of emergent infectious diseases. Understanding how virulence relates to viral fitness is critical for disease management by identifying the most influential drivers of evolution towards or away from virulence.

II. IHNV evolution

Infectious hematopoietic necrosis virus (IHNV) is a single-stranded, negative-sense RNA virus in the family Rhabdoviridae (26). Consistent with other members of the family such as rabies, virions have a bullet shape apparent by electron microscopy (27). IHNV targets the kidney and spleen of salmonids, and once a virion enters a host cell via receptor-mediated endocytosis, virus replication begins within hours (28–30). *De novo* assembly by host cell machinery produces progeny virions which are released by budding from the hijacked cells (31, 32). While adaptive immunity certainly matters to survivors of IHNV, as exemplified by vaccine-induced protection, initial cellular defenses are largely dependent on the innate immune system and constitutive response of the host (30, 33).

IHNV is primarily transmitted horizontally in fish populations as the host body sheds virions through excretions (27). Transmission may also occur directly from skin, and the virus is believed to enter new hosts through the gills and fin bases (29, 34). Because IHNV is shed through reproductive fluids, spawning adult fish may also vertically transmit the virus to juveniles, although this route of infection is effectively eliminated in aquaculture by treating eggs with iodine (35). Clinical disease signs include externally visible hemorrhage, darkened skin, exophthalmia, distended abdomens, whirling or erratic swimming behavior, and necrosis of the kidney, spleen, and liver (26, 27, 35, 36). Among age classes, juvenile salmonids experience the most severe disease caused by IHNV. Clinical disease is often followed by mortality. Some isolates of IHNV have resulted in 50-90% mortality in juveniles, although mortality rates are variable between species, age classes, and environmental conditions (37–39).

IHNV is generally thought to have co-evolved in North America with sockeye salmon (*Oncorhyncus nerka*) as its ancestral host over possibly millennia but was first described and documented in the 1950s in Washington and later in British Columbia (26, 35, 40). Within its endemic region, with the advent of industrialized aquaculture, IHNV jumped hosts from sockeye salmon to farmed rainbow trout (*O. mykiss*) in the mid-1960s, where it diversified into myriad

new genotypes in decades (26, 41). This host jump was facilitated by the use of unpasteurized salmon viscera as feed for juvenile rainbow trout (33–36,39).

Thousands of IHNV strains originating in sockeye and rainbow trout farms from the 1970s-present have been isolated and genotyped (42). The resulting phylogeny is consistent with rapid geographic proliferation of IHNV in and among trout farms in the western US (38, 43, 44). IHNV phylogeny is organized into genogroups and termed with letters: U, M, L, J, E (45). Genogroups are primarily associated with geographic distribution and with host species. The IHNV phylogenetic tree is large and complex, with some genogroups exhibiting an internal structure, and others appearing more homogenous (43, 46, 47).

The U and L-genogroups are considered the evolutionarily oldest branches of IHNV phylogeny (45). It is unknown whether U or L arose first, or if they both evolved from an older, unknown ancestor. The U group is primarily associated with sockeye salmon, although isolates have been collected from multiple geographically overlapping endemic salmonid species. The L group is chiefly comprised of strains isolated from Chinook salmon (*O. tshawytscha*) and is attributed to ancestral coevolution outside of sockeye species (43).

More recently evolved IHNV isolates, associated with the novel rainbow trout host, have been termed the M-genogroup, which appears to have emerged within farmed *O. mykiss* systems (43). The M-genogroup is estimated to contain three to four times higher genetic diversity than either the U or L groups, and has the most complex subgroup structure (43, 46). M viruses are also believed to have adapted to a higher temperature range (15°C rather than 10°C, the colder temperature preferred by sockeye), attributed to emergence and rapid diversification at the standard rearing temperature for the Hagerman Valley region in Idaho where intensive trout farming occurs (48, 49). M viruses are the predominant IHNV threat in contemporary North American rainbow trout aquaculture and present significant disease risk to wild and hatchery-reared trout populations via spillover events (50).

The J- and E-genogroups have been recognized more recently than U, M, and L. The J group is comprised of Asian-endemic strains that resulted from geographic spread and an independent host jump of IHNV from North Pacific sockeye salmon to rainbow trout farming in Japan (27). The E group is understood to be a subset of M viruses that were transported to Europe from North America via either eggs or fry (51). Increasing virulence within both the J- and E-genogroups has been documented in recent years (52, 53).

Due to its heavy impacts on salmonid aquaculture and conservation, an archive of thousands of IHNV isolates has been collected and maintained by the US Geological Survey (USGS) (42, 54). Samples are primarily from North American field sites. The archive spans the time before, during, and since the host jump, and can be used to examine the evolutionary relationship between fitness and virulence.

III. Host ecology

The host study species utilized in this dissertation were sockeye salmon (*Oncorhynchus nerka*) and rainbow trout (*O. mykiss*). Salmon and trout are culturally, ecologically, and economically important members of the fish Family Salmonidae. Broadly, rainbow trout and sockeye salmon are teleosts native to the Northeastern Pacific Ocean and Pacific Northwest region of North America. The native ranges of *O. nerka* and *O. mykiss* overlap significantly, with both species often utilizing the same watersheds (55). Both species occupy a shared northern range, stretching as far west as Siberia, through the Aleutian Islands and southeast through Washington (55, 56). The western extent of *O. nerka* ranges into Korea and Japan, and the southeastern extent of *O. mykiss* ranges into (55–57). Life histories of specific populations of each species can differ at the regional scale (54). Several common names exist for each species, such as ‘kokanee’ for landlocked populations of *O. nerka*, ‘rainbow trout’ for freshwater resident *O. mykiss*, or ‘steelhead’ for ocean-going *O. mykiss* (58).

Sockeye salmon and steelhead trout are textbook examples of fishes with anadromous life histories. Adult fish spawn in freshwater lakes and riverbeds in the late fall, leaving gravel nests full of fertilized eggs. Eggs hatch in spring; the new hatchlings are called alevins. The alevins forage in their natal streams or lakes for months or up to a couple of years, depending on the species and population. Juveniles migrate seaward and spend their adult years feeding on zooplankton and small prey (55). Reproductively mature adults migrate back to their river of origin for a single spawning season before dying (55). This annual upriver shift in population biomass constitutes a massive nutrient transport from the ocean to riparian systems where carcasses are deposited or consumed (59). Salmonid fish also alter spawning grounds through bioturbation and spawning activities. Due to their effect on both nutrient cycling and physical processes, salmonid fish are considered ecosystem engineers (60).

It is easy to superficially classify salmon and trout as similar animals, but *Oncorhynchus* species are estimated to have diverged 2-5 million years ago and have since developed complex life histories adapted to their diverse environments (55). While steelhead populations of *O. mykiss* are anadromous, rainbow trout populations are not. Rainbow trout are adapted to living entirely in freshwater and their life history may be applied to the majority of the species' populations, making steelhead life history the exception rather than the rule (55, 58). Generally rainbow trout develop along the same timeline as sockeye salmon, feeding opportunistically on invertebrates and small prey at all life stages (55). Rainbow trout do not undergo any physiological changes associated with anadromous migration and usually achieve smaller maximum sizes relative to steelhead and Pacific salmon species (55, 57). Unlike salmon, rainbow trout may survive spawning season to reproduce multiple times in their lifetime (56).

Salmon and trout constitute valuable food items in the food web, not least for humans. Salmonids have been an important food source for subsistence groups in North America throughout recorded history, establishing themselves as culturally vital species. Cultural status and culinary appeal of these fishes have not diminished over time, but many populations of both

sockeye and steelhead have become threatened or endangered due to anthropogenic activities such as habitat degradation (61, 62).

IV. Rainbow trout aquaculture

Commercial aquaculture is among the fastest growing industrial sectors on the planet (63, 64). In response to a growing global market for farm-raised finfishes, the increasing demand for sport and commercial fisheries, and conservation concerns, aquaculture facilities have become commonplace in the last century. Rainbow trout are one of the primary salmonid species used for aquaculture due to their desirable end product and flexible requirements for rearing conditions. For example, unlike many seafood products requiring saltwater, farmed trout do not need to be raised in watersheds with ocean access.

The term aquaculture here includes both hatcheries and farms. Hatcheries in North America are typically state-, tribal-, or federally-run entities located and designed to support natural wild populations for the benefit of the environment, sport fisheries, and commercial fisheries. Fish produced via hatchery typically spend only their juvenile stages in the hatchery before being released into the wild. Farms are commercial operations that raise fish from egg to marketable products, often using domesticated lines. It is important to note that different production styles have unique balances of health practices and biosecurity needs. For instance, trout hatcheries often have conservation goals which dictate different prioritization of genetic diversity and growth rate goals compared to commercial trout farms.

Modern rainbow trout aquaculture started in the 1870s on the McCloud River in northern California (65). Eggs were transferred out of the McCloud River to establish subsequent trout breeding stocks across the United States (US) as early as 1874, and by 1888 when the McCloud station was closed, eggs had been shipped internationally as far as Japan, the United Kingdom, and Denmark (57, 65). Egg transfers from northern California were so successful in broodstock establishment that most current farmed rainbow trout stocks are assumed to be

descendants of McCloud River resident populations or nearby steelhead populations (55, 65). Most current US production of rainbow trout occurs in the Pacific Northwest region, in the Snake and Columbia River watersheds. The densest production region of farmed trout in the US is the Hagerman Valley region of Idaho, a roughly 100km stretch of river which comprises close to 75% of total US production (57). The Hagerman Valley provides ideal trout farming conditions due to the year-round supply of aquifer-derived water at the optimal growing temperature of 15°C (66).

The first trout farm in Idaho opened in 1909, starting what would become a major area for intensified rainbow trout farming (67). By the 1940s, Idaho was recognized as a major fish culturing region and seasonally produced up to 60 million eggs for continued shipments to other regions (57, 66, 67). By the 1970s, farming practices included manipulation of the trout breeding cycle to enable year-round production (66, 67). Augmentation of trout breeding cycles and the advent of pelleted fish feed were major contributors to trout farming success and rapid expansion from the 1950s to 1980s (66, 67). In the early 1980s, Idaho rainbow trout farms produced up to 16 million metric tons of fish annually, the vast majority destined for food processors (66). At the turn of the 21st century, annual production had increased to 25 million metric tons (57). Most producers in the US rainbow trout farming industry are small businesses, but less than 20% of producers account for 80% of total production (57, 66).

On a global scale, rainbow trout aquaculture remains a lucrative and growing industry. Annual global production of finfish increased by a rate of 5.8% between 2000-2016, translating to an annual global production of 800 million metric tons for rainbow trout in 2016 (63). In 2022, the annual export market for salmon and trout reached USD 38 billion (64). Of this market, Idaho rainbow trout accounted for USD 57 million (68). Egg production and trout processors in Idaho continue to be major players in the global trout farming industry.

Despite improvements in biosecurity, research in disease biology and ecology, and management, viral disease remains one of the most significant threats to aquaculture

production and sustainable practices (69–73). Among rainbow trout, over 70% of total losses are attributed to disease (57, 68). IHNV remains a significant health risk across production styles and is one of the top infectious diseases impacting the trout farming industry worldwide. There is no treatment to eliminate IHNV infection from adult fish, and efforts to produce IHNV-resistant families of fish based on immune function and differential survival rates have had mixed success (30, 32, 74–77). A DNA vaccine for IHNV is commercially available but expensive to administer and does not confer disease resistance across generations. At present vaccination is not an economically feasible option for the majority of salmonid production operations (27).

V. Aquaculture-specific disease risks

Commercial aquaculture has been the fastest growing agricultural sector for several decades. Matching global aquaculture trends, rainbow trout farming in the US has emerged and rapidly expanded in the last century (57, 78). The expansion of this industry offers sustainable economic and dietary opportunities for humans, but also offers novel circumstances to the pathogens and parasites inherent to fish populations. Evolutionary drivers unique to or strengthened by aquaculture settings may be shaping virulence evolution (79).

There are several aspects of typical farm layouts that could contribute to increased disease risk. Farms typically stock trout in concrete, outdoor raceways at 15°C (57). Though salmonid fish are inherently social, stocking density is maximized to the point of creating stressful environments, often with subpar water quality, (even in the most responsible operations). Raceway design, which may necessitate effluent flowing from one raceway to another, may facilitate pathogen spread. Furthermore, manipulation of the trout life cycle has allowed for continuous production, where young fish are replenished as the largest individuals are harvested. This results in the overlap of various fish age cohorts on farms, and high turnover

among individual hosts with increased growth rates (either due to intentional husbandry or selective breeding). Fish cohorts, by age, size, and family, are frequently kept together which may benefit IHNV rapid evolution (79). For pathogens, these methods result in a constant supply of naïve, susceptible hosts in fragmented but concurrent lots.

Conditions on trout farms are ripe for driving virus evolution, particularly virulence. High host density and a compressed host life cycle allows virus particles circulating in raceways to encounter a new, susceptible host quickly. Theoretically, high virulence comes at the cost of reduced transmission duration (80, 81). Farm environments, with high stocking densities and turnover, may diminish the necessity of long transmission durations and effectively negate the cost of high virulence. This creates a potential path to increasingly virulent viruses in an unnatural but enduring set of environmental conditions. Other potential drivers of virulence evolution include farm variables such as low broodstock genetic diversity and vaccination practices (79).

Blue economies such as aquaculture are tapping into global aquatic resources to meet human needs while staying in line with climate goals, but require additional tools and data to effectively manage emergent diseases.

VI. Research objectives

The main goals of these studies were to describe what happened evolutionarily during and after a host jump in an aquaculture setting, using an archive of IHNV isolates. Studies were designed to quantify viral virulence and fitness through *in vivo* survival, shedding, and transmission assays followed by analysis using molecular quantification techniques. The experiments were organized into the following sections:

Chapter 1. Virulence evolution of a salmonid virus following a host jump

Chapter 2. Evolution of viral shedding post-host jump in salmonid fish

Chapter 3. Linking virulence and shedding fitness of three sublineages of M-genogroup IHNV following the North American host jump into rainbow trout (*Oncorhynchus mykiss*)

Chapter 4. Quantifying viral transmission rate over the course of IHNV infection in rainbow trout (*Oncorhynchus mykiss*)

References

1. M. C. Fisher, T. W. J Garner, Chytrid fungi and global amphibian declines. *Nature Reviews Microbiology* **18**, 332–343 (2020).

2. C. M. Miner, *et al.*, Large-scale impacts of sea star wasting disease (SSWD) on intertidal sea stars and implications for recovery. (2018). https://doi.org/10.1371/journal.pone.0192870.

3. J. R. Hoyt, A. M. Kilpatrick, K. E. Langwig, Ecology and impacts of white-nose syndrome on bats. *Nature Reviews Microbiology* 33–36 (2021). https://doi.org/10.1038/s41579-020-00493-5.

4. D. Ruiz-Moreno, *et al.*, Global coral disease prevalence associated with sea temperature anomalies and local factors. *Diseases of Aquatic Organisms* **100**, 249–261 (2012).

5. T. Goldstein, *et al.*, Spillover of ebolaviruses into people in eastern Democratic Republic of Congo prior to the 2018 Ebola virus disease outbreak. *One Health Outlook* **2**, 21 (2020).

6. D. Baud, D. J. Gubler, B. Schaub, M. C. Lanteri, D. Musso, An update on Zika virus infection. *The Lancet* **390**, 2099–2109 (2017).

7. T. J. D. Knight-Jones, J. Rushton, The economic impacts of foot and mouth disease - What are they, how big are they and where do they occur? *Preventive Veterinary Medicine* **112**, 161–173 (2013).

8. M. Bchetnia, C. Girard, C. Duchaine, C. Laprise, The outbreak of the novel severe acute respiratory syndrome coronavirus 2 (SARS-CoV-2): A review of the current global status. *Journal of Infection and Public Health* **13**, 1601–1610 (2020).

9. A. R. Wargo, G. Kurath, Viral fitness: Definitions, measurement, and current insights. *Current Opinion in Virology* **2**, 538–545 (2012).

10. R. Breban, R. Vardavas, S. Blower, Theory versus data: How to calculate R0? *PLoS ONE* **2**, e282 (2007).

11. R. M. Anderson, R. M. May, Coevolution of hosts and parasites. *Parasitology* **85**, 411–426 (1982).

12. R. M. Anderson, R. M. May, Population biology of infectious diseases: Part I. *Nature* **280**, 361–367 (1979).

13. S. Alizon, A. Hurford, N. Mideo, M. Van Baalen, Virulence evolution and the trade-off hypothesis: History, current state of affairs and the future. *Journal of Evolutionary Biology* **22**, 245–259 (2009).

14. S. Alizon, Y. Michalakis, Adaptive virulence evolution: The good old fitness-based approach. *Trends in Ecology and Evolution* **30**, 248–254 (2015).

15. J. J. Bull, A. S. Lauring, Theory and Empiricism in Virulence Evolution. *PLOS Pathogens* **10**, e1004387 (2014).

16. G. Saunders, B. Cooke, K. Mccoll, R. Shine, T. Peacock, Modern approaches for the biological control of vertebrate pests: An Australian perspective. (2009). https://doi.org/10.1016/j.biocontrol.2009.06.014.

17. B. Spiesschaert, G. McFadden, K. Hermans, H. Nauwynck, G. R. Van De Walle, The current status and future directions of myxoma virus, a master in immune evasion. *Veterinary Research* **42**, 1–18 (2011).

18. J. W. Edmonds, I. F. Nolan, R. C. H. Shepherd, A. Gocs, Myxomatosis: the virulence of field strains of myxoma virus in a population of wild rabbits (Oryctolagus cuniculus L.) with high resistance to myxomatosis. *J. Hyg., Camb* **74**, 417–421 (2020).

19. P. J. Kerr, *et al.*, Myxoma virus and the leporipoxviruses: An evolutionary paradigm. *Viruses* **7**, 1020–1061 (2015).

20. S. Alizon, M. T. Sofonea, SARS-CoV-2 virulence evolution: Avirulence theory, immunity and trade-offs. *Journal of Evolutionary Biology* **34**, 1867–1877 (2021).

21. M. A. Acevedo, F. P. Dillemuth, A. J. Flick, M. J. Faldyn, B. D. Elderd, Virulence-driven trade-offs in disease transmission: A meta-analysis*. *Evolution* **73**, 636–647 (2019).

22. D. L. Medica, M. V. K. Sukhdeo, Estimating Transmission Potential in Gastrointestinal Nematodes (Order: Strongylida). *Journal of Parasitology* **87**, 439–442 (2001).

23. M. Hatta, Y. Kawaoka, The continued pandemic threat posed by avian influenza viruses in Hong Kong. *Trends in Microbiology* **10**, 340–344 (2002).

24. D. T. Mandell, *et al.*, Pathogenic features associated with increased virulence upon Simian immunodeficiency virus cross-species transmission from natural hosts. *J Virol* **88**, 6778–6792 (2014).

25. A. R. Wargo, G. Kurath, R. J. Scott, B. Kerr, Virus shedding kinetics and unconventional virulence tradeoffs. *PLOS Pathogens* **17**, e1009528 (2021).

26. D. F. Amend, W. T. Yasutake, R. W. Mead, A Hematopoietic Virus Disease of Rainbow Trout and Sockeye Salmon. *Transactions of the American Fisheries Society* **98**, 796–804 (1969).

27. L. M. Bootland, J. C. Leong, “Infectious Hematopoietic Necrosis Virus” in *Fish Diseases and Disorders*, (2011), pp. 66–95.

28. R. G. Dietzgen, H. Kondo, M. M. Goodin, G. Kurath, N. Vasilakis, The family Rhabdoviridae: mono- and bipartite negative-sense RNA viruses with diverse genome organization and common evolutionary origins. *Virus Research* **227**, 158–170 (2017).

29. P. Dixon, R. Paley, R. Alegria-Moran, B. Oidtmann, Epidemiological characteristics of infectious hematopoietic necrosis virus (IHNV): A review. *Veterinary Research* **47**, 1–26 (2016).

30. M. K. Purcell, S. E. LaPatra, J. C. Woodson, G. Kurath, J. R. Winton, Early viral replication and induced or constitutive immunity in rainbow trout families with differential resistance to

Infectious hematopoietic necrosis virus (IHNV). *Fish and Shellfish Immunology* **28**, 98–105 (2010).

31. N. J. Maclachlan, E. J. Dubovi, Eds., “Ch 2: Virus Replication” in *Fenner’s Veterinary Virology*, (2010), pp. 21–42.

32. M. K. Purcell, K. J. Laing, J. R. Winton, Immunity to fish rhabdoviruses. *Viruses* **4**, 140–166 (2012).

33. D. R. Jones, B. J. Rutan, A. R. Wargo, Impact of vaccination and pathogen exposure dosage on shedding kinetics ofinfectious hematopoietic necrosis virus (IHNV) in rainbow trout. *Journal of Aquatic Animal Health* (2020). https://doi.org/10.1007/978-1-4614-7495-1_23.

34. D. Mulcahy, R. J. Pascho, C. K. Jenes, Detection of infectious haematopoietic necrosis virus in river water and demonstration of waterborne transmission. *Journal of Fish Diseases* **6**, 321–330 (1983).

35. D. F. Amend, Detection and transmission of infectious hematopoietic necrosis virus in rainbow trout. *Journal of wildlife diseases* **11**, 471–8 (1975).

36. N. J. Maclachlan, E. J. Dubovi, Eds., “Ch 18: Rhabdoviridae, Properties of Rhabdoviruses” in *Fenner’s Veterinary Virology*, (2010), pp. 327–330.

37. S. E. LaPatra, Factors Affecting Pathogenicity of Infectious Hematopoietic Necrosis Virus (IHNV) for Salmonid Fish. *Journal of Aquatic Animal Health* **10**, 121–131 (1998).

38. R. Breyta, D. Mckenney, T. Tesfaye, K. Ono, G. Kurath, Increasing virulence, but not infectivity, associated with serially emergent virus strains of a fish rhabdovirus. *Virus Evolution* **2**, 1–14 (2016).

39. R. W. Guenther, S. W. Watson, R. R. Rucker, “Etiology of sockeye salmon ‘virus’ disease” (Dept. of the Interior, Fish and Wildlife Service, 1959).

40. T. J. Parisot, W. T. Yasutake, G. W. Klontz, Virus Diseases of the Salmonidae in Western United States. I. Etiology and Epizootiology. *Annals New York Academy of Sciences* 502–519 (1965).

41. J. A. Plumb, A Virus-Caused Epizootic of Rainbow Trout (Salmo gairdneri) in Minnesota. *Transactions of the American Fisheries Society* **1**, 121–123 (1972).

42. G. Kurath, E. Emmenegger, T. Tesfaye, R. Breyta, Molecular epidemiology of aquatic pathogens- Infectious hematopoietic necrosis virus (MEAP-IHNV) database. *USGS WFRC* (2016). Available at: http://gis.nacse.org/ihnv/ [Accessed 28 June 2021].

43. G. Kurath, *et al.*, Phylogeography of infectious haematopoietic necrosis virus in North America. *Journal of General Virology* **84**, 803–814 (2003).

44. R. M. Troyer, S. E. LaPatra, G. Kurath, Genetic analyses reveal unusually high diversity of infectious haematopoietic necrosis virus in rainbow trout aquaculture. *Journal of General Virology* **81**, 2823–2832 (2000).

45. G. Kurath, “Molecular Epidemiology and Evolution of Fish Novirhabdoviruses” in *Rhabdoviruses: Molecular Taxonomy, Evolution, Genomics, Ecology, Host-Vector Interactions, Cytopathology and Control*, R. G. Dietzgen, I. V. Kuzmin, Eds. (Caister Academic Press, 2012), pp. 423–445.

46. R. Breyta, A. Black, J. Kaufman, G. Kurath, Spatial and temporal heterogeneity of infectious hematopoietic necrosis virus in Pacific Northwest salmonids. *Infection, Genetics and Evolution* **45**, 347–358 (2016).

47. A. Black, R. Breyta, T. Bedford, G. Kurath, Geography and host species shape the evolutionary dynamics of U genogroup infectious hematopoietic necrosis virus. *Virus Evolution* **2**, 1–13 (2016).

48. K. A. Garver, W. N. Batts, G. Kurath, Virulence comparisons of infectious hematopoietic necrosis virus U and M genogroups in sockeye salmon and rainbow trout. *Journal of Aquatic Animal Health* **18**, 232–243 (2006).

49. M. M. D. Peñaranda, A. R. Wargo, G. Kurath, In vivo fitness correlates with host-specific virulence of Infectious hematopoietic necrosis virus (IHNV) in sockeye salmon and rainbow trout. *Virology* **417**, 312–319 (2011).

50. R. Breyta, *et al.*, Emergence of MD type infectious hematopoietic necrosis virus in Washington State coastal steelhead trout. *Diseases of Aquatic Organisms* **104**, 179–195 (2013).

51. P. J. Enzmann, G. Kurath, D. Fichtner, S. M. Bergmann, Infectious hematopoietic necrosis virus: Monophyletic origin of European isolates from North American Genogroup M. *Diseases of Aquatic Organisms* **66**, 187–195 (2005).

52. M. Mochizuki, H. J. Kim, H. Kasai, T. Nishizawa, M. Yoshimizu, Virulence Change of Infectious Hematopoietic Necrosis Virus against Rainbow Trout Oncorhynchus mykiss with Viral Molecular Evolution. *Fish Pathology* **44**, 159–165 (2009).

53. M. Abbadi, *et al.*, Increased virulence of Italian infectious hematopoietic necrosis virus (IHNV) associated with the emergence of new strains. *Virus Evolution* **7**, 1–14 (2021).

54. E. J. Emmenegger, *et al.*, Development of an aquatic pathogen database (AquaPathogen X) and its utilization in tracking emerging fish virus pathogens in North America. *Journal of Fish Diseases* **34**, 579–587 (2011).

55. R. Behnke, J. Tomelleri, *Trout and Salmon of North America*, G. Scott, Ed. (The Free Press, 2002).

56. C. Groot, L. Margolis, *Pacific Salmon Life Histories* (UBC Press, 1991).

57. G. Fornshell, Rainbow Trout - Challenges and Solutions. *Reviews in Fisheries Science* **10**, 545–557 (2002).

58. N. W. Kendall, *et al.*, Anadromy and residency in steelhead and rainbow trout (oncorhynchus mykiss): A review of the Processes and Patterns. *Canadian Journal of Fisheries and Aquatic Sciences* **72**, 319–342 (2015).

59. J. W. Moore, *et al.*, Biotic control of stream fluxes: spawning salmon drive nutrient and matter export. *Ecology* **88**, 1278–1291 (2007).

60. R. J. Naiman, R. E. Bilby, D. E. Schindler, J. M. Helfield, Pacific Salmon, Nutrients, and the Dynamics of Freshwater and Riparian Ecosystems. *Ecosystems* **5**, 399–417 (2002).

61. T. H. Williams, S. T. Lindley, B. C. Spence, D. A. Boughton, "Status Review Update for Pacific Salmon and Steelhead listed under the Endangered Species Act: Southwest" (National Marine Fisheries Service, 2011).

62. P. S. Rand, *et al.*, Global Assessment of Extinction Risk to Populations of Sockeye Salmon Oncorhynchus nerka. *PLoS ONE* **7** (2012).

63. FAO, *The State of World Fisheries and Aquaculture 2018* (2018).

64. FAO, "The State of World Fisheries and Aquaculture 2024 - Blue Transformation in action." (2024).

65. G. A. E. Gall, P. A. Crandell, The rainbow trout. *Aquaculture* **100**, 1–10 (1992).

66. R. A. Busch, Workshop proceedings: Viral diseases of salmonid fishes in the Columbia River Basin. (1982).

67. J. M. Hinshaw, G. Fornshell, R. Kinnunen, "A profile of the aquaculture of trout in United States" (USDA Risk Management Agency, 2004).

68. USDA, Trout Production. *National Agricultural Satistics Service* (2024).

69. A. Rico, *et al.*, Use of models for the environmental risk assessment of veterinary medicines in European aquaculture: current situation and future perspectives. *Reviews in Aquaculture* **11**, 969–988 (2019).

70. A. Assefa, F. Abunna, Maintenance of Fish Health in Aquaculture: Review of Epidemiological Approaches for Prevention and Control of Infectious Disease of Fish. *Veterinary Medicine International* **2018**, 1–10 (2018).

71. K. Scutt, I. Ernst, Sharing responsibility between public and private sectors for the management of aquatic emergency animal diseases. *Revue scientifique et technique (International Office of Epizootics)* **38**, 533–570 (2019).

72. E. J. Peeler, I. Ernst, A new approach to the management of emerging diseases of aquatic animals. *Revue scientifique et technique (International Office of Epizootics)* **38**, 537–551 (2019).

73. E. Georgiades, B. Jones, R. Fraser, "Options to Strengthen On-farm Biosecurity Management for Commercial and Non-commercial Aquaculture" (Ministry for Primary Industries, 2016).

74. M. M. D. Peñaranda, M. K. Purcell, G. Kurath, Differential virulence mechanisms of infectious hematopoietic necrosis virus in rainbow trout (Oncorhynchus mykiss) include host entry and virus replication kinetics. *Journal of General Virology* **90**, 2172–2182 (2009).

75. S. Yamamoto, I. Sanjyo, M. Kohara, H. Tahara, R. Sato, Estimation of the Heritability for Resistance to Infectious Hematopoietic Necrosis in Rainbow Trout. *Nippon Suisan Gakkaishi (Japanese Edition)* **57**, 1519–1522 (1991).

76. J. D. McIntyre, D. F. Amend, Heritability of Tolerance for Infectious Hematopoietic Necrosis in Sockeye Salmon (Oncorhynchus nerka). *Transactions of the American Fisheries Society* **107**, 305–308 (2004).

77. S. E. LaPatra, K. A. Lauda, G. R. Jones, Antigenic variants of infectious hematopoietic necrosis virus and implications for vaccine development. *Diseases of Aquatic Organisms* **20**, 119–126 (1994).

78. FAO, *World Fisheries and Aquaculture, FAO:Rome,2022* (2022).

79. D. A. Kennedy, *et al.*, Potential drivers of virulence evolution in aquaculture. *Evolutionary Applications* **9**, 344–354 (2016).

80. T. Day, S. R. Proulx, A general theory for the evolutionary dynamics of virulence. *The American naturalist* **163** (2004).

81. A. F. Read, The evolution of virulence. *Trends in Microbiology* **2**, 73–76 (1994).

CHAPTER 1: Virulence evolution of a salmonid virus following a host jump

ABSTRACT

Emergent viral diseases remain a critical obstacle to welfare across landscapes and species, encompassing humans, wildlife, and agriculture. Following a jump to a novel host, whether a virus confers high or low virulence determines the severity of a continuing disease threat. Classical evolutionary theory posits that virulence attenuates over time as a virus adapts to a novel host, but this is largely based on data from just one system, myxoma virus, which was used as a biocontrol agent in rabbits in mid-1900s Australia. In this study, we demonstrate that infectious hematopoietic necrosis virus (IHNV) in salmonid fishes does not to conform to this classical theory. Since IHNV emerged in fish farming following a host jump into rainbow trout (*Oncorhynchus mykiss*) from its endemic sockeye salmon (*O. nerka*) host in the 1960s, the virus has posed serious challenges to aquaculture and conservation efforts. We utilized 16 archival IHNV isolates collected across five decades, which span the host jump to near-present day collection years as well as two major phylogenetic groups, to examine virulence evolution in the ancestral and novel hosts. Our results indicated a significant trend of increasing IHNV virulence through time in novel isolates that emerged since the host jump. This was met with losses in virulence of emergent isolates in the ancestral host, whereas ancestral isolates collected across the same time range showed no clear pattern of virulence evolution. Some possible indication of a temperature adaption after the host jump was present, but the effect was not as pronounced as previously speculated. This represents one of only a handful of systems to characterize virulence evolution across a host jump and subsequent adaptation using this diversity of isolates in common garden *in vivo* experiments. The work contributes to a growing body of evidence that challenges the classical theory of viral attenuation after adaptation to novel hosts.

INTRODUCTION

Emergent viruses constitute a major threat across species and ecosystems. Virulence, here defined as host morbidity and mortality as a direct result of infection, is the most obvious and urgent consequence of viral emergence. The direction of viral virulence evolution is a critical determinant for assessing the severity of an emergence event, but our ability to infer this trajectory remains limited (1). Contemporary virulence evolution theory postulates high virulence begets high viral transmission rates through greater replication and reduced infection clearance, while it diminishes viral transmission duration through host mortality (2–4). This creates what has been termed the virulence tradeoff, which was classically demonstrated by myxoma virus in Australia's naïve introduced rabbit population (3, 5, 6). In mid-1900s Australia, myxoma virus was used as a biocontrol measure for invasive rabbits with decimating effects in the early years after its release. However, after several decades, myxoma virulence attenuated towards intermediate levels, which provided optimal viral fitness (7, 8). The myxoma story was so compelling that conventional wisdom quickly became that pathogens will evolve decreased virulence after emergence (9), although the theory has been subsequently challenged (10).

Numerous observational and epidemiological studies have tracked viral virulence evolution after emergence. Systems such as ebolavirus in humans and feline calicivirus in domesticated cats, indicate the evolution of increased virulence over time (11–13). For HIV, there is evidence that the virus evolved increased virulence in some countries and decreased virulence in others since it emerged in humans, with postulated mechanisms by which intermediate virulence could maximize viral fitness (10, 14). The evolution of emergent SARS-CoV-2 has been an area of high public concern with evidence that the virus initially increased in virulence, and despite the circulation of less virulent variants such as Omicron, the long-term virulence trajectory remains uncertain (15–17). The effect of confounding variables such as

intervention and host immunity on virulence epidemiology has been difficult to parse out of many of these observational studies (18).

Virulence evolution in the context of trade-off theory is an area that has received a great deal of research attention, particularly in mathematical-modeling studies reviewed in (19). Nonetheless, few empirical studies exist beyond myxoma that investigate how viral pathogens evolve following a host jump, and those that do offer contrasting conclusions (3). A particularly recent and compelling example is *Mycoplasma gallisepticum* bacterium in North American house finches (*Haemorhous mexicanus*), which demonstrated increased virulence evolved over two epidemics spanning the mid-1990s to 2010s (20). Higher *M. gallisepticum* loads and subsequently increased transmission suggest that higher virulence may confer greater overall fitness for some pathogens (20–22).

Collectively, the available research indicates that the evolutionary arc of attenuation after emergence found in the textbook case of myxoma cannot be applied to all pathogens. As such, additional empirical studies are warranted to determine if generalities can be found, or what specific mechanisms might be most important for driving virulence evolution. The trajectory of virulence evolution after pathogen emergence remains a difficult theory to test. A common limitation is that concurrent changes in host genetics, the environment, or management that occur alongside viral evolution can mask changes in virulence (23, 24). Conclusive evidence requires experiments across the same host genotype and environmental conditions (i.e. common garden) examining the virulence of multiple viral isolates spanning the host jump and subsequent adaptation. Few systems allow for such investigations. A rare exception is infectious hematopoietic necrosis virus (IHNV) in rainbow trout (*Oncorhynchus mykiss*). This system has unique resources and background knowledge necessary to empirically characterize the trajectory of virulence evolution after an emergence event. Furthermore, the natural history of IHNV provides contrasting features to previously studied systems, and insights into disease emergence in aquatic environments, which is an area of increasing global importance.

IHNV is an RNA virus in the genus *Novirhabdoviridae* that can infect many members of the fish family Salmonidae (25). Fish mortality can reach up to 50-95% during epidemics and IHNV is one of the most important pathogens hindering salmonid conservation and aquaculture worldwide (26–31). Virulence of IHNV is highly variable and driven by factors such viral genotype and dosage, host species and age, and environmental factors such as temperature and rearing conditions (28, 32–34). Due to the important economic, ecological, and cultural status of wild and farmed salmon and trout hosts (35–38), intensive efforts have been put into IHNV surveillance, yielding an archive of thousands of virus isolates (39). This has allowed for extensive evolutionary analysis indicating that IHNV has been endemic in sockeye salmon (*Oncorhynchus nerka*) for several millennia in the upper Pacific Northwest of North America (40, 41). This long evolutionary history in sockeye resulted in a distinct phylogenetic clade of the virus, classified as genogroup U, which represents the ancestral state of IHNV (41–43). A new lineage of IHNV, classified as M, arose following a host jump to rainbow trout (*O. mykiss*) in the 1960s, attributed to using unpasteurized *O. nerka* viscera as feed for juvenile *O. mykiss* aquaculture sites in Washington and British Columbia (31, 44). Reports of IHNV epidemics were documented as early as the 1950s in sockeye salmon aquaculture in Washington (31) and in rainbow trout facilities by the 1970s. Since then, M-genogroup viruses spread through the Hagerman Valley region of Idaho, a 100 km stretch of the Snake River where aquaculture rapidly expanded in the 1970s-80s and approximately 70% of the food-grade rainbow trout in North America is currently produced (45, 46).

Historical records also indicate that the IHNV host jump into rainbow trout was soon followed by a virus temperature adaption. In wild environments, salmonids such as sockeye and rainbow trout experience a wide range of temperatures but optimally reside at cooler temperatures (~10°C), whereas farmed rainbow trout in the Hagerman Valley of Idaho are maintained at a constant 15°C by a spring-fed aquifer (29, 47). Early after emergence of IHNV in rainbow trout, epidemics were reported at farms rearing fish at lower temperatures (9-10°C),

but no such reports originated at facilities that used higher temperatures (16-20°C) even though they were likely receiving contaminated eggs from the same source (44, 48–51). Subsequent studies have indicated that M-genogroup virus is more virulent at 15°C and U-genogroup at 10°C, although the number of isolates tested was limited (29, 34, 52–54).

Since its emergence, IHNV has continued to cause epidemics in Idaho rainbow trout farming facilities (55, 56), and spread globally through aquaculture activities (26). Comprehensive phylogenetic analysis of known IHNV diversity in North America, including the Idaho Hagerman Valley region, indicates that the M-genogroup represents the most genetically diverse and rapidly evolving clade, despite a narrower geographic range than the U-genogroup (42). Follow-up phylogenetic analyses confirming directional selection of IHNV suggest that M viruses continue to adapt, whereas the ancestral U-genogroup shows patterns of stabilizing selection (42). Field observations and previous empirical investigations indicate high and potentially increasing virulence of the M-genogroup circulating in trout farms since the late 1970s (29, 56–60). A similar pattern of increasing virulence across dominant genotypes during field displacement events was observed with the MD subgroup, which spilled out of aquaculture and subsequently evolved in wild and hatchery managed *O. mykiss* populations (30). During the global spread of IHNV, M-genogroup isolates also gave rise to the E-genogroup in Europe (61). Although this was not a separate host-jump event, increasing virulence among emergent E isolates in Italian rainbow trout farms has been recently documented (62). An independent host jump from the U-genogroup virus in sockeye salmon to rainbow trout did occur in Asia, giving rise to the J-genogroup, with some evidence of the evolution of increased virulence among the few isolates tested (63, 64). As such, there is an urgent need to definitively determine the trajectory or IHNV virulence evolution, particularly among rainbow trout aquaculture-derived isolates of IHNV.

Extensive empirical studies of IHNV provide evidence of mechanisms by which virulence evolution could occur in this system. This work indicates that IHNV gained a high degree of

host-specificity after the emergence event, such that representative U and M isolates demonstrate greater fitness and virulence in sockeye salmon and rainbow trout respectively (30, 57, 58, 60). Studies also indicate that for M-genogroup virus in rainbow trout, higher virulence is associated with higher replication and transmission rates, as well as lower recovery rates (1, 60, 65, 66). Furthermore, there is evidence that the cost associated with transmission duration truncation due to mortality is minimal for IHNV at the virulence levels of isolates tested to date (4). Thus increased virulence appears to provide a fitness advantage for IHNV, particularly in rainbow trout. Despite compelling evidence for this relationship between virulence and fitness, no previous IHNV studies have specifically focused on the virulence evolution trajectory across the host-jump event and subsequent adaptation.

Here we used a common garden *in vivo* experimental design to compare the virulence of sixteen isolates of IHNV, from the ancestral U-genogroup and the emergent M-genogroup, in the ancestral and novel hosts sockeye salmon and rainbow trout. Isolate selection represents five decades of IHNV evolution, from immediately after the host jump to the present, with isolates collected from 1974–2017. These studies were replicated across two laboratories, exposure doses, and temperatures, to confirm the repeatability of results and explore the process of adaption of the virus. This work broadens the understanding of how virulence evolves after emergence with robust empirical data, particularly in the context of aquaculture. Pathogen evolution studies in aquaculture remain limited, despite aquaculture being one of the fastest growing sectors of the global economy and a critical component of food security (1, 67, 68). Additionally, this research imparts system-specific insights into the variable phenotypes of IHNV, a pathogen of considerable economic and ecological importance. Ultimately, successful disease mitigation in this and other vital systems depends on a holistic understanding of pathogen natural history and evolutionary trends.

METHODS

1. Virus selection

Sixteen genetically unique IHNV isolates from the USGS archive (39), previously collected in the field, were used in this study (Table 1.1). All isolates were previously confirmed to be unique sequences via mid-glycoprotein gene (mid-G) sequencing as described in (42, 69). Five U isolates of known dominance in the field were selected to represent the ancestral state of IHNV (42, 69). Eleven M-genogroup isolates were selected to span the temporal, spatial, and phylogenetic history of IHNV emergence and subsequent evolution in North American rainbow trout aquaculture. The isolates were propagated on EPC fish cells in Minimum Essential Media supplemented with 10 % fetal bovine serum, 2mM L-glutamine, 50 units/mL penicillin, 50 µg/mL streptomycin, 20 µg/mL gentamycin, 2.5 µg/mL amphotericin B, and 0.15 mg/mL sodium bicarbonate (MEM-10) to generate viral stocks, which were titered by plaque assays independently at both the Virginia Institute of Marine Science (VIMS) and USGS Western Fisheries Research Center (WFRC) then stored at -80°C for later use (70, 71).

2. Host species

To represent the ancestral IHNV host, sockeye salmon (*Oncorhynchus nerka*) were provided by Baker Lake Fish Hatchery (WDFW, Washington, USA), produced as part of state hatchery salmon conservation. To represent the emergent IHNV host, rainbow trout (*O. mykiss*) were obtained from a commercial trout producer. Trout were produced from a minimum of twelve parental steelhead lines (anadromous stocks of *O. mykiss*). Neither the sockeye salmon nor rainbow trout lines are believed to have undergone artificial selective breeding for IHNV resistance. All fish were obtained as eggs shipped directly to the respective research institutions

(VIMS and WFRC), with the same cohort of fish used across locations. Eggs were iodine treated (10-minute soak in 1% solution) to remove IHNV and external pathogens and then reared in flow-through (2-4 tank exchanges/hour), specific pathogen-free, UV-irradiated fresh water maintained at 10°C or 12.5°C for sockeye and rainbow trout respectively. After hatching and complete digestion of yolk-sacs, fish fry were fed a standard trout diet (Zeigler- VIMS, Skretting - WFRC) at 2-4% body weight until 1-2 grams of size when they were used for experiments. To alleviate stress rainbow trout were split into two identical tanks and water temperature gradually stepped up or down to 15 or 10°C over three weeks. Fish were then allowed to acclimate for a minimum of two weeks prior to the beginning of experiments. All sockeye experiments were conducted at 10°C, so acclimatization was not required. All research animals were handled according to William & Mary IACUC protocols (IACUC-2018-06-21-12998-arwargo and IACUC-2021-07-02-15072-arwargo).

3. *In vivo* challenge

To quantify viral isolate virulence, a standard *in vivo* batch challenge method was used (34, 60, 65, 72). Briefly triplicate groups of 15-20 fish were exposed to a High (2 x 10^5 pfu/mL) or Low (2 x 10^3 pfu/mL) dosage of each viral isolate (Table 1.1), diluted in MEM-10 or mock exposed to culture media, by adding 5ml of inoculum to 995 mL of static water in 6 L tanks under aeration. Fish were held static for 1 hour, then maintained on aerated flow-through water (~150 mL/min), until mortality plateaued (28-56 days, Fig. 1). Sockeye were monitored for longer than rainbow trout due to known slower mortality kinetics (34, 72). Mortality was recorded daily, and dead fish were removed from tanks daily. The experiments were separated into three blocks: sockeye at 10°C, rainbow trout at 10°C, and rainbow trout at 15°C. These were replicated at both the VIMS and WFRC labs, for a total of 6 independent experiments. Experiments within host species were

conducted within 1-2 weeks of each other to control for age (degree-days) and size (1.52 ± 0.36 grams).

4. Statistical analysis

Statistical tests and visualizations were carried out in R Statistical Software (version 4.2.3) (73) and RStudio (version 2023.12.1+402) (74). All data was analyzed using generalized linear models (75) with a binomial error structure (lme4 and stats packages) to elucidate virulence differences between treatments, measured as the total number of dead and live fish at the end of the experiment (i.e. logistic regression on cumulative probability of fish death). The analysis was then broken into three parts.

[1] To investigate how emergent IHNV virulence evolved since the host jump, the first analysis focused on the data from M-genogroup isolates in rainbow trout. Dose (categorical), temperature (10 vs 15°C – categorical) and year of virus isolate collection (continuous) centered around median year (2000), were included as fixed effects. Location of experiment (VIMS or WFRC), isolate (see Table 1.1), and tank [1-3] were included (all categorical) as random effects. Many treatments had no mortality, so to facilitate model convergence, one additional “dead” fish and “alive” fish were added to the dataset for every tank. In addition to examining isolate evolution, the isolates were also directly compared to each other at each exposure dose to estimate proportionate changes in virulence at the most environmentally critical temperature (15°C). For this part of the analysis, isolate (categorical) alone was included as a fixed effect and location of the experiment was included as a random effect. Year of collection and tank were explored as additional random effects but resulted in overfitting.

[2] A similar approach was used to compare differences between M and U-genogroup virus. The two host species were analyzed separately, to account for independent experiments and different temperature treatments. For both hosts, factors in the model were the same as

analysis 1 with the addition of genogroup (U or M – categorical). Temperature was dropped for the sockeye since only one temperature treatment is environmentally relevant to the host species. Including all random effects resulted in overfitting for sockeye, so location and tank were dropped from that analysis.

[3] To compare the virulence of ancestral isolates in the ancestral host, the analysis focused on data from U isolates in sockeye salmon, with isolate name (categorical) and dose included as fixed factors. Models with the random effects experiment and tank did not converge or were deemed a poorer fit, so the terms were dropped. The GLM model from the “stats” package (version 4.2.3) function was then employed to allow for exclusion of all random terms (73).

For all analyses, model selection was conducted using corrected Akaike Information Criterion (AICc), where maximal models (all main effects and interactions) were fit to the data and the dredge function from the “MuMIn” package (version 1.47.5) was used to select the lowest AICc value from all possible combinations (76). Results of the selected model are presented in the main text and models within Δ2 AICc are shown in the supplementary materials. Because AICc selection was used, p-values are not provided, and instead ΔAICc for model without the factor of discussion is presented in the results. Coefficients from summaries of best fit models, as well as plotting of predicted values, were used to determine the magnitude and direction of factor level differences for best fit models. The predicted probability of fish death and 95% confidence intervals were calculated using the predictSE function from the “AICcmodavg” package (version 2.3-3) and multiplying the standard error by 1.96 (assuming a normal distribution of the population variance), for the factors of interest in the AICc selected models (77). In cases of interaction terms or where factors contained more than two levels post-hoc pairwise comparisons of the estimated marginal means were performed with the “emmeans” package (version 1.8.8) (78), to determine significant differences between factor levels.

RESULTS

Survival kinetics trends

Rainbow trout mortality peaked at 5-10 days and plateaued between days 10-14 post-infection (Figure 1.1). In general, the kinetics of mortality were slightly faster at 15°C compared to 10°C, as well as for M compared to U-genogroup isolates. For sockeye, mortality peaked between days 10-15, then continued at a steady rate until slowing between days 20-25. M-genogroup isolates caused virtually no mortality among sockeye hosts, and in the few cases where it was observed, mortality rates were slower than those produced by U-genogroup isolates. Within hosts and genogroups, there was substantial between isolate variation in survival kinetics, with more virulent isolates (measured as cumulative mortality) typically causing more acute mortality with a clear peak incidence period and less virulent isolates resulting in more protracted mortality. Survival kinetics patterns were consistent across experiments duplicated at two different laboratories, with the exception of one experiment (experiment 6, Figure 1.1) generally having higher mortality at the WFRC than its paired experiment at VIMS (experiment 5, Figure 1.1). To account for any location effects, location was included as a random term in all subsequent analyses. In all challenges, no mortality occurred for fish exposed to the mock treatment in the first three weeks, by which time most survival curves had plateaued in virus exposed fish. A small amount of mortality (10-20%) was observed in 2 experiments at the WFRC on days 17-30 in the mock tanks, but this was much lower and later than the kinetics observed in virus treatment tanks.

Evolution of M virulence through time in rainbow trout

Logistic regression analysis of M-genogroup isolates in rainbow trout indicated that on average every unit increase in virus collection year resulted in a 1.02 times increase in the

probability of fish death (Table S1.5, ΔAICc = 2.70). As such, more recent M-isolates caused significantly greater mortality than older isolates. However, this trend depended on temperature, such that the rate of increase in the probability of death as a function of viral isolation year was 2.5 times greater at 15°C compared to 10°C (Figure 1.2, year * temp interaction, ΔAICc = 0.90, Table S1.5). When isolates were directly compared to one another at 15°C, the probability of death increased by 0.56 from the oldest to the most recent isolate following higher dose exposure or by 0.62 following lower exposure dose (Figure 1.2). The highest probability of death at high dose exposure was from the second-most recent isolate, at 0.96 (Figure 1.2D). In general, the higher viral exposure dose resulted in a greater probability of death than the low dose regardless of viral isolation year. However, the dose effect was more pronounced at 10°C compared to 15°C (Figure 1.4, logistic regression, dose * temp interaction, ΔAICc =1.8, Table S1.5). This interaction also resulted in a significantly higher probability of fish death at 15°C compared to 10°C at the low dose, but a proportionally smaller temperature effect at the high dose.

Comparison of M to U virulence within hosts

For sockeye salmon hosts, logistic regression analysis indicated that the cumulative probability of fish mortality was 43 times more likely when fish were exposed to a U-genogroup isolate compared to a M-genogroup isolate (Genotype main effect, ΔAICc = 22.58, Table S1.1), with predicted probabilities of death ranging from 20-70% versus 0-5% respectively (Figure 1.3a). Sockeye in the higher dose treatment were also three times more likely to die compared to the lower dose treatment (Dose main effect, ΔAICc = 62.78, Table S1.1), although mortality of sockeye exposed to M isolates was generally low (Figure 1.3a).

Rainbow trout hosts displayed the opposite relationship with viraL-genogroup compared to sockeye; M isolates were 14 times more likely to produce death compared to U isolates

(Genogroup main effect, ΔAICc = 14.69, Table S1.3). The predicted probability of rainbow trout mortality was 0-20% versus 25-80% for U compared to M-genogroup isolates respectively (Figure 1.3b). Although not directly tested, in general, mortality was higher in rainbow trout for U isolates compared to that of M isolates in sockeye (Figures 1, 2). The analysis indicated that rainbow trout were more susceptible to mortality at 15°C compared to 10°C, regardless of the virus isolate (Figure 1.3b, Temperature main effect, ΔAICc = 47.83, Table S1.3). Like results in sockeye hosts, the higher dose treatments resulted in 5 times greater likelihood of death compared to low dose treatments (Figure 1.3c, Dose main effect, ΔAICc = 164.88, Table S1.3).

Variation in virulence among U isolates in sockeye salmon

Overall, U isolates incurred cumulative mortality ranging from 19 to 60% in sockeye salmon (Figure 1.1A and 1B). The best fit model indicated that the probability of fish death significantly differed between isolates, with Blk12 being the least virulent and isolates Wck74 and Blk94 being the most virulent (Figure 1.5, Isolate main effect, ΔAICc = 80.2, Table S1.9). Isolates GF77 and Blk15 caused moderate levels of mortality, the probability of which was significantly different from the other three isolates but not from each other. As such, there was no indication of a temporal trend of year of virus isolation for U-genogroup isolates in sockeye. A significant effect of dose was observed, such that fish death was more probable in treatments which received the higher dose of viral exposure (Dose main effect, ΔAICc = 56.8, Table S1.9).

DISCUSSION

Collectively, our results indicate that M-genogroup IHNV rapidly gained virulence after a host jump from sockeye salmon into rainbow trout, and then continued to increase in virulence through time. This resulted in average fish mortality induced by emergent M-genogroup IHNV increasing by 2-3 times in the novel rainbow trout host over the five decades of isolate collection

(Figure 1.3). These findings are supported by 6 independent studies of sixteen viral isolates temporally spanning the host jump event to present day; replicated across the ancestral and novel salmonid hosts, two research facilities, two viral exposure dosages, and two temperatures. Our results therefore offer a compelling contrast to the textbook case of myxoma virus in Australian rabbits (8) and conventional theory which predicts virus virulence will attenuate following a host jump (9). The evolution of IHNV towards increased virulence observed here indicates that virulence is an adaptive trait or a consequence of an adapted trait for the virus.

Our findings are in line with other recent IHNV studies investigating the virulence of emerging IHNV genogroups MD (a subgroup within the M-genogroup) in North America (79), (62, 63, 79) and J in Asia (62, 63, 79), all indicating the continued evolution of increased virulence. Among E isolates circulating in Italy, rapid increases in virulence have been documented in two different genetic groups, where virulence is positively correlated with viral replication and emergence time rather than genetic clustering (62, 63, 79). Similarly, J isolates circulating in Japan demonstrated increased virulence over collection date but the shift in phenotype did not correlate with genetic divergence (62, 63, 79). Whether M-genogroup IHNV circulating in North American aquaculture is moving towards an unknown virulence endpoint or stable equilibrium as predicted after a host-jump (80), is unknown. We note that among the most recent isolates assayed in this study (2014-2017), some variation in virulence was observed, but the most recent isolate (Ht134-17) was also one of the most virulent. This indicates IHNV virulence has not yet stabilized and may have more evolutionary space to explore.

These results also agree with a growing body of literature from systems such Ebola, feline calicivirus, HIV, SARS-CoV-2, and *M. gallisepticum*, which indicate the evolution of increased pathogen virulence after host-jump events. The question remains as to what system properties drive virulence evolution and whether generalities can be reached. In the case of

myxoma virus in Australia, an anthropogenically induced strain was specifically chosen for its extreme virulence, potentially precluding the virus for attenuation (81). For *M. gallisepticum*, virulence evolution appeared to be driven in part by anthropogenically supplemented feeding behavior, facilitating increased virulence (21). In the case of SARS-CoV-2, immune invasion and routes of transmission modulated by human behavior heavily influenced which strains became dominant (15, 18). Similar anthropogenic drivers of virulence have been observed in other systems, such as the evolution of increased virulence in Marek's disease attributed to vaccination and poultry farming intensification (82).

For IHNV, the specificity of U-genogroup to sockeye and M-genogroup to rainbow trout is well established (29, 34, 41, 57, 58, 79, 83). Theory predicts that specialist pathogens will be more virulent than generalists (84, 85). We observed evidence of this here, in that ancestral U-genogroup isolates were able to produce low levels of mortality in the novel rainbow trout host in addition to high virulence in sockeye, indicating they had a small amount of generalist capability. However, U-genogroup isolates in sockeye were qualitatively less pathogenic than M isolates in rainbow trout. In contrast, the M-genogroup appears to have a high degree of host-specific virulence, with gains in the novel host and losses in the ancestral host. This is supported by our finding that in all but one case, M-genogroup isolates were more virulent than U isolates in rainbow trout. Almost no mortality from M isolates was observed in the ancestral host. External studies of IHNV sub-genogroups also indicate that generalist life histories across host species are typically met with lower virulence and replicative fitness than specialists (83, 86). Specialism may therefore be a mechanism by which M-genogroup IHNV is able to optimize fitness at higher levels of virulence, which has been observed in a variety of systems through serial passage experiments (87).

Our results indicated that U-genogroup IHNV did not evolve increased virulence in the ancestral host, given that no correlation with isolate collection date was found. The U-genogroup has possibly had several millennia of evolution with its sockeye host, and therefore

selection over the last 50 years was not expected. An interesting finding was the high variability of U-genogroup virulence, indicating that even this clade of the virus is still exploring evolutionary space. Anthropogenic impacts have drastically changed sockeye salmon ecology over the past century and how this has affected IHNV evolution is unknown. The fundamentally different ecology between these species and environments could offer an interesting contrast between viral evolution in rainbow trout aquaculture compared to declining wild and hatchery-managed sockeye populations. Factors such as climate change might also have greater impacts on evolution in sockeye, which are exposed to more variable environments than temperature-controlled rainbow trout aquaculture. Others have shown that the strength of the virulence-replication link may be modulated by environmental temperature and subsequent host tolerance, thusly subject to predicted climate variability (88). These topics could not be fully explored because the number of U isolates tested in this study was limited due to the focus on M-genogroup evolution.

A fundamental system-specific question to the IHNV host jump is whether it involved a temperature adaptation (34). Our results provide support for such an adaptation, most compelling of which was that the predicted rate of virulence evolution across the date of viral isolate collection was greater at 15°C compared to 10°C (Figure 1.2). In other words, M isolates were on average more virulent at 15°C compared to 10°C (Figure 1.4), but the difference was smallest for the oldest isolates. Among the oldest M isolates, collected in 1974 and 1976, there was not a consistent relationship between temperature and survival kinetics, but mean cumulative mortality indicated higher virulence occurred at 15°C (Figures 1-2). This supports the idea that virulence had already increased in the novel host relative to virulence seen in the ancestral sockeye host but exhibited lower cumulative mortality relative to more recently collected isolates (Figure 1.1). It is possible that a more pronounced temperature adaptation did occur, but prior to the earliest M isolates used in this study. We note that U isolates were also more virulent at 15°C compared to 10°C in rainbow trout, although the effect was much smaller

(Figure 1.3B). This may indicate a general increased rainbow trout susceptibility to IHNV at 15°C, regardless of genogroup, and previous studies show some evidence of this, although results are varied (32, 34, 58, 89).

Another question is whether the temperature adaptation occurred before, during, or after the host adaptation. Historical records of early epidemics (up to the mid 1970s) in rainbow trout occurring exclusively at 10°C before emerging at 15°C, indicate that the host adaptation occurred first. If IHNV adapted to the novel host before increased temperature, in our study we would expect to see the old M isolates were more virulent at 10°C compared to 15°C in rainbow trout. There was a suggestive pattern that this was true for the oldest isolate, HaVT74, but only at the highest exposure dosage and the effect was small (Figure 1.2). However, comparison of the old M isolates (HaVT74 and SV76) to U isolates clearly shows that a major change in virulence had already occurred following the host jump (Figure 1.1). All other M isolates were collected after the first major epidemics of the Hagerman Valley had been reported, indicating that while the host jump facilitated a change in virulence for IHNV, other selection factors continue to drive virulence changes (47, 56). Characterization of the virulence-temperature interaction for additional M isolates collected immediately after the time of the host jump and their nearest U-genogroup ancestor would better resolve the timing of the temperature adaptation, but their availability is limited. Regardless, our results, and that of others, indicated that the temperature adaption likely occurred very early in the emergence event (90). Most importantly for our study, M-genogroup IHNV was significantly more virulent than U-genogroup in rainbow trout regardless of temperature, indicating that a host adaptation occurred during emergence and not simply a temperature adaptation.

The role of aquaculture in the virulence evolution of IHNV is another pertinent question. It is theorized that aquaculture may create novel selection opportunities for increased virulence evolution not seen in wild ecosystems, such as higher rearing density, accelerated growth rates, genetically homogenous host populations, vaccination, overlapping age cohorts among hosts,

and landscape fragmentation (1, 29, 56). Many of these factors are common features of the intensive trout farming region of the Hagerman Valley in Idaho where M-genogroup IHNV evolved after the host jump (45). Links between the implementation of specific farm practices and the evolution of IHNV have not been explored, but could shed light on the drivers of virulence and warrant further investigation. In other salmonid aquaculture systems, intensive farming practices have been linked to increased virulence among newly emergent parasites and pathogens, including *Flavobacterium columnaris* bacterial strains and *Lepeophtheirus salmonis* salmon lice, and it has been suggested for infectious salmon anemia virus (91–93). Given that aquaculture is globally the most rapidly expanding sector of food production (68), understanding how its practices may drive virulence evolution of emergent pathogens is paramount for long-term disease management.

The evolving HNV-salmonid system continues to provide a valuable set of investigative resources. A remaining mechanistic question is whether IHNV evolved increased virulence via increased transmission rate, as observed in other systems (11, 21, 82, 94). A positive link between virulence, viral replication, and viral shedding is established in rainbow trout, but direct assessment of transmission has not yet been conducted (4, 60). Likewise, linking IHNV genetics to virulence represents a ripe opportunity for continued investigation of host-pathogen genomics and transcriptomics. Achieving a nuanced understanding of virulence is key as even small changes in virulence can enable epidemic-proportion outbreaks, which may lead to continued emergence and displacement events like those documented among MD isolates in the Columbia River Basin (30, 95).

These findings highlight the importance of understanding evolutionary trajectories and the diversity among viral phenotypes for effective pathogen management. Increasing virulence represents a major disease mitigation challenge, particularly given the increase in pathogen emergence events across systems (24, 96, 97). For salmonids specifically, it presents a serious threat to fish production and natural biodiversity via risk of spillback events. Next steps include

of how virulence evolution could be managed. Control over stocking density, vaccination, selective breeding, and culling are tools that could be modified for curbing IHNV virulence in aquaculture (1, 4), and also have relevance to a variety of agricultural, wildlife, and human systems. Identification and integration of effective management may guide pathogen evolution away from the most damaging outcomes, thus safeguarding resources including essential food production, managed species, agriculture, and services provided by resilient natural ecosystems (3, 11, 96, 98–101). Gaining a comprehensive understanding of viral traits, host and environmental factors, and the strength of their relationships is critical for modeling the host-pathogen coevolutionary pathway, risk landscapes, and feasible management options.

References

1. D. A. Kennedy, *et al.*, Potential drivers of virulence evolution in aquaculture. *Evolutionary Applications* **9**, 344–354 (2016).

2. R. M. Anderson, R. M. May, Coevolution of hosts and parasites. *Parasitology* **85**, 411–426 (1982).

3. S. Alizon, A. Hurford, N. Mideo, M. Van Baalen, Virulence evolution and the trade-off hypothesis: History, current state of affairs and the future. *Journal of Evolutionary Biology* **22**, 245–259 (2009).

4. A. R. Wargo, G. Kurath, R. J. Scott, B. Kerr, Virus shedding kinetics and unconventional virulence tradeoffs. *PLOS Pathogens* **17**, e1009528 (2021).

5. G. Kurath, A. R. Wargo, "Evolution of Viral Virulence: Empirical Studies" in *Virus Evolution: Current Research and Future Directions*, S. C. Weaver, M. Denison, M. J. Roossinck, M. Vignuzzi, Eds. (2003), pp. 53–60.

6. S. L. Messenger, I. J. Molineux, J. J. Bull, Virulence evolution in a virus obeys a trade-off. *Proceedings of the Royal Society of London - Biological Sciences* **266**, 397–404 (1999).

7. F. Fenner, M. Day, G. M. Woodroofe, THE MECHANISM OF THE TRANSMISSION OF MYXOMATOSIS IN THE EUROPEAN RABBIT (*ORYCTOLAGUS CUNICULUS*) BY THE MOSQUITO *AEDES AEGYPTI*. *Australian Journal of Experimental Biology and Medical Science* **30**, 139–152 (1952).

8. P. J. Kerr, *et al.*, Myxoma virus and the leporipoxviruses: An evolutionary paradigm. *Viruses* **7**, 1020–1061 (2015).

9. R. M. May, R. M. Anderson, Epidemiology and genetics in the coevolution of parasites and hosts. *Proceedings of the Royal Society of London - Biological Sciences* **219**, 281–313 (1983).

10. Á. Kun, *et al.*, Do pathogens always evolve to be less virulent? The virulence–transmission trade-off in light of the COVID-19 pandemic. *Biologia Futura* **74**, 69–80 (2023).

11. K. E. Atkins, *et al.*, Vaccination and reduced cohort duration can drive virulence evolution: Marek's disease virus and industrialized agriculture. *Evolution* **67**, 851–860 (2013).

12. M. T. Sofonea, L. Aldakak, L. F. V. . V. Boullosa, S. Alizon, Can Ebola virus evolve to be less virulent in humans? *Journal of Evolutionary Biology* **31**, 382–392 (2018).

13. A. Radford, *et al.*, Feline calicivirus To cite this version : Review article Feline calicivirus. *Veterinary Research* **38**, 319–335 (2007).

14. C. Fraser, *et al.*, Virulence and pathogenesis of HIV-1 infection: An evolutionary perspective. *Science* **343** (2014).

15. P. V. Markov, *et al.*, The evolution of SARS-CoV-2. *Nature Reviews Microbiology* **21**, 361–379 (2023).

16. S. Alizon, M. T. Sofonea, SARS-CoV-2 virulence evolution: Avirulence theory, immunity and trade-offs. *Journal of Evolutionary Biology* **34**, 1867–1877 (2021).

17. S. P. Otto, *et al.*, The origins and potential future of SARS-CoV-2 variants of concern in the evolving COVID-19 pandemic. *Current Biology* **31**, 918–929 (2021).

18. S. Gupta, Evolution of pathogen virulence. *EMBO reports* **24**, 1–5 (2023).

19. C. E. Cressler, D. V. McLeod, C. Rozins, J. Van Den Hoogen, T. Day, The adaptive evolution of virulence: A review of theoretical predictions and empirical tests. *Parasitology* **143**, 915–930 (2016).

20. D. M. Hawley, *et al.*, Parallel Patterns of Increased Virulence in a Recently Emerged Wildlife Pathogen. *PLoS Biology* **11** (2013).

21. D. M. Hawley, C. A. Thomason, M. A. Aberle, R. Brown, J. S. Adelman, High virulence is associated with pathogen spreadability in a songbird-bacterial system. *Royal Society Open Science* **10** (2023).

22. A. E. Henschen, *et al.*, Rapid adaptation to a novel pathogen through disease tolerance in a wild songbird. *PLoS Pathogens* **19**, 1–20 (2023).

23. M. Gallana, M. P. Ryser-Degiorgis, T. Wahli, H. Segner, Climate change and infectious diseases of wildlife: altered interactions between pathogens, vectors, and hosts. *Current Zoology* **59**, 427–437 (2013).

24. E. J. Peeler, I. Ernst, A new approach to the management of emerging diseases of aquatic animals. *Revue scientifique et technique (International Office of Epizootics)* **38**, 537–551 (2019).

25. L. M. Bootland, J. C. Leong, “Infectious Hematopoietic Necrosis Virus” in *Fish Diseases and Disorders*, (2011), pp. 66–95.

26. R. Breyta, C. Samson, M. Blair, A. Black, G. Kurath, Successful mitigation of viral disease based on a delayed exposure rearing strategy at a large-scale steelhead trout conservation hatchery. *Aquaculture* **450**, 213–224 (2016).

27. T. R. Meyers, *et al.*, Infectious hematopoietic necrosis virus (Ihnv) in alaskan sockeye salmon culture from 1973 to 2000: Annual virus prevalences and titers in broodstocks compared with juvenile losses. *Journal of Aquatic Animal Health* **15**, 21–30 (2003).

28. P. Dixon, R. Paley, R. Alegria-Moran, B. Oidtmann, Epidemiological characteristics of infectious hematopoietic necrosis virus (IHNV): A review. *Veterinary Research* **47**, 1–26 (2016).

29. R. M. Troyer, G. Kurath, Molecular epidemiology of infectious hematopoietic necrosis virus reveals complex virus traffic and evolution within southern Idaho aquaculture. *Diseases of Aquatic Organisms* **55**, 175–185 (2003).

30. R. Breyta, D. Mckenney, T. Tesfaye, K. Ono, G. Kurath, Increasing virulence, but not infectivity, associated with serially emergent virus strains of a fish rhabdovirus. *Virus Evolution* **2**, 1–14 (2016).

31. R. W. Guenther, S. W. Watson, R. R. Rucker, "Etiology of sockeye salmon 'virus' disease" (Dept. of the Interior, Fish and Wildlife Service, 1959).

32. S. E. LaPatra, Factors Affecting Pathogenicity of Infectious Hematopoietic Necrosis Virus (IHNV) for Salmonid Fish. *Journal of Aquatic Animal Health* **10**, 121–131 (1998).

33. R. Breyta, A. Jones, G. Kurath, Differential susceptibility in steelhead trout populations to an emergent MD strain of infectious hematopoietic necrosis virus. *Diseases of Aquatic Organisms* **112**, 17–28 (2014).

34. K. A. Garver, W. N. Batts, G. Kurath, Virulence comparisons of infectious hematopoietic necrosis virus U and M genogroups in sockeye salmon and rainbow trout. *Journal of Aquatic Animal Health* **18**, 232–243 (2006).

35. K. R. Criddle, I. Shimizu, "Economic importance of wild salmon" in *Salmon: Biology, Ecological Impacts, and Economic Importance*, (2014), pp. 269–306.

36. V. L. Butler, J. E. O'Connor, 9000 years of salmon fishing on the Columbia River, North America. *Quaternary Research* **62**, 1–8 (2004).

37. S. K. Campbell, V. L. Butler, Archaeological evidence for resilience of pacific northwest salmon populations and the socioecological system over the last ~7,500 years. *Ecology and Society* **15** (2010).

38. D. H. Johnson, T. A. O'Neil, *Wildlife-Habitat Relationships in Oregon and Washington Project Sponsors and Contributing Sponsors Managing Directors' Dedication* (Oregon State University Press, 2001).

39. E. J. Emmenegger, *et al.*, Development of an aquatic pathogen database (AquaPathogen X) and its utilization in tracking emerging fish virus pathogens in North America. *Journal of Fish Diseases* **34**, 579–587 (2011).

40. A. Black, R. Breyta, T. Bedford, G. Kurath, Geography and host species shape the evolutionary dynamics of U genogroup infectious hematopoietic necrosis virus. *Virus Evolution* **2**, 1–13 (2016).

41. G. Kurath, *et al.*, Phylogeography of infectious haematopoietic necrosis virus in North America. *Journal of General Virology* **84**, 803–814 (2003).

42. R. Breyta, A. Black, J. Kaufman, G. Kurath, Spatial and temporal heterogeneity of infectious hematopoietic necrosis virus in Pacific Northwest salmonids. *Infection, Genetics and Evolution* **45**, 347–358 (2016).

43. G. Kurath, "Molecular Epidemiology and Evolution of Fish Novirhabdoviruses" in *Rhabdoviruses: Molecular Taxonomy, Evolution, Genomics, Ecology, Host-Vector Interactions, Cytopathology and Control*, R. G. Dietzgen, I. V. Kuzmin, Eds. (Caister Academic Press, 2012), pp. 423–445.

44. D. F. Amend, W. T. Yasutake, R. W. Mead, A Hematopoietic Virus Disease of Rainbow Trout and Sockeye Salmon. *Transactions of the American Fisheries Society* **98**, 796–804 (1969).

45. J. M. Hinshaw, G. Fornshell, R. Kinnunen, “A profile of the aquaculture of trout in United States” (USDA Risk Management Agency, 2004).

46. G. Fornshell, Rainbow Trout - Challenges and Solutions. *Reviews in Fisheries Science* **10**, 545–557 (2002).

47. R. A. Busch, Workshop proceedings: Viral diseases of salmonid fishes in the Columbia River Basin. (1982).

48. D. F. Amend, Control of Infectious Hematopoietic Necrosis Virus Disease by Elevating the Water Temperature. *Journal of the Fisheries Research Board of Canada* **27**, 265–270 (1970).

49. D. F. Amend, Detection and transmission of infectious hematopoietic necrosis virus in rainbow trout. *Journal of wildlife diseases* **11**, 471–8 (1975).

50. R. R. Rucker, W. J. Whipple, J. R. Parvin, C. A. Evans, A contagious disease of salmon, possibly of virus origin. *Fishery Bulletin* **54**, 35–46 (1953).

51. T. J. Parisot, J. Pelnar, An interim report on sacramento river chinook disease: A viruslike disease of chinook salmon. *Progressive Fish-Culturist* **24**, 51–55 (1962).

52. D. W. Welch, Y. Ishida, K. Nagasawa, Thermal limits and ocean migrations of sockeye salmon (Oncorhynchus nerka): Long-term consequences of global warming. *Canadian Journal of Fisheries and Aquatic Sciences* **55**, 937–948 (1998).

53. E. G. Martins, S. G. Hinch, S. J. Cooke, D. A. Patterson, Climate effects on growth, phenology, and survival of sockeye salmon (Oncorhynchus nerka): A synthesis of the current state of knowledge and future research directions. *Reviews in Fish Biology and Fisheries* **22**, 887–914 (2012).

54. D. J. Páez, *et al.*, Temperature variation and host immunity regulate viral persistence in a salmonid host. *Pathogens* **10**, 1–18 (2021).

55. E. J. Emmenegger, T. R. Meyers, T. O. Burton, G. Kurath, Genetic diversity and epidemiology of infectious hematopoietic necrosis virus in Alaska. *Diseases of Aquatic Organisms* **40**, 163–176 (2000).

56. R. M. Troyer, S. E. LaPatra, G. Kurath, Genetic analyses reveal unusually high diversity of infectious haematopoietic necrosis virus in rainbow trout aquaculture. *Journal of General Virology* **81**, 2823–2832 (2000).

57. M. M. D. Peñaranda, A. R. Wargo, G. Kurath, In vivo fitness correlates with host-specific virulence of Infectious hematopoietic necrosis virus (IHNV) in sockeye salmon and rainbow trout. *Virology* **417**, 312–319 (2011).

58. M. K. Purcell, K. A. Garver, C. Conway, D. G. Elliott, G. Kurath, Infectious haematopoietic necrosis virus genogroup-specific virulence mechanisms in sockeye salmon, Oncorhynchus nerka (Walbaum), from Redfish Lake, Idaho. *Journal of Fish Diseases* **32**, 619–631 (2009).

59. D. G. McKenney, G. Kurath, A. R. Wargo, Characterization of infectious dose and lethal dose of two strains of infectious hematopoietic necrosis virus (IHNV). *Virus Research* **214**, 80–89 (2016).

60. A. R. Wargo, K. A. Garver, G. Kurath, Virulence correlates with fitness in vivo for two M group genotypes of Infectious hematopoietic necrosis virus (IHNV). *Virology* **404**, 51–58 (2010).

61. P. J. Enzmann, G. Kurath, D. Fichtner, S. M. Bergmann, Infectious hematopoietic necrosis virus: Monophyletic origin of European isolates from North American Genogroup M. *Diseases of Aquatic Organisms* **66**, 187–195 (2005).

62. M. Abbadi, *et al.*, Increased virulence of Italian infectious hematopoietic necrosis virus (IHNV) associated with the emergence of new strains. *Virus Evolution* **7**, 1–14 (2021).

63. M. Mochizuki, H. J. Kim, H. Kasai, T. Nishizawa, M. Yoshimizu, Virulence Change of Infectious Hematopoietic Necrosis Virus against Rainbow Trout Oncorhynchus mykiss with Viral Molecular Evolution. *Fish Pathology* **44**, 159–165 (2009).

64. T. Nishizawa, S. Kinoshita, W. S. Kim, S. Higashi, M. Yoshimizu, Nucleotide diversity of Japanese isolates of infectious hematopoietic necrosis virus (IHNV) based on the glycoprotein gene. *Diseases of Aquatic Organisms* **71**, 267–272 (2006).

65. A. R. Wargo, G. Kurath, In Vivo Fitness Associated with High Virulence in a Vertebrate Virus Is a Complex Trait Regulated by Host Entry, Replication, and Shedding. *Journal of Virology* **85**, 3959–3967 (2011).

66. A. R. Wargo, R. J. Scott, B. Kerr, G. Kurath, Replication and shedding kinetics of infectious hematopoietic necrosis virus in juvenile rainbow trout. *Virus Research* **227**, 200–211 (2017).

67. A. Mennerat, F. Nilsen, D. Ebert, A. Skorping, Intensive Farming: Evolutionary Implications for Parasites and Pathogens. *Evolutionary Biology* **37**, 59–67 (2010).

68. FAO, *World Fisheries and Aquaculture, FAO:Rome,2022* (2022).

69. R. Breyta, I. Brito, G. Kurath, S. Ladeau, “Infectious hematopoietic necrosis virus virological and genetic surveillance 2000-2012” (2017).

70. N. Fijan, *et al.*, Some properties of the Epithelioma papulosum cyprini (EPC) cell line from carp cyprinus carpio. *Annales de l’Institut Pasteur Virology* **134**, 207–220 (1983).

71. W. N. Batts, J. R. Winton, Enhanced Detection of Infectious Hematopoietic Necrosis Virus and Other Fish Viruses by PreTreatment of Cell Monolayers with Polyethylene Glycol. *Journal of Aquatic Animal Health* **1**, 284–290 (1989).

72. M. M. D. Peñaranda, M. K. Purcell, G. Kurath, Differential virulence mechanisms of infectious hematopoietic necrosis virus in rainbow trout (Oncorhynchus mykiss) include host entry and virus replication kinetics. *Journal of General Virology* **90**, 2172–2182 (2009).

73. R Core Team, R: A Language and Environment for Statistical Computing. (2023).

74. Posit team, RStudio: Integrated Development Environment for R. (2024). Deposited 2024.

75. D. Bates, M. Mächler, B. Bolker, S. Walker, Fitting Linear Mixed-Effects Models Using {lme4}. *Journal of Statistical Software* **67**, 1–48 (2015).

76. K. Bartoń, MuMIn: Multi-Model Inference. (2023). Deposited 2023.

77. M. J. Mazerolle, AICcmodavg: Model selection and multimodel inference based on (Q)AIC(c). (2023).

78. R. V. Lenth, emmeans: Estimated Marginal Means, aka Least-Squares Means. (2023).

79. R. Breyta, *et al.*, Emergence of MD type infectious hematopoietic necrosis virus in Washington State coastal steelhead trout. *Diseases of Aquatic Organisms* **104**, 179–195 (2013).

80. J. J. Bull, D. Ebert, Invasion thresholds and the evolution of nonequilibrium virulence. *Evolutionary Applications* **1**, 172–182 (2008).

81. P. J. Kerr, *et al.*, Next step in the ongoing arms race between myxoma virus and wild rabbits in Australia is a novel disease phenotype. *Proceedings of the National Academy of Sciences of the United States of America* **114**, 9397–9402 (2017).

82. A. F. Read, *et al.*, Imperfect vaccination can enhance the transmission of highly virulent pathogens. *PLoS Biology* **13**, 1–18 (2015).

83. D. J. Páez, D. McKenney, M. K. Purcell, K. A. Naish, G. Kurath, Variation in within-host replication kinetics among virus genotypes provides evidence of specialist and generalist infection strategies across three salmonid host species. *Virus Evolution* **8**, 1–12 (2022).

84. H. C. Leggett, A. Buckling, G. H. Long, M. Boots, Generalism and the evolution of parasite virulence. *Trends in Ecology and Evolution* **28**, 592–596 (2013).

85. S. Remold, Understanding specialism when the jack of all trades can be the master of all. *Proceedings of the Royal Society B: Biological Sciences* **279**, 4861–4869 (2012).

86. D. J. Páez, G. Kurath, R. L. Powers, K. A. Naish, M. K. Purcell, Local and systemic replicative fitness for viruses in specialist, generalist, and non-specialist interactions with salmonid hosts. *Journal of General Virology* **105** (2024).

87. D. Ebert, Experimental evolution of parasites. *Science* **282**, 1432–1436 (1998).

88. T. E. Hector, A. M. Gehman, K. C. King, Infection burdens and virulence under heat stress : ecological and evolutionary considerations. *Philosophical Transactions of the Royal Society B: Biological Sciences* **378** (2023).

89. R. G. Dietzgen, H. Kondo, M. M. Goodin, G. Kurath, N. Vasilakis, The family Rhabdoviridae: mono- and bipartite negative-sense RNA viruses with diverse genome organization and common evolutionary origins. *Virus Research* **227**, 158–170 (2017).

90. J. A. Plumb, A Virus-Caused Epizootic of Rainbow Trout (Salmo gairdneri) in Minnesota. *Transactions of the American Fisheries Society* **1**, 121–123 (1972).

91. L. R. Sundberg, *et al.*, Intensive aquaculture selects for increased virulence and interference competition in bacteria. *Proceedings of the Royal Society B: Biological Sciences* **283** (2016).

92. M. S. Ugelvik, A. Skorping, O. Moberg, A. Mennerat, Evolution of virulence under intensive farming: salmon lice increase skin lesions and reduce host growth in salmon farms. *Journal of Evolutionary Biology* **30**, 1136–1142 (2017).

93. D. H. Christiansen, *et al.*, First field evidence of the evolution from a non-virulent HPR0 to a virulent HPR-deleted infectious salmon anaemia virus. *Journal of General Virology* **98**, 595–606 (2017).

94. J. C. De Roode, S. Altizer, Host-parasite genetic interactions and virulence-transmission relationships in natural populations of monarch butterflies. *Evolution* **64**, 502–514 (2010).

95. L. M. Gomez, V. A. Meszaros, W. C. Turner, C. B. Ogbunugafor, The Epidemiological Signature of Pathogen Populations That Vary in the Relationship between Free-Living Parasite Survival and Virulence. *Viruses* **12**, 1–16 (2020).

96. R. Fan, S. A. H. Geritz, Virulence management: Closing the feedback loop between healthcare interventions and virulence evolution. *Journal of Theoretical Biology* **531**, 110900 (2021).

97. V. Trivellone, E. P. Hoberg, W. A. Boeger, D. R. Brooks, Food security and emerging infectious disease: Risk assessment and risk management. *Royal Society Open Science* **9** (2022).

98. M. L. Groner, *et al.*, Managing marine disease emergencies in an era of rapid change. *Philosophical Transactions of the Royal Society B: Biological Sciences* **371** (2016).

99. C. A. Burge, *et al.*, Climate Change Influences on Marine Infectious Diseases: Implications for Management and Society. (2013). https://doi.org/10.1146/annurev-marine-010213-135029.

100. K. S. Traynor, *et al.*, Varroa destructor: A Complex Parasite, Crippling Honey Bees Worldwide. *Trends in Parasitology* **36**, 592–606 (2020).

101. D. Ebert, J. J. Bull, “Challenging the trade-off model for the evolution of virulence: is virulence management feasible?” (2003).

Table 1.1. IHNV Isolate information. Rows list IHNV isolates used in the study obtained from WFRC freezer archive and originally collected from the field, with accompanying metadata. For isolate name, letters typically signify location, and last two numbers date of isolation. Phylogenetic genogroup, subgroup, and sequence type were determined by mid-G gene sequencing. *Isolate 14 was not tested in VIMS experiments. **Isolate 16 was not tested in sockeye hosts.

Label	Isolate Name	Collection Location	Collection Year	Species of Isolation	Genogroup	Subgroup	Sequence type
1	Wck74	Weaver Creek, B.C.	1974	*O. nerka*	U	UP	mG004U
2	GF77	Glacier Flats, AK	1977	*O. nerka*	U	UP	mG003U
3	Blk94	Baker Lake Hatchery, WA	1994	*O. nerka*	U	UP	mG002U
4	Blk12	Baker Lake Hatchery, WA	2012	*O. nerka*	U	UP	mG050U
5	Blk15	Baker Lake Hatchery, WA	2015	*O. nerka*	U	UP	mG265U
6	HaVT-74	Hagerman Valley, ID	1974	*O. mykiss*	M	MN	mG400M
7	SV76	Sun Valley Trout, B.C.	1976	*O. mykiss*	M	MN	mG401M
8	220-90	Hagerman Valley, ID	1990	*O. mykiss*	M	MB	mG009M
9	Ha20-91	Hagerman Valley, ID	1991	*O. mykiss*	M	MB	mG079M
10	Ha30-91	Hagerman Valley, ID	1991	*O. mykiss*	M	MC	mG119M
11	Ha39-91	Hagerman Valley, ID	1991	*O. mykiss*	M	MD	mG107M
12	Ht508k-14	Hagerman Valley, ID	2014	*O. mykiss*	M	MB	mG296M
13	Ht511-14	Hagerman Valley, ID	2014	*O. mykiss*	M	MD	mG298M
14*	HtBrG-16	Hagerman Valley, ID	2016	*O. mykiss*	M	MB	mG342M
15	HtBrK-16	Hagerman Valley, ID	2016	*O. mykiss*	M	MB	mG331M
16**	Ht134-17	Hagerman Valley, ID	2017	*O. mykiss*	M	MC	mG335M

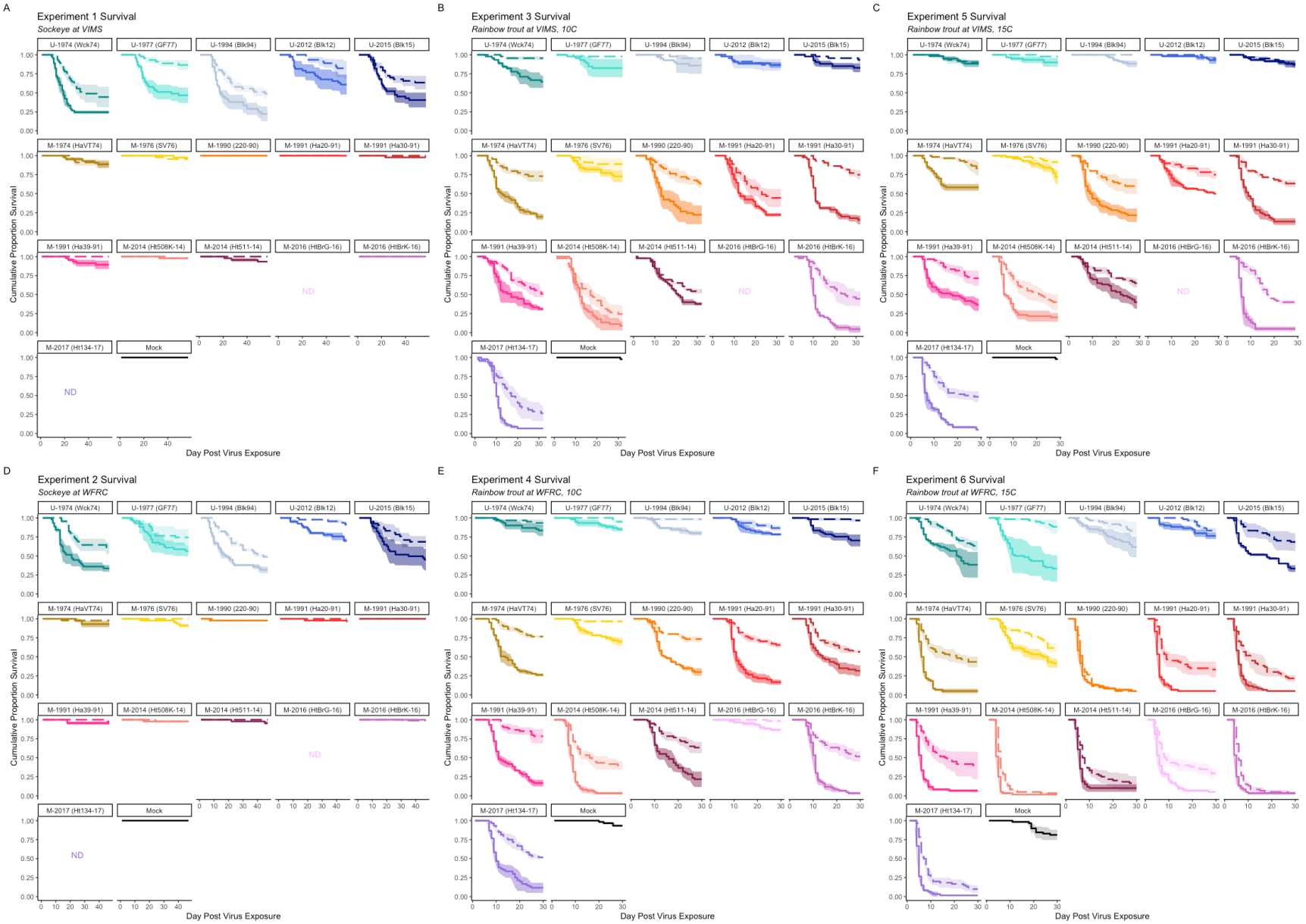
A
Experiment 1 Survival
Sockeye at VIMS
B
Experiment 3 Survival
Rainbow trout at VIMS, 10C
C
Experiment 5 Survival
Rainbow trout at VIMS, 15C
D
Experiment 2 Survival
Sockeye at WFRC
E
Experiment 4 Survival
Rainbow trout at WFRC, 10C
F
Experiment 6 Survival
Rainbow trout at WFRC, 15C
U-1974 (Wck74)
U-1977 (GF77)
U-1994 (Blk94)
U-2012 (Blk12)
U-2015 (Blk15)
M-1974 (HaVT74)
M-1976 (SV76)
M-1990 (220-90)
M-1991 (Ha20-91)
M-1991 (Ha30-91)
M-1991 (Ha39-91)
M-2014 (Ht508K-14)
M-2014 (Ht511-14)
M-2016 (HtBrG-16)
M-2016 (HtBrK-16)
M-2017 (Ht134-17)
Mock
ND
Cumulative Proportion Survival
Day Post Virus Exposure

Figure 1.1. Cumulative survival data from virulence assays. Panels show mean cumulative proportion survival through time, for triplicate tanks in each experiment treatment. Tanks contained 20 fish each, except for experiment 3 which contained 15 fish each. (A) Experiment 1; sockeye hosts held at 10°C at VIMS. (B) Experiment 3; rainbow trout hosts held at 10°C at VIMS. (C) Experiment 5; rainbow trout hosts held at 15°C at VIMS. (D) Experiment 2; sockeye hosts held at 10°C at WFRC. (E) Experiment 4; rainbow trout hosts held at 10°C at WFRC. (F) Experiment 6; rainbow trout hosts held at 15°C at WFRC. For all panels, solid lines indicate high dose (2×10^5 pfu/mL); dashed lines indicate low dose (2×10^3 pfu/mL) virus exposure. Standard error (± 1) between the triplicate tanks is indicated by a shaded ribbon. Treatments that were not included in an experiment are marked ND. Treatment plots are ordered by IHNV genogroup (U top row, M bottom rows), followed by year of isolation and isolate name. Mortality was tracked for longer in sockeye experiments so x-axis scale is different (panels A and D).

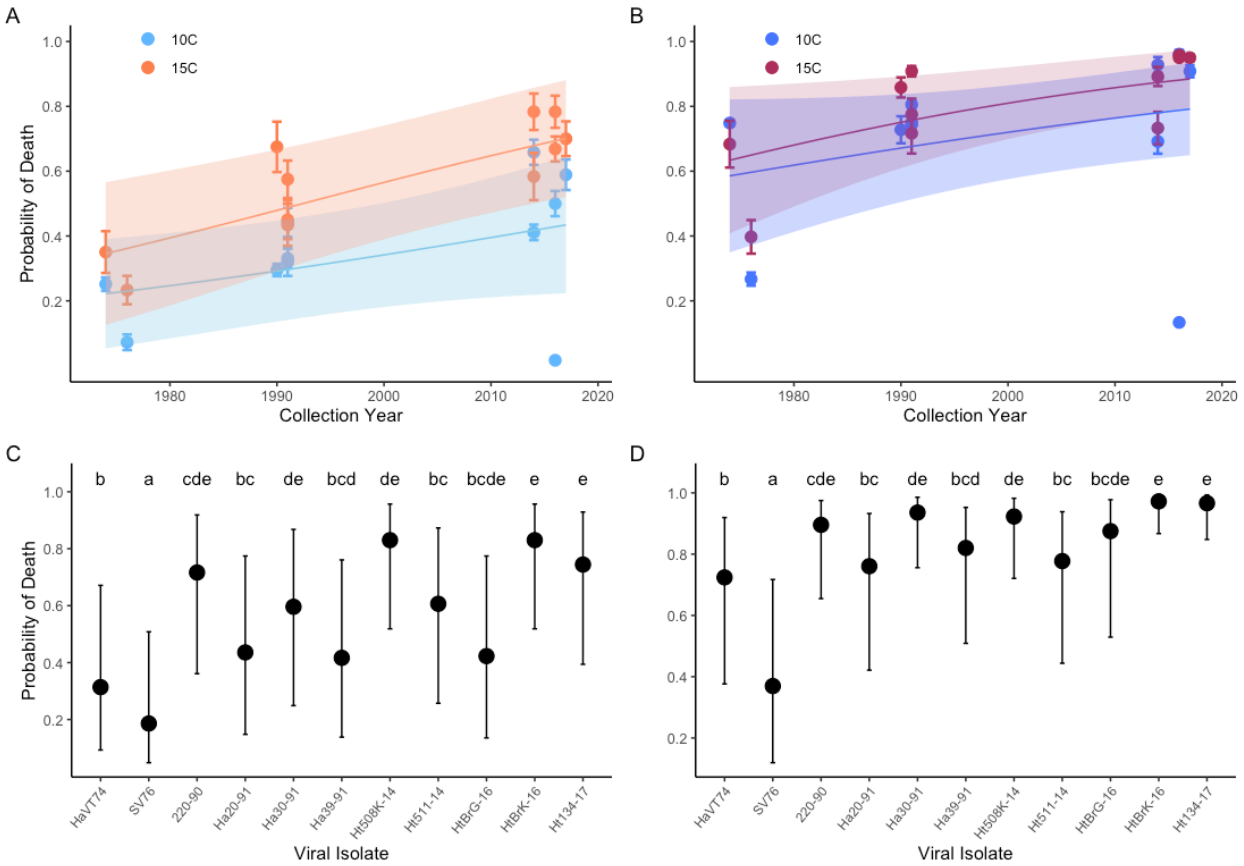

Figure 1.2. Virulence evolution and variation of M-genogroup isolates through time. (A,B) Lines show predicted probability of fish death as a function of year of viral collection, obtained from AICc-selected statistical models (see methods and Tables S5-S6) for 15°C (orange and red) and 10°C (blue and purple) for low dose (A - 2 x 10^3 pfu/mL) and high dose (B - 2 x 10^5 pfu/mL) experiments in rainbow trout. Predicted probabilities are back transformed from log odds (logit) and shading shows 95% confidence interval. Points represent mean raw data across six replicate tanks (WFRC and VIMS data combined) with standard error bars, annotated by Isolate number (refer to Table 1.1 for Isolate information). Although the dosages are shown separately, the analysis indicated that there was no dose interaction with factors, so the slopes of the lines across dosages and within temperatures are the same in the untransformed logit scale. (C, D) Predicted probability of fish mortality for M isolates when compared directly to one another in rainbow trout at 15°C at low dose (C - 2 x 10^3 pfu/mL), and high dose (D - 2 x 10^5 pfu/mL), obtained from AICc-selected models (see methods and Tables S7-S8). Differing letter symbols indicate statistical differences at $p < 0.05$ (Tables S7-S8). Bars represent 95% confidence intervals.

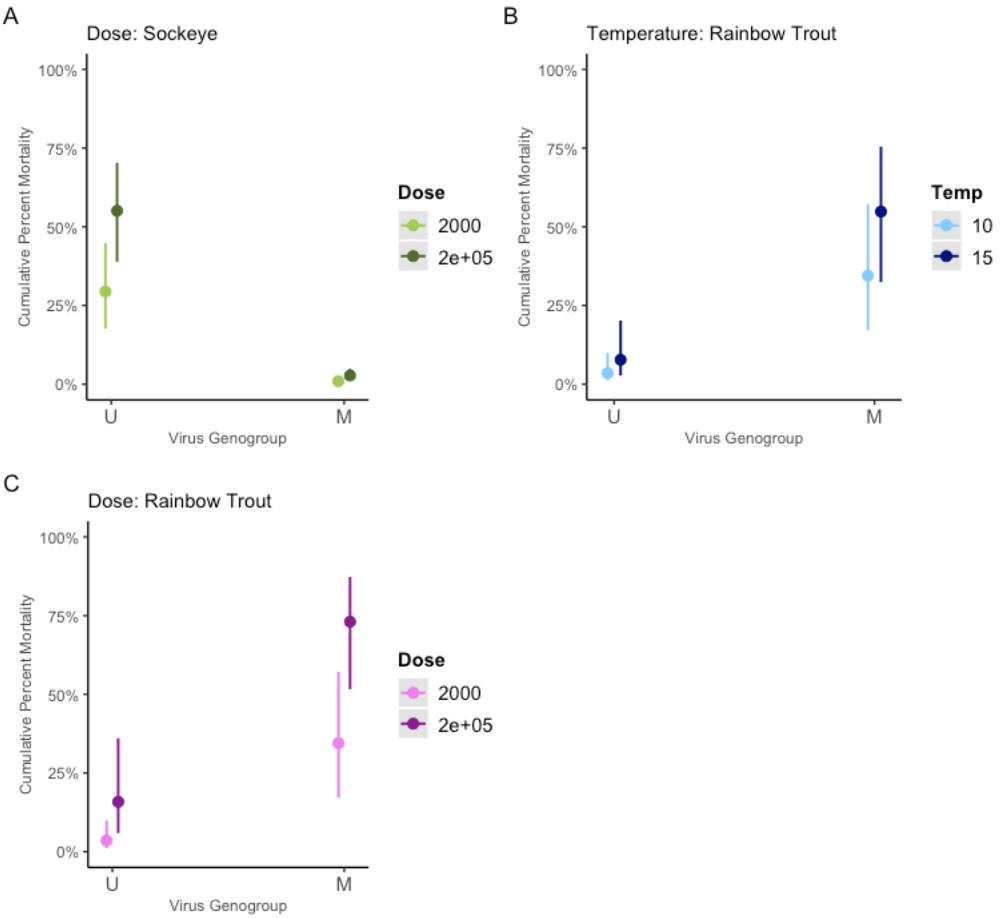

Figure 1.3. Predicted probability of mortality between genogroups within hosts. Panels show predicted probability of fish death for significant interactions obtained from AICc selected statistical models comparing U and M-genogroups within hosts (see methods and Tables S1-S4). Panels A and D show genogroup * dose interaction for sockeye salmon and rainbow trout respectively. Panel B shows the genogroup * temperature interaction for rainbow trout hosts. For all panels, bars are 95% confidence intervals. No other interactions or factors were found to be significant in the analyses.

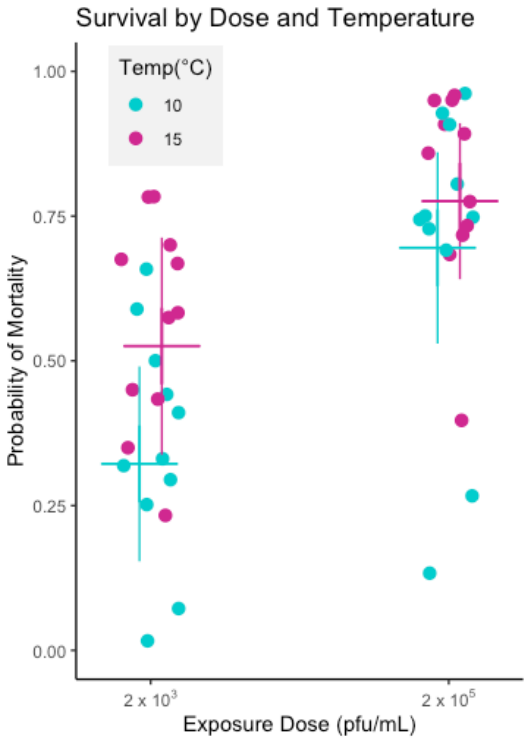

Figure 1.4. Dose by temperature interaction for M-genogroup evolution. Predicted probability of cumulative percent mortality (horizontal bars) for M-genogroup isolates in rainbow trout hosts at different doses (2 x 10^3 or 2 x 10^5 pfu/mL) of IHNV at two temperatures (10°C in cyan or 15°C in magenta). Mean experimental data (solid circles) are shown for all isolates. Predicted data are obtained from selected AICc models (Tables S5-S6), plotted with 95% confidence intervals (whiskers).

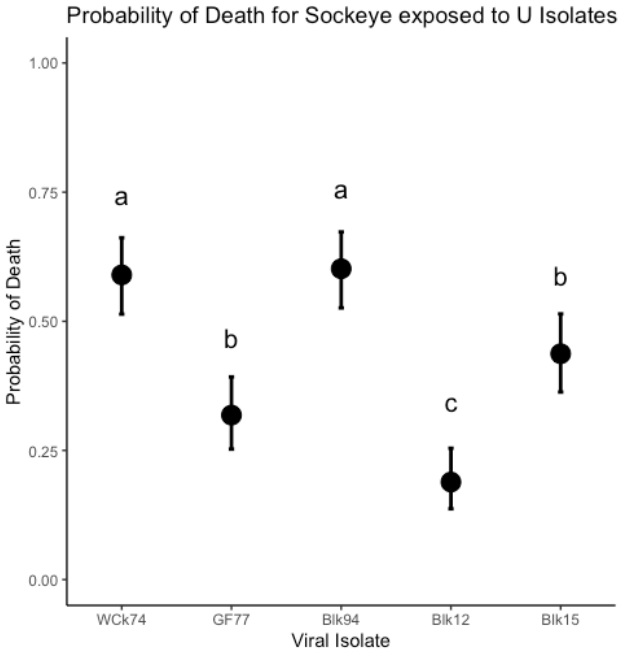

Figure 1.5. Probability of fish mortality in ancestral host and virus. Points shown predicted probability of fish mortality for U isolates in sockeye salmon, obtained from AICc selected models (see methods and Table S1.9). Differing letter symbols indicate statistical differences at $p < 0.05$ (Table S1.9). Bars represent 95% CI. No dose effect was observed so data was combined in the mean.

Supplemental Materials

Table S1.1. Model summary comparing U versus M virulence in sockeye hosts. Estimates and associated error are on logit scale. Residual degrees of freedom = 170.

Fixed effect	Estimate	Standard error	Z-value	Degrees of freedom
Intercept	-4.6355	0.3219	-14.401	
Genogroup (U)	3.7627	0.4501	8.359	1
Dose (High)	1.0772	0.1371	7.859	1
cbind(Dead, Alive) ~ (1|Isolate) + Genogroup + Dose, family="binomial"				

Table S1.2. Candidate models for comparing U versus M virulence in sockeye hosts. Model 1 is the best-fit model; all other models within ΔAICc of 2 are shown with a '+' indicating whether or not the parameter was included in the respective model.

Model	Isolate	Dose	Genogroup	Dose* Genogroup	ΔAICc	AICc weight
1	+	+	+		0.00	0.694
2	+	+	+	+	1.63	0.306

Table S1.3. Model summary for comparing U versus M virulence in rainbow trout hosts. Estimates and associated error are on logit scale. The degrees of freedom for residuals were 170.

Fixed effect	Estimate	Standard error	Z-value	Degrees of freedom
Intercept	-3.3091	0.5637	-5.871	
Genogroup (M)	2.6673	0.4855	5.494	1
Dose (High)	1.6391	0.1165	14.070	1
Temperature (15℃)	0.8354	0.1146	7.287	1
cbind(Dead, Alive) ~ (1|Isolate) + (1|Tank) +(1|Lab) + Genogroup + Dose + Temp, family="binomial"				

Table S1.4. GLME candidate models for comparing U versus M virulence in rainbow trout hosts. Model 1 is the best-fit model; all other models within ΔAICc of 2 are shown with a '+' indicating whether or not the parameter was included in the respective model.

Model	Isolate	Tank	Lab Location	Dose	Genogroup	Temperature	Temperature* Genogroup	ΔAICc	AICc weight
1	+	+	+	+	+	+		0.00	0.701
2	+	+	+	+	+	+	+	1.71	0.298

Table S1.5. GLME model output for examining M isolate evolution since host jumping to rainbow trout. Estimates and associated error are on logit scale. The degrees of freedom for residuals were 365.

Fixed effect	**Estimate**	**Standard error**	**Z-value**	**Degrees of freedom**
Intercept	-0.655611	0.364417	-1.799	
Year of Isolation	0.023017	0.013510	1.704	6
Dose (High)	1.599523	0.146394	10.926	1
Temperature (15℃)	0.918181	0.142626	6.438	1
Year*Temp	0.011591	0.006586	1.760	13
Dose*Temp	-0.414032	0.207136	-1.999	3

cbind(Dead, Alive) ~ (1|Lab) + (1|Tank) + (1|Isolate) + CenterYr + Dose + Temp + CenterYr:Temp + Dose:Temp, family="binomial"

Table S1.6. GLME candidate models for M virulence over time.

Model	Isolation Year	Dose	Temp	Year*Temp	Dose*Temp	Year*Dose	ΔAICc	AICc weight
1	+	+	+	+	+		0.00	0.276
2	+	+	+		+		0.90	0.176
3	+	+	+	+			1.78	0.114

Table S1.7. GLME model output for M isolate variation in virulence following low dose exposure (2 x 10^3 pfu/mL) at 15°C. Coefficient estimates for each isolate and associated error are on logit scale. Total degrees of freedom for residuals in the model were 51.

Coefficient	Estimate	Standard error	Z-value
Intercept	-0.7825	0.7637	-1.025
Isolate (SV76)	-0.6931	0.3165	-2.190
Isolate (220-90)	1.7098	0.3090	5.534
Isolate (Ha20-91)	0.5238	0.2988	1.753
Isolate (Ha30-91)	1.1717	0.3015	3.887
Isolate (Ha39-91)	0.4459	0.2995	1.489
Isolate (Ht508K-14)	2.3688	0.3271	7.242
Isolate (Ht511-14)	1.2154	0.3019	4.026
Isolate (HtBrG-16)	0.4714	0.3557	1.325
Isolate (HtBrK-16)	2.3688	0.3271	7.242
Isolate (Ht134-17)	1.8518	0.3119	5.937
cbind(Dead,Alive) ~ (1|Lab) + Isolate, family="binomial"			

Table S1.8. GLME model output for M isolate variation in virulence following high dose exposure (2 x 10^5 pfu/mL) at 15°C. Coefficient estimates for each isolate and associated error are on logit scale. Total degrees of freedom for residuals in the model were 51.

Coefficient	Estimate	Standard error	Z-value
Intercept	0.9653	0.7498	1.287
Isolate (SV76)	-1.4995	0.3087	-4.857
Isolate (220-90)	1.1847	0.3492	3.393
Isolate (Ha20-91)	0.1909	0.3089	0.618
Isolate (Ha30-91)	1.7130	0.3914	4.377
Isolate (Ha39-91)	0.5523	0.3190	1.732
Isolate (Ht508K-14)	1.5157	0.3735	4.058
Isolate (Ht511-14)	0.2852	0.3115	0.916
Isolate (HtBrG-16)	0.9826	0.6436	1.527
Isolate (HtBrK-16)	2.5885	0.5113	5.063
Isolate (Ht134-17)	2.3921	0.4777	5.007
cbind(Dead,Alive) ~ (1|Lab) + Isolate, family="binomial"			

Table S1.9. GLM model output for U isolate variation in virulence. Coefficient estimates for each isolate and associated error are on logit scale. Residual degrees of freedom = 54.

Coefficient	Estimate	Standard error	Z-value	Degrees of freedom
Intercept	-2.0183	0.2163	-9.333	
Isolate (Blk15)	1.2055	0.2502	4.817	4
Isolate (Blk94)	1.8706	0.2514	7.442	4
Isolate (GF77)	0.6967	0.2541	2.742	4
Isolate (Wck74)	1.8211	0.2509	7.259	4
Dose (High)	1.1210	0.1492	7.514	1
cbind(Dead,Alive) ~ Isolate + Dose, family="binomial"				

CHAPTER 2: Evolution of viral shedding post-host jump in salmonid fish

ABSTRACT

Viral shedding is a critical component of viral fitness, which is the ability of a virus to persist and spread within host populations. Measuring shedding is an efficient method to confirm infection and estimate potential transmission rates, which are key to identifying epidemiological patterns of emergent pathogens. Success of an emergent virus is contingent on maximizing transmission in response to a new host and environmental factors. In the commercially and ecologically important species rainbow trout (*Oncorhynchus mykiss*), the previous chapter as well as studies by other researchers have identified temporal trends of increased virulence among emergent isolates of the virus infectious hematopoietic necrosis virus (IHNV). A fundamental question remains as to the mechanism of virulence for IHNV. Contemporary theory posits that high virulence may constitute high fitness if mortality facilitates greater viral shedding. This chapter uses a selection of IHNV isolates spanning the ancestral and novel IHNV genogroups, from the time of host jump to the present, to quantify viral shedding phenotypes over evolutionary time.

INTRODUCTION

Infectious hematopoietic necrosis virus (IHNV) is endemic to most watersheds in the Pacific Northwest region of North America. As an RNA virus, IHNV exhibits a relatively high mutation rate, and has undergone rapid genetic diversification in recent decades since its host jump from the ancestral host sockeye salmon (*Oncorhynchus nerka*) to rainbow trout (*O. mykiss*) (1–4). Emergence in a new host confers possible evolutionary advantages to IHNV such as abilities to adapt to changing environmental conditions, evade host immune responses, or acquire increased virulence or transmissibility. Currently IHNV poses a significant threat to the global aquaculture industry, particularly among salmon and trout species. Since its emergence in the novel host of rainbow trout in the 1970s, IHNV has been responsible for devastating outbreaks of increasing frequency and magnitude, resulting in substantial economic losses and ecological impacts. Understanding the dynamics of its viral transmission, including shedding kinetics and virus evolution, is paramount for effective management strategies in both industry and conservation.

We previously demonstrated that IHNV has continued to evolve increased virulence since the time of the host jump into rainbow trout through the near-present (Chapter 1). Viral shedding dynamics are theorized to be linked to virulence, here defined as host mortality directly attributed to viral infection. As virulence continues to evolve after a host jump, it is critical to understand how shedding and virulence phenotypes may interact. Virulence changes have previously been documented within the IHNV-salmonid system. Most notably, virulence differs between ancestral U-genogroup strains which are associated with sockeye salmon, and M-genogroup strains which are considered to be the novel group which emerged in North American trout aquaculture and gave rise to subsequent sub-lineages (5). U isolate shedding measured in the context of Atlantic salmon (*Salmo salar*) net pen aquaculture found high variation in individual susceptibility but also found that even 1% prevalence of acute IHNV

disease had potential for initiating epizootics given peak shedding rates, demonstrating how important understanding the shedding characteristics of strains is in the context of host population health (6). Virulence phenotypes have been described for IHNV across both genetic and geographic spectra in North America, Asia, and Europe (Chapter 1; (7–10)). In each of these major regions, increasing virulence has been detected among emergent IHNV isolates in rainbow trout. If IHNV continues to explore evolutionary space in terms of virulence phenotypes, shedding traits under selection may be part of the explanatory mechanism.

While virulence evolution has been documented and shedding kinetics have been broadly characterized for IHNV, a direct association has not been made between these traits for the specific IHNV isolates studied across the host jump event. Viral fitness describes the ability of a virus to persist and spread within host populations. Fitness is the result of interconnected viral shedding duration, transmission rate, and host recovery rate, according to evolutionary theory (11). According to tradeoff theory, transmission is the driver behind virulence evolution. Transmission may be estimated by a variety of methods, including *in vitro* assays and mathematical models. *In vivo* assays that examine viral replication via body burden or viral shedding via environmental samples offer a significant advantage in modeling transmission dynamics in host-pathogen systems with fewer degrees of separation from natural environments. Furthermore, shedding is the most direct metric of transmission since it encompasses both viral replication and release, and can be measured over multiple timepoints since it is a non-destructive sampling method. Viral shedding refers to the release of virus particles from infected hosts into the environment, where particles may encounter and infect susceptible individuals. Horizontal transmission and recovery rates can be captured by measuring viral shedding from a host to the environment. Recovery, or the duration over which hosts continue to shed virus, is also theorized to be a key factor in population-level incidence and transmission, where shortening the duration of shedding via recovery or host death may be a cost to the virus (11–13). However, if duration is shortened due to massive host damage via

viral shedding and transmission, the benefit of an extremely high and short-lived shedding peak may outweigh the costs of a truncated shedding duration. Quantifying the shedding kinetics, or the shedding dynamics including onset, duration, and magnitude, of infection may identify critical periods of contagiousness in infected hosts. This information would inform the potential for transmission, thus guiding risk management and mitigation at a population level.

Shedding intensity (quantity) can be quantified by sampling viral shedding through environmental sampling and has been demonstrated in multiple systems, spanning human health, wildlife epidemiology, agriculture and food systems. Examples include widespread wastewater testing for SARS-CoV2 to estimate COVID prevalence and severity (14), comparison of shedding modes to assess risk of transmission of Ebola (15), prevalence of avian viruses shed by wild reservoir species which threaten public health (16), transmission and clearance rate of Marek's disease in broiler chicken farms (17), and surveillance of ostreid herpesvirus-μvar in oyster farms (18). Most empirical studies use endpoint samples, but where a repeated-measures sampling design can be employed to take multiple temporal samples from individuals, variation in shedding magnitude and duration may be quantified to estimate the instantaneous rate of transmission. A repeated sampling design has been demonstrated with IHNV in rainbow trout previously, indicating that IHNV produces acute infections within a few days of exposure and continues to shed for a couple weeks (19–22).

Significant work has been done to elucidate the natural history of IHNV, yielding a broad understanding of infection and transmission routes, clinical disease and mortality, increased virulence on the landscape, multiple host jumps, and resulting phylogenetics and geographic range. Viral replication is known to differ between the U and M-genogroups, which are adapted to different host species (24). Shedding profiles have been described for representative M-genogroup isolates dubbed 'high virulence' or 'low virulence' and were determined to correlate with within-host replication quantities 3 days post-exposure (21, 23). The shedding kinetics of these strains follow a pattern of rapidly peaking within 1-4 days post-exposure among all

individuals, decreasing through day 7, and generally falling below detection limits within 2 weeks (19). A followup study expanded both the number of IHNV isolates included (from two to four isolates considered to have different virulence levels) as well as the time period over which samples were analyzed (from three to 30 days) and used a coinfection design with three distinct isolate pairs to detect differences between isolates (20). This study explicitly examined possible tradeoffs between virulence, transmission rate, and transmission duration by using shedding as a proxy for transmission. The four isolates spanned the known range of IHNV virulence in rainbow trout at the time of the study. Early shedding kinetics were consistent with previous descriptions of the shedding peak followed by decreased shedding, but the rate depended on isolate (20). Overall the study found a positive association between virulence and shedding duration, but not shedding intensity (20). The results from the four included isolates lent support to the theory that these viral traits are linked, and suggested that higher virulence phenotypes would have a fitness advantage (20).

On an individual host level, the quantity of virus shed by infected fish can vary significantly. As seen in past IHNV studies high levels of viral shedding may be associated with acute or severe infections, but a high level of individual variation appears to be common (19, 25). It is unknown to what extent individual host variability contributes to viral evolutionary dynamics. Viral shedding kinetics are theorized to play a crucial role in IHNV transmission dynamics within aquaculture facilities, where aquaculture-specific factors may increase susceptibility to infection via direct contact with infected fish or indirect exposure to contaminated water (4, 25–27).

Given the economic implications of IHNV, there is significant interest in teasing apart the associations between IHNV shedding kinetics and virulence. Previous IHNV studies in rainbow trout found more virulent strains exhibited longer transmission durations due to lower recovery rates of infected hosts, ultimately providing an overall fitness advantage without a constraint on increased virulence evolution, but only four isolates were tested, selected for virulence

representation rather than temporal representation (20). A key question lingers for the IHNV evolutionary arc: is increased shedding quantity or duration enabling the observed gain in virulence post-host jump event?

In this study, we describe and examine the shedding phenotypes for 15 isolates of IHNV in the novel host rainbow trout to investigate viral fitness following the host jump. Fitness at different temperatures was examined to investigate the possibility of a temperature adaptation. Additionally, we examine whether a consistent relationship exists between virulence and shedding, essentially searching for optimal fitness 'type' that may be emerging in trout farms. Understanding the mechanisms of viral transmission dynamics, shedding kinetics, and virus evolution is crucial for effective disease management and sustainable food production. Existing management strategies for controlling IHNV transmission often focus on preventing horizontally transmitted infection, such as implementing biosecurity measures and vaccination programs to reduce disease prevalence and severity (6, 25). Not only do salmonid conservation and sustainable global aquaculture depend on informed management, but advancing our understanding of viral fitness across systems furthers our grasp of epidemiology and risk management.

METHODS

1. Virus and host

Fifteen genetically distinct IHNV isolates collected in the field from the estimated time of host jump (1970s) to 2017 were used. Isolates were obtained from the USGS archive (28), and previously described (Chapter 1). Of these, five isolates were from the ancestral U-genogroup to serve as a baseline for dominant U isolates on the landscape at the time of the host-jump (see

Table 2.2.1). Ten isolates of the emergent M-genogroup were collected from intensive trout farming regions were also used (Table 2.2.1). These isolates were chosen to represent the virus immediately after the time of host jump through the subsequent decades of evolution within North American rainbow trout farms, separated into roughly three temporal periods. All fifteen isolates have been previously typed for virulence and stand for the temporal as well as spatial diversification of endemic IHNV in North America rainbow trout aquaculture (Chapter 1; (2, 5)). Virus stocks were obtained by inoculating fish cell lines and harvesting supernatant after observing terminal cytopathic effect (CPE) progression (typically 5 – 7 days) (29). Stocks were stored at -80°C before titering via plaque assay a minimum of three times [see Chapter 1 methods]. In addition to the virus isolates, a mock exposure with MEM-10 (Chapter 1) was used to control for effects of the exposure method.

Farmed rainbow trout (*O. mykiss*) eggs were supplied by a commercial trout producer and reared as previously described (Chapter 1). Briefly, rainbow trout were specific pathogen free research-grade fish, bred from a minimum of twelve parental pairs, and selected as the best available genetic representative of *O. mykiss* populations in which the M group host jump is theorized to have occurred. Eggs were maintained in egg trays under 2 gpm flow until hatching, when they were transferred to 50-gallon flow trout tanks maintained at 1gpm flow. Eggs and fish were supplied with pathogen free, UV-irradiated fresh water at 12.5°C. Approximately 5 weeks before experiments, fish were split into two identical pools and gradually stepped up or down to 15 or 10°C respectively over three weeks then allowed to acclimate for a minimum of an additional two weeks before experiments began, to minimize temperature stress. At the time of experiments fish were 1.8 grams. Juvenile fish were fed a daily diet of semi-moist pellets equivalent to 2-3% biomass (Zeigler). These represent that same lot of fish that were characterized for IHNV virulence evolution, and those experiments were run concurrently (Chapter 1).

All fish care and subsequent experiments were conducted at the Virginia Institute of Marine Science (Virginia, USA) in accordance with William & Mary IACUC protocols (IACUC-2018-06-21-12998-arwargo and IACUC-2021-07-02-15072-arwargo).

2. In vivo shedding experiment

We conducted two independent experiments to quantify IHNV shedding kinetics across the 15 isolates of IHNV in the novel rainbow trout host. Experiment 1 was conducted at 10°C and experiment 2 at 15°C to assess potential temperature adaptation of isolates during or after the host jump and impacts on shedding kinetics. On Day 0 of each experiment, groups of 15 (10°C experiment) or 20 (15°C experiment) fish were exposed via bath immersion to one of the IHNV isolates at a dose of 2×10^5 pfu/mL in one liter of aerated, static water for one hour, with aeration. A mock control group of five fish per experiment was exposed to MEM in water (no virus). Immediately following exposure, the fish were transferred to a new tank with aeration and water flow at 750mL/min for 1 hour to remove any residual virus (data not shown) for a minimum of 7.5 complete water changes. The fish were subsequently distributed to individual 0.8L tanks (one fish per tank) with aeration and water flow at 150mL/min in a tower rack system (Aquaneering Systems). A 700ul volume of water was sampled from each tank immediately following distribution on Day 0, and placed in a 96- well, 1 mL collection plate. The tanks were sampled again on days 1-3, 5, 7, 10, and 20 for experiment 1 at 10°C and days 1-5, 7, 10, 20, and 29 for experiment 2 at 15°C. For each sampling timepoint, flow to tanks was halted for 22 hours prior to the sampling time to allow shed virus to accumulate in static conditions. After sampling, flow was restored for a minimum of 2 hours to flush remaining virus from the tank (equivalent to over twenty water changes per tank). This sampling method allowed the shed IHNV load of every replicate fish to be quantified for both temperatures, all virus isolates, at every timepoint. Fish were also monitored daily for mortality for 30 days. Dead fish were left in

tanks and water samples continued to be collected. Samples were stored at -80°C until processing. Of the 5 mock fish included per experiment, 1 fish died in the 15°C experiment on day 1, presumably the result of handling stress rather than viral contamination because no other fish in virus-exposed groups died prior to day five (data not shown).

3. Virus quantification

Virus shed loads in water samples were analyzed via RNA extraction followed by RT-qPCR. RNA was extracted from a 210uL sample with the *cador* Pathogen 96-well kit (Indical, formerly produced by Qiagen) using a Tecan Evo 100 liquid handler as previously described (22). An 11uL volume of extracted RNA was then converted to cDNA, in a 20ul reaction using oligo-dT, random hexamers, and Moloney murine leukemia virus (M-MLV) reverse transcriptase (Promega) as previously described (21). The cDNA was diluted 1:2 in RNAase-free water and at 5 uL volume quantified via qPCR using IHNV N-gene specific primers IHNV N 796F, IHnVN 875R, TaqMan probe IHNV N 818MGB, and Universal PCR Master Mix No AmpErase UNG (all Life Technologies) on a QuantStudio 6 qPCR machine as previously described (30). Each qPCR plate included an 8-step, 10-fold dilution series of plasmid (experiment 1) or g-block gene fragment (experiment 2) generated artificial positive control (APC) to allow for absolute quantification of RNA (30). The data from experiment 1 was normalized against the g-block standard using linear regression, to allow for comparison between experiments. The qPCR method provides viral RNA copies per mL water, which is presented as copies/mL and represents the amount of virus shed into the environment. The sensitivity, specificity, and limit of detection for the qPCR assay have been previously characterized (30) and limit of detection was validated here by averaging the highest CT value obtained across all qPCR runs.

4. Statistical analyses

Statistical tests and visualizations were carried out in R Statistical Software (version 4.2.3) and RStudio (version 2023.12.1+402) (31, 32). Data were visually inspected to identify possible shedding metrics of interest using correlation plots with the pairs.panels() function of the psych package (Figures S2.1 – S2.6).

Analyses were then organized into four sections to focus on [1] how the kinetics of surviving and shedding over the course of the experiment varied across IHNV isolates and temperatures, [2] whether shedding phenotypes differed across emergent M isolate collection dates, indicating evolutionary patterns in the field, [3] how virulence and shedding are associated, and [4] how shedding phenotypes varied between the ancestral U and novel M-genogroups of IHNV.

[1] To determine if shedding and survival kinetics followed the same pattern over experiment days, both shedding and mortality data were analyzed via generalized linear mixed effects models (GLME) using the lme4 package and a binomial error distribution (33). Genogroups were analyzed separately due to the majority of U isolate fish never shedding. For the shedding kinetics models, the response variable was the shedding status of each individual fish on each day (binomial – yes or no), with fixed effects predictors day (numerical), temperature (categorical), viral isolate (categorical), interaction terms between all combinations of effects, and the random effect of individual fish to account for repeated measures taken from fish across experimental days. Data was only analyzed from day 2 forward to capture the kinetics of shedding from the peak onwards. A similar model approach was used for analyzing cumulative survival over the course of the experiment, with the ratio of living to dead fish on the terminal day of the experiment as the dependent variable. The fixed effects included temperature (categorical), viral isolate (categorical), an interaction term between temperature and isolate, and no random effects.

[2] Within the M-genogroup, the association between isolate collection year and the shedding phenotypes (0) frequency of shedding, (i) mean intensity, (ii) peak intensity, (iii) post-

peak quantity shed, (iv) time of peak, and (v) duration of shedding were analyzed using regression models from the lme4 package. In all models, predictors included year (continuous) as a fixed effect and isolate (categorical) as a random effect. Temperatures were analyzed separately due to independent experiments with different sampling time points. (0) Frequency of shedding was calculated as the proportion of fish shedding out of total fish included per treatment. (i) Mean intensity was calculated as the average amount of virus shed (RNA copies determined by qPCR) by each fish, across all sampling days excluding points where shedding was not detected. (ii) Peak intensity was calculated as the maximum amount of virus shed from each fish, excluding fish that never shed. Mean and peak intensity were $\log_{10}(x)$ transformed to normalize the response distribution (iii) Post-peak quantity shedding per fish was calculated as the sum of all shedding that occurred from day 7 post-exposure onwards, including even those fish without detectable shedding (set to 0), then log (x+1) transformed. Peak and post-peak periods were examined separately due to the pattern of high levels of acute shedding in the peak period (days 0-5) followed by exponentially lower quantity but prolonged shedding in post-peak period (days 7-30). This allowed for increased resolution of shedding differences within the peak and post-peak periods. (iv) Time of peak was calculated as the day of peak shedding for each individual fish. (v) The duration of shedding was calculated as the number of sampling days positive versus negative for shedding, for each fish. Shedding from dead fish was not included in any of the analyses, with the assumption that dead fish are removed daily in aquaculture so their contribution to transmission is minimal. Data were also dropped from fish that never shed for the analyses of peak intensity, time of peak, and post-peak shedding. Total quantity shed over experiment days (including positive and negative fish) was observed to correlate nearly perfectly with peak intensity and was not analyzed (Figures S2.1-S2.6). Quantity response data (mean intensity, peak intensity, and post-peak quantity shed) was analyzed with linear mixed effects models (LME) and a Gaussian error distribution. Time of peak

and duration of shedding were analyzed with generalized mixed effects linear models (GLME), with Poisson and binomial error distributions respectively.

[3] To examine how virulence was associated with the shedding of emergent IHNV isolates, survival status (binomial – yes or no) of individual fish at the experiment end was modeled as a response variable with peak period shedding quantity (continuous), isolate collection year (continuous), and their interaction, as fixed effects, and viral isolate as a random effect, using a generalized linear mixed effects model. The experiments at the two different temperatures were analyzed separately. Another set of analyses were conducted using post-peak shedding quantity as a fixed predictor instead of the peak shedding term. The goal of these analyses was to determine how the relationship between virulence and shedding has evolved in emergent IHNV, and as such U isolates, which also experienced very little mortality, were not included. The second analysis was conducted with day of individual fish death as the response variable and the same predictors as above, using a linear mixed effects model with a Gaussian error distribution. The analysis included only fish that died before the last sampling day and was separated by experiment.

[4] To investigate shedding differences between emergent M and ancestral U IHNV genogroups, total quantity of shed virus ($\log_{10}(x+1)$ transformed) per fish was analyzed using regression analyses from the lme4 and glmmTMB packages (33). Evidence of excess zeros in the data was identified by the performance package; correspondingly zero-inflated models were used with a tweedie distribution. Predictor variables were genogroup (categorical) as a fixed effect and isolate as a random effect. The analysis was run separately for the two experiments due a different number of sampling days.

For all analyses, model selection was conducted using corrected Akaike Information Criterion (AICc), where maximal models (all main effects and interactions) were fit to the data and the model with the lowest AICc value was selected as the best fit model. In some cases where exploration of multiple random effects was appropriate, a cutoff of Δ10 AICc was used to

select random effects before exploration of main effects. This involved AICc comparison between models with all possible factor combinations, including interaction terms, sometimes using the dredge() function of the MuMIn package when the number of possible models was large (>4). Any models within Δ2 AICc are shown in the supplementary materials; only results of the best fit model are presented in the main text. Because AICc selection was used, p-values are not provided, and instead ΔAICc for model without the factor of discussion is presented in the results. Coefficients from summaries of best fit models, as well as plotting of predicted values, were used to determine the magnitude and direction of factor level differences for best fit models. 95% confidence intervals were used to determine significant differences between levels.

RESULTS

1. Shedding and survival kinetics

The number of juvenile rainbow trout hosts shedding IHNV rapidly peaked on days 2-3 following host exposure and then decreased after days 5-7 (Figures 2.1A-2.1B). Shedding intensity (quantity among positive hosts) generally followed the same pattern of peaking within 3 days of initial exposure at 15°C but was more variable at 10°C (Figures 2.1C-2.1D). The statistical models indicated that the likelihood of shedding decreased with experimental day, from day 2 onward for both U and M-genogroup isolates (Figure 2.2, day main effect, delta AICc = 10.24, Tables S2.3, S2.4). There was a higher likelihood of shedding at 15°C compared to 10°C for U isolates (Figure 2.2), but the probability of shedding was not found to differ between isolates within the genogroup (no isolate main effect). Some fish never shed at all, mostly among U-genogroup treatments where less than half the fish shed at 10°C and about half the

fish shed at 15°C (Appendix A; Figures A1-A5, Figure 2.1A-2.1B). In comparison, almost all fish in M isolate treatments at both temperatures shed detectable virus within 2 days post-exposure (Appendix A; Figures A6-A15, Figures 2.1A-2.1B).

For the M-genogroup, the effect of temperature was dependent on virus isolate (Figure 2.3, temperature * isolate interaction). For half of the M-isolates, shedding was higher at 10°C compared to 15°C, although the difference was only significant for one isolate (Ht511-14). There was also a general pattern of more recently collected M-isolates having a higher probability of shedding compared to older isolates, with SV76 (collected 1976) having the lowest probability and Ht134-17 (collected 2017) having the highest probability at 15°C. At 10°C, Ha39-91 (collected 1991) had the lowest and Ht511-14 (collected 2014) had the highest shedding probability. For each genogroup data subset, a second candidate model was within ΔAICc 2 of the best fit model, indicating an interaction between day and temperature, suggesting that the rate of decrease in shedding probability through experiment day depended on temperature (Tables S2.1, S2.2).

When examining survival kinetics in the shedding experiments, mortality for each isolate presented a pattern similar to shedding kinetics for each isolate, with a 2-4 day lag. Mortality typically began around day 5, peaked between days 5-10, and then began to plateau, although it remained high in some groups until the end of the experiment (Table 2.2). Day of death ranged between day 4-28 for M isolates at 10°C, day 4-29 for M isolates at 15°C, 8-22 for U isolates at 10°C, and day 4-26 for U isolates at 15°C (Table 2.2). Very little mortality occurred in U-isolate treatments; with only 14 total fish dying during the experiment, and no difference between temperatures. For both genogroups, the best fit model for total mortality included an interaction between viral isolate and temperature (Figure 2.4, Tables S2.5-S2.6). No post-hoc comparisons between factor levels were significant among U isolates (Figure 2.4A). Mortality among M-isolates was much higher, ranging from 10-90% by the end of the experiment (Figure 2.4B). Lower mortality was observed among 10°C treatments relative to 15°C for seven of the

ten isolates, but the 95% confidence intervals overlapped between temperatures for all isolates. For some isolates, the 15°C treatment produced more mortality such that it was significantly different from the mean total mortality of a milder virulence isolate at either temperature. For example, the least virulent isolate (SV76 collected in 1976) produced less than 20% cumulative mortality at both temperatures and was not significantly different from the Ht508k-14 at 10°C (50% mortality), but was different from Ht508k-14 at 15°C (80% mortality) (Figure 2.4B). Qualitatively, more recently collected isolates appeared to induce higher mortality, although there were some notable exceptions such as Ha39-91 which was less virulent than the other two isolates collected in the same year and the oldest isolate HaVT-74. Again, in many cases 95% confidence intervals in survival between isolates overlapped, with the exception of the most and least virulent isolates (HtBrk-16 and SV76 respectively).

Shedding intensity (magnitude of shedding from only those fish actively shedding) kinetics generally matched kinetics of shedding frequency (Figure 2.1C-2.1D). Differences in peak intensity among isolates at 15°C appeared minimal, typically reaching approximately 10^4 copies/mL among M isolates or slightly lower among U isolates (Figure 2.1D). Greater variation was observed at 10°C such that peak intensity did not occur on a consistent day or with consistent magnitude across isolates and genogroups (Figure 2.1C). Shedding at the individual fish level also exhibited high variability (Appendix A). Four individuals, all within U isolate treatments, produced shed virus over $10^{5.5}$ copies/mL, up to 10^6 copies/mL (Appendix A; Figures A1, A2, A4). Given the wide range of shedding and survival kinetics, we continued to examine genogroups separately to better detect differences among isolates. A total of 3 of the 80 samples processed from Mock-exposed fish tested positive for virus by qPCR (1 fish tested positive on 1 sampling day in Experiment 1 and 1 fish tested positive on 2 sampling days in Experiment 2; data not shown), near the threshold of detection and outside the pattern of shedding kinetics of virus exposed fish.

2. Evolution of emergent M isolate shedding

The virus shedding parameters (0) shedding frequency, (i) mean intensity, (ii) peak intensity, (iii) post-peak quantity shed, (iv) time of peak, and (v) duration of shedding were further analyzed for their association with year of M-isolate collection. Based on the observed shedding kinetics, these were found to be the most informative parameters for elucidating evolutionary trends in emergent IHNV shedding phenotypes (Figures S2.1-S2.6). U isolates were not included in this analysis.

Recent collection years were associated with increased shedding frequency, represented by the proportion of positive fish relative to total number of fish replicates included in the treatment, estimated at 0.024 increased proportion per year at 10°C, and a slightly greater slope for 15°C (respectively, delta AICc = 10.8, Table S2.7 and delta AICc = 41.47, Table S2.8; Figure 2.5).

The effect of collection year exhibited a weakly positive relationship with (i) mean shedding intensity per fish, estimated at 0.0014 times increase in quantity of virus shed with each unit increase in collection year, for both experimental temperatures (respectively, delta AICc = 10.6, Table S2.9 and delta AICc = 10.7, Table S2.10; Figure 2.6). While this year-to-year change is minimal, over the 40-year range this viral selection encompasses, this translates to an estimated 400-500 copies/mL increase in intensity (Figure 2.6).

M isolate collection year was positively associated with the (ii) peak shedding quantity for both 10°C (delta AICc = 9.42, Table S2.11) and 15°C (delta AICc = 8.72, Table S2.12). At 10°C, every increase in year resulted in a predicted increase of 0.006 times viral copies shed and at 15°C the predicted increase was 0.009 times peak viral copies shed (Figure 2.7A). As such, at 15°C the oldest isolates collected in the 1970s were predicted to have a sum quantity of 6,300 viral copies/mL over the peak shedding period and those in 2010s were predicted to have 14,100 viral copies/mL (Figure 2.7A).

At 15°C, recency of collection year was negatively associated with (iii) post-peak shedding such that each year increase coincided with 0.003 times fewer log viral copies/mL (delta AICc = 3.17, Figure 2.7B, Table S2.13). Over the 40-year span in collection years, this resulted in only a 0.1 decrease in post-peak shedding on the logarithmic scale. At 10°C the opposite trend was detected, where each unit increase in isolate collection year resulted in an increase of 0.02 times more viral copies/mL (delta AICc =1.84, Figure 2.7B, Table S2.14). This resulted in almost an order of magnitude increase in post-peak shedding across the 40 years of isolate collection.

The analysis of (iv) day of peak shedding indicated that every increase in collection year resulted in 0.0027 times increase in peak shedding day (delta AICc = 1.34, Table S2.15). Temperature also influenced peak shedding day, such that fish exposed at 15°C peaked 0.4 days earlier than fish exposed at 10°C (delta AICc = 42.54, Figure 2.7C, Table S2.15). As such, fish exposed to isolates collected in the 1970s were predicted to reach peak shedding on days 2.5 and 3.7 at 15 and 10°C respectively, compared to 2.8 and 4.2 days respectively with isolates collected in the 2010s.

The (v) duration of detectable virus shedding was correlated with collection year such that exposure to more recent isolates increased the log-odds of positive sampling days by 0.02 times (Figure 2.7D, Table S2.17). Over the evolutionary time range examined, this resulted in a 30% longer shedding duration. An effect of temperature on shedding duration was indicated by a secondary model within ΔAICc 2 of best fit model (Table S2.16).

3. Association between virulence and shedding for emergent IHNV

Emergent M-genogroup isolates were analyzed to determine how mortality and day of fish death (virulence) were associated with peak and post-peak shedding quantities at both temperatures (Figure 2.8, Tables S2.18-S2.23). The analysis indicated that every collection year unit increase result in a 0.07 time increase in the log-odds of death (year effect delta AICc =

12.04, Table S2.21). For the 15°C dataset, every log unit increase in peak quantity was estimated to result in increased log-odds of death by 2.29 (peak shed effect delta AICc= 35.89, Table S2.21, Figure 2.8A), such that at the lowest peak shedding values (2 log copies/mL) the probability of fish death was zero and at the highest (4.6 log copies/mL) it was close to 1 (Figure 2.8A). Estimates for the 10°C relationship between peak shedding and probability of death followed the same trend (Figure 2.8A). However, there were subtle differences compared to the 15°C estimates: the rate of change was initially faster and slowed at higher peak quantities (4 log copies/mL) such that the maximum probability of death was predicted at 0.75 (Figure 2.8A, Table S2.18). The relationship between post-peak shedding and probability of fish death depended on temperature. For 15°C post-peak shedding decreased the log-odds of death by 0.25 (Figure 2.8B, post-peak shed effect delta AICc = 0.24, Table S2.23) and every increase in isolate collection year resulted in increasing the log-odds by 0.07 (year effect delta AICc = 5.84, Table S2.19). At 10°C, post-peak shedding quantity was positively associated with virulence at 10°C such that every log unit increase resulted in a log-odds increase of death by 0.705 (Figure 2.8B, shedding effect delta AICc = 37.83, Table S2.19) and every increase in isolate collection year resulted in increasing the log-odds by 0.052 (year effect delta AICc = 5.84, Table S2.19).

Earlier death day was associated with a higher magnitude of peak shedding regardless of temperature (Figure 2.9, Tables S2.24-S2.25). At the peak shedding extrema observed at 10°C, fish were estimated to succumb between days 7-9 at high shedding rates or days 15-25 at low shedding rates (Figure 2.9A). Among lower shedding rates, predicted death day was modulated by collection year, with the most recent isolates having an earlier day of death (Figure 2.9A). ore recently collected isolates generally had the earlier death days except at high temperature and very low shedding peak rate (< 2.3 log copies/mL) where the relationship between collection year and death day was reversed (Figure 2.9B). Exploration of the data including fish that did not die during the experiment found the same relationships between shedding and virulence.

4. Phenotype differences between major IHNV genogroups

Isolates from the emergent M genogroup elicited higher shedding intensity than U isolates across all fish at both temperatures. At 10°C, trout shed 0.097 more M virus than U virus on the log scale (Genogroup effect, delta AICc= Table S2.26). The same positive relationship was present at 15°C where M virus-exposed fish shed more, but the observed difference was greater where they shed 0.27 log fold more virus (Genogroup effect, delta AICc= Table S2.27, Figure 2.10). The higher temperature appeared to exacerbate the genogroup differences.

DISCUSSION

Our study revealed that within the novel M-genogroup, which is of paramount concern to trout aquaculture and conservation, most recently collected isolates shed up to 1.6 times more during peak shedding, relative to the oldest isolates. Recency had little effect on post-peak shedding quantity at the environmentally relevant temperature of 15°C, but was positively correlated with later peak days and longer shedding durations. Virulence analysis identified a relationship between higher shedding loads and greater probability of death, and was consistent with previous findings, although the same relationship did not hold when only post-peak shed quantity was examined. Viral shedding kinetics followed a similar pattern across genogroups and isolates within the rainbow trout host species, peaking within 2-3 days post-exposure and then declining to undetectable levels after 2-3 weeks. Shedding decreased more slowly at 10°C relative to 15°C, which was largely driven by peak probability of shedding being much lower for 10°C. At the genogroup level, M isolates resulted in 70-100% prevalence, greater shedding intensity and total quantity, and higher mortality than U isolates, which produced 50% or less prevalence and almost no mortality. These differences at the genogroup levels were consistent

with past studies that have compared high and low virulence types of IHNV within a host as well as kinetics of U and M virus.

This study measured individual shedding fitness at discrete sampling timepoints to produce data at both the individual host level, and population level. Base probability of U shedding was always lower than M isolates and was especially notable during the acute peak window of shedding prevalence. Patterns were consistent across genogroups but individual variability was high, including later peaks than the mean in a minority of fish hosts and variable post-mortem shedding, with some fish never shedding after peak and others shedding at multiple timepoints. The observed increase in both probability of shedding and shedding intensity over evolutionary time among emergent M isolates indicates a trend towards increased transmission potential as more virus is released to the environment per host.

Since peak and mean intensity are positively correlated with virulence and recency of emergence, this could be interpreted as a shift towards more explosive infectious periods where virulence confers only low fitness costs to IHNV. Past work has explored virulence tradeoffs of IHNV empirically and mathematically and found that high virulent types of IHNV had longer transmission periods measured by viral shedding, and were more fit than low virulence types (20). Further work on acute viral infections in other systems such as human papillomavirus has demonstrated how viruses which infect and replicate in hosts in short time frames may evade host innate immune responses and are subject primarily to selection by the adaptive host immune system (34). Among shedding hosts, peak intensity was similar across viral genogroups but longer duration of shedding for M isolates indicates greater fitness for M-genogroup. Since increased transmission (approximated by probability and intensity of shedding) as well as increased shedding duration (recovery) both correlated with virulence changes, these results suggest that IHNV evolution aligns with virulence evolution theory, which posits that these viral traits are linked.

Relationships between shedding metrics and time indicate that later peaks and subsequently longer recovery periods may be stronger drivers of virulence than shedding magnitude. When a virus adapts to a new host, as IHNV in rainbow trout, we may expect that a wide variety of traits are initially explored by the virus as it moves towards equilibrium with its host (35). Early shedding dynamics would be expected to significantly influence its fitness after emergence where earlier peaks could result in virus strains reaching maximum infectious potential more quickly, in turn leading to rapid spread in a naïve population. Acute shedding windows like those seen with SARS-coV-2 in the early months of the COVID-19 pandemic were an example of rapid spread and rapid change as viral strains quickly adapted to human populations and were subsequently displaced as fitness increased (36). Paired with acute shedding, longer recovery periods (shedding duration) allow viruses a longer period of potential transmission, which can amplify the cumulative fitness of a virus allowed to circulate in a chronically shedding host. Considering the compounding effect of more transmission potential to additional naïve hosts, it is reasonable to expect that the timing of viral shedding may be equally or even more important to overall viral fitness than the frequency or quantity of virus shed.

Lower mortality was seen in the 10°C experiment, despite reaching similar infection prevalence. Higher probability of shedding and earlier peaks were associated with 15°C. These temperature differences continue to allow the possibility of a temperature adaptation to 15°C, beyond the intrinsic rate increase of viral replication as a function of host cellular metabolism at increased temperatures, but do not necessarily point to a temperature adaptation. Had a temperature adaptation occurred for IHNV alongside its host jump, the shedding kinetics of old M isolates would be expected to align more with U isolates than with recently collected M isolates, at both 10°C and 15°C. Both reduced probability of shedding as well as reduced intensity might be expected for 10°C treatments too, but a uniform difference between the temperature treatments could just as easily be attributed to host biology. Temperature is a

strong modulator of both host factors such as immune response as well as viral replication dynamics (24, 37, 38).

In this study system, the difference in shedding suppression (recovery rate) between temperatures is likely due in part to the differential activation of the teleost immune system at different temperatures since teleost organisms are highly sensitive to temperature (37). Recent work in steelhead (anadromous *O. mykiss*) found that viral replication was accelerated at higher temperatures, resulting in shorter shedding durations, whereas colder temperatures resulted in longer persistence and increased virulence due to enhanced host immune response (38). A link between cold temperature and extended shedding duration has been observed in common carp infected with koi herpesvirus (KHV), indicating greater risk of infection over time in cold freshwater conditions (39). KHV has also been examined in seawater, where higher water temperatures were found to induce host immune responses that limited viral entry, adding to the body of work that underscores the importance of temperature for endotherm species particularly in aquatic environments (40).

The variation in shedding intensity observed at the individual and isolate levels is minute in many cases. Nonetheless, these differences may have considerable implications for opportunities of evolutionary trajectories for IHNV. Variable shedding rates observed in small scale experiments result in differential transmission fitness of foot-and-mouth disease (FMDV) in cattle and other livestock, but scaling these effects to natural outbreaks has proven difficult given the moderate longevity (weeks) of virions in the environment, potential for transmission via indirect contact, and variability in agricultural methods (41, 42). While events such as aerosol dispersal of FMDV virions represent low probability for transmission, when they do occur they may translate to outbreaks and subsequent pathogen adaptation in naïve livestock populations (37). In the context of aquatic environments, indirect exposure to pathogens via shared water sources is of considerable concern. Salmonid aquaculture managers expend enormous effort to curtail biosecurity risks of spillover and spillback events that could occur by

contaminated water entering or leaving aquaculture facilities (43). Despite these precautions, spillback events have been documented for IHNV in the Columbia River Basin watershed (44–46). Subsequent displacements of IHNV genotypes in the same region indicate that emergence of new genetic strains can have significant effect on the subsequent evolution of viral phenotypes. A separate study conducted with Chinook salmon (*O. tshawytscha*) in the Columbia River Basin found that spring-run salmon shed significantly more IHNV virus than fall-run salmon, indicating a higher transmission potential and dominance in virus ecology also depend on host factors (47).

Continuing questions for this system include whether shedding virus is equivalent to absolute transmission potential. One drawback to measuring released virus with molecular methods in this study is the unknown viability of detected virus. Further work directly measuring transmission would greatly add to the body of information available on the IHNV-salmonid system and serve to either confirm shedding avenues as transmission routes, or scale how to interpret the infection risk of shed virions. Another question that remains for the system is the infectious dose required for IHNV and how it varies across isolates; some individual fish release enormous amounts of virus in the days following infection, but given the vast ratio of water volume to fish biomass in field environments, transmission events would still appear to be rare if experimental results are to be directly extrapolated (48). Is shedding detectable virus a prerequisite to transmission success among trout? Does infectivity differ among genetic types? A study conducted with vaccinated, sialodacryoadenitis virus (SDAV)-seropositive rats found that transmission was possible even among low shedding individuals, indicating that even very low titers of virus represent risk (49). Conversely, the role of super shedder individuals, which release exponentially higher loads of virus and may represent disproportionately high risk, is difficult to measure due to their rarity. Among fish used in this study, outliers in the high range of shedding intensity were unusual but not unknown; three individuals in the Blk12 treatment shed much more than any other fish in their group, but inconsistently. Modeling these rare

occurrences in controlled experiments is difficult but raises questions about how often these events occur in the field.

Downstream ecological impacts associated with the sequential displacement of virus genotypes and phenotypes reach beyond the initial host species. As seen in the case study of myxomavirus evolution in European rabbits introduced to Australia, changes in virulence and transmission fitness may be linked to feedback loops intrinsically linked to the local environment like vector presence, climate-related modulation, and interaction with other local species such as the native plant community of Australia (12, 50). If the same trends hold true for IHNV shedding kinetics such as intensifying shedding along with virulence, we may see altered shedding and transmission pathways fundamentally different from historic disease events. For IHNV and the multitude of ecological niches directly and indirectly impacted by salmonid host species, the many potential environmental selection pressures represented by managed aquaculture populations as well as wild populations provide myriad opportunities to evolve. Which paths IHNV may take depend partly on these external factors but also appear to be subject to the balance of viral phenotypic traits of shedding intensity, duration, and prevalence. Untangling their relationships will guide disease management strategies across commercial landscapes, ultimately serving to protect biodiversity among salmonid populations and ecosystem stability.

References

1. L. M. Bootland, J. C. Leong, “Infectious Hematopoietic Necrosis Virus” in *Fish Diseases and Disorders*, (2011), pp. 66–95.

2. G. Kurath, *et al.*, Phylogeography of infectious haematopoietic necrosis virus in North America. *Journal of General Virology* **84**, 803–814 (2003).

3. R. M. Troyer, G. Kurath, Molecular epidemiology of infectious hematopoietic necrosis virus reveals complex virus traffic and evolution within southern Idaho aquaculture. *Diseases of Aquatic Organisms* **55**, 175–185 (2003).

4. R. M. Troyer, S. E. LaPatra, G. Kurath, Genetic analyses reveal unusually high diversity of infectious haematopoietic necrosis virus in rainbow trout aquaculture. *Journal of General Virology* **81**, 2823–2832 (2000).

5. R. Breyta, A. Black, J. Kaufman, G. Kurath, Spatial and temporal heterogeneity of infectious hematopoietic necrosis virus in Pacific Northwest salmonids. *Infection, Genetics and Evolution* **45**, 347–358 (2016).

6. K. A. Garver, *et al.*, Estimation of parameters influencing waterborne transmission of infectious hematopoietic necrosis virus (IHNV) in atlantic salmon (Salmo salar). *PLoS ONE* **8** (2013).

7. M. Abbadi, *et al.*, Increased virulence of Italian infectious hematopoietic necrosis virus (IHNV) associated with the emergence of new strains. *Virus Evolution* **7**, 1–14 (2021).

8. M. Abbadi, *et al.*, Molecular Evolution and Phylogeography of Co-circulating IHNV and VHSV in Italy. *Frontiers in Microbiology* | *www.frontiersin.org* **1**, 1306 (2016).

9. M. Mochizuki, H. J. Kim, H. Kasai, T. Nishizawa, M. Yoshimizu, Virulence Change of Infectious Hematopoietic Necrosis Virus against Rainbow Trout Oncorhynchus mykiss with Viral Molecular Evolution. *Fish Pathology* **44**, 159–165 (2009).

10. S. S. Kim, *et al.*, Differential virulence of infectious hematopoietic necrosis virus (IHNV) isolated from salmonid fish in Gangwon Province, Korea. *Fish and Shellfish Immunology* **119**, 490–498 (2021).

11. R. M. Anderson, R. M. May, Coevolution of hosts and parasites. *Parasitology* **85**, 411–426 (1982).

12. F. Fenner, M. Day, G. M. Woodroofe, THE MECHANISM OF THE TRANSMISSION OF MYXOMATOSIS IN THE EUROPEAN RABBIT (*ORYCTOLAGUS CUNICULUS*) BY THE MOSQUITO *AEDES AEGYPTI*. *Australian Journal of Experimental Biology and Medical Science* **30**, 139–152 (1952).

13. J. J. Bull, A. S. Lauring, Theory and Empiricism in Virulence Evolution. *PLOS Pathogens* **10**, e1004387 (2014).

14. O. Puhach, B. Meyer, I. Eckerle, SARS-CoV-2 viral load and shedding kinetics. *Nat Rev Microbiol* (2022). https://doi.org/10.1038/s41579-022-00822-w.

15. P. Vetter, *et al.*, Ebola Virus Shedding and Transmission: Review of Current Evidence. *J Infect Dis.* **214**, S177–S184 (2016).

16. M. D. Jankowski, M. D. Jankowski, C. J. Williams, J. M. Fair, J. C. Owen, Birds shed RNA-viruses according to the pareto principle. *PLOS ONE* **8** (2013).

17. D. A. Kennedy, P. A. Dunn, A. F. Read, Modeling Marek's disease virus transmission: A framework for evaluating the impact of farming practices and evolution. *Epidemics* **23**, 85–95 (2018).

18. O. Evans, Transmission of Ostreid herpesvirus-1 microvariant in seawater: Detection of viral DNA in seawater, filter retentates, filter membranes and sentinel Crassostrea gigas spat in upwellers. (2017).

19. A. R. Wargo, R. J. Scott, B. Kerr, G. Kurath, Replication and shedding kinetics of infectious hematopoietic necrosis virus in juvenile rainbow trout. *Virus Research* **227**, 200–211 (2017).

20. A. R. Wargo, G. Kurath, R. J. Scott, B. Kerr, Virus shedding kinetics and unconventional virulence tradeoffs. *PLOS Pathogens* **17**, e1009528 (2021).

21. A. R. Wargo, K. A. Garver, G. Kurath, Virulence correlates with fitness in vivo for two M group genotypes of Infectious hematopoietic necrosis virus (IHNV). *Virology* **404**, 51–58 (2010).

22. D. R. Jones, B. J. Rutan, A. R. Wargo, Impact of vaccination and pathogen exposure dosage on shedding kinetics ofinfectious hematopoietic necrosis virus (IHNV) in rainbow trout. *Journal of Aquatic Animal Health* (2020). https://doi.org/10.1007/978-1-4614-7495-1_23.

23. A. R. Wargo, G. Kurath, In Vivo Fitness Associated with High Virulence in a Vertebrate Virus Is a Complex Trait Regulated by Host Entry, Replication, and Shedding. *Journal of Virology* **85**, 3959–3967 (2011).

24. M. M. D. Peñaranda, M. K. Purcell, G. Kurath, Differential virulence mechanisms of infectious hematopoietic necrosis virus in rainbow trout (Oncorhynchus mykiss) include host entry and virus replication kinetics. *Journal of General Virology* **90**, 2172–2182 (2009).

25. S. E. LaPatra, *et al.*, Negligible risk associated with the movement of processed rainbow trout, Oncorhynchus mykiss (Walbaum), from an infectious haematopoietic necrosis virus (IHNV) endemic area. *Journal of Fish Diseases* **24**, 399–408 (2001).

26. K. A. Garver, W. N. Batts, G. Kurath, Virulence comparisons of infectious hematopoietic necrosis virus U and M genogroups in sockeye salmon and rainbow trout. *Journal of Aquatic Animal Health* **18**, 232–243 (2006).

27. D. A. Kennedy, *et al.*, Potential drivers of virulence evolution in aquaculture. *Evolutionary Applications* **9**, 344–354 (2016).

28. E. J. Emmenegger, *et al.*, Development of an aquatic pathogen database (AquaPathogen X) and its utilization in tracking emerging fish virus pathogens in North America. *Journal of Fish Diseases* **34**, 579–587 (2011).

29. W. N. Batts, J. R. Winton, Enhanced Detection of Infectious Hematopoietic Necrosis Virus and Other Fish Viruses by PreTreatment of Cell Monolayers with Polyethylene Glycol. *Journal of Aquatic Animal Health* **1**, 284–290 (1989).

30. M. K. Purcell, *et al.*, Universal reverse-transcriptase real-time PCR for infectious hematopoietic necrosis virus (IHNV). *Diseases of Aquatic Organisms* **106**, 103–115 (2013).

31. R Core Team, R: A Language and Environment for Statistical Computing. (2023).

32. Posit team, RStudio: Integrated Development Environment for R. (2024). Deposited 2024.

33. D. Bates, M. Mächler, B. Bolker, S. Walker, Fitting Linear Mixed-Effects Models Using {lme4}. *Journal of Statistical Software* **67**, 1–48 (2015).

34. S. Alizon, C. L. Murall, I. G. Bravo, Why Human Papillomavirus Acute Infections Matter. *Viruses* **9**, 293 (2017).

35. R. M. May, R. M. Anderson, Epidemiology and genetics in the coevolution of parasites and hosts. *Proceedings of the Royal Society of London - Biological Sciences* **219**, 281–313 (1983).

36. S. P. Otto, *et al.*, The origins and potential future of SARS-CoV-2 variants of concern in the evolving COVID-19 pandemic. *Current Biology* **31**, 918–929 (2021).

37. M. K. Purcell, K. A. Garver, C. Conway, D. G. Elliott, G. Kurath, Infectious haematopoietic necrosis virus genogroup-specific virulence mechanisms in sockeye salmon, Oncorhynchus nerka (Walbaum), from Redfish Lake, Idaho. *Journal of Fish Diseases* **32**, 619–631 (2009).

38. D. J. Páez, *et al.*, Temperature variation and host immunity regulate viral persistence in a salmonid host. *Pathogens* **10**, 1–18 (2021).

39. Cano, Irene; Mulhearn, Brian; Akter, Sabhia; Paley, Richard, Seroconversion and Skin Mucosal Parameters during Koi Herpesvirus Shedding in Common Carp, Cyprinus carpio. *International Journal of Molecular Sciences* **21** (2020).

40. K. Yuasa, M. Sano, Koi Herpesvirus: Status of Outbreaks, Diagnosis, Surveillance, and Research. (2009).

41. C. Colenutt, *et al.*, Quantifying the Transmission of Foot-and-Mouth Disease Virus in Cattle via a Contaminated Environment. *mBio* **11**, 10.1128/mbio.00381-20 (2020).

42. D. J. Paton, S. Gubbins, D. P. King, Understanding the transmission of foot-and-mouth disease virus at different scales. *Current Opinion in Virology* **28**, 85–91 (2018).

43. J. M. Hinshaw, G. Fornshell, R. Kinnunen, “A profile of the aquaculture of trout in United States” (USDA Risk Management Agency, 2004).

44. D. G. Hernandez, W. Brown, K. A. Naish, G. Kurath, Virulence and infectivity of UC, MD, and L strains of infectious hematopoietic necrosis virus (IHNV) in four populations of Columbia River Basin chinook salmon. *Viruses* **13** (2021).

45. R. Breyta, A. Jones, G. Kurath, Differential susceptibility in steelhead trout populations to an emergent MD strain of infectious hematopoietic necrosis virus. *Diseases of Aquatic Organisms* **112**, 17–28 (2014).

46. K. Garver, R. Troyer, G. Kurath, Two distinct phylogenetic clades of infectious hematopoietic necrosis virus overlap within the Columbia River basin. *Dis. Aquat. Org.* **55**, 187–203 (2003).

47. D. G. Hernandez, G. Kurath, Shedding Kinetics of Infectious Hematopoietic Necrosis Virus (IHNV) in Juvenile Spring- and Fall-Run Chinook Salmon of the Columbia River Basin. *Animals* **12**, 1887 (2022).

48. D. G. McKenney, G. Kurath, A. R. Wargo, Characterization of infectious dose and lethal dose of two strains of infectious hematopoietic necrosis virus (IHNV). *Virus Research* **214**, 80–89 (2016).

49. C. J. Zeiss, J. L. Asher, B. V. Wyk, H. G. Allore, S. Compton, Viral shedding and transmission after natural infection and vaccination in an animal model of SARS-CoV-2 propagation. [Preprint] (2021). Available at: https://www.biorxiv.org/content/10.1101/2021.05.11.443477v1 [Accessed 7 June 2024].

50. J. W. Edmonds, I. F. Nolan, R. C. H. Shepherd, A. Gocs, Myxomatosis: the virulence of field strains of myxoma virus in a population of wild rabbits (Oryctolagus cuniculus L.) with high resistance to myxomatosis. *J. Hyg., Camb* **74**, 417–421 (2020).

Table 2.2.1. List of IHNV isolates included in the study, with relevant metadata. Data includes: collection location, year in which the isolate was collected, host species from which the sample was collected, genogroup, subgroup, and unique genetic identifier based on midG-gene sequencing.

Label	Isolate Name	Location of Isolation	Year of Isolation	Species of Isolation	Genogroup	Subgroup	midG sequence [Breyta; et al.
1	Wck74	Weaver Creek, B.C.	1974	*O. nerka*	U	UP	mG004U
2	GF77	Glacier Flats, AK	1977	*O. nerka*	U	UP	mG003U
3	Blk94	Baker Lake Hatchery, WA	1994	*O. nerka*	U	UP	mG002U
4	Blk12	Baker Lake Hatchery, WA	2012	*O. nerka*	U	UP	mG050U
5	Blk15	Baker Lake Hatchery, WA	2015	*O. nerka*	U	UP	mG265U
6	HaVT-74	Hagerman Valley, ID	1974	*O. mykiss*	M	MN	mG400M
7	SV76	Sun Valley Trout, B.C.	1976	*O. mykiss*	M	MN	mG401M
8	220-90	Hagerman Valley, ID	1990	*O. mykiss*	M	MB	mG009M
9	Ha20-91	Hagerman Valley, ID	1991	*O. mykiss*	M	MB	mG079M
10	Ha30-91	Hagerman Valley, ID	1991	*O. mykiss*	M	MC	mG119M
11	Ha39-91	Hagerman Valley, ID	1991	*O. mykiss*	M	MD	mG107M
12	Ht508k-14	Hagerman Valley, ID	2014	*O. mykiss*	M	MB	mG296M
13	Ht511-14	Hagerman Valley, ID	2014	*O. mykiss*	M	MD	mG298M
14	HtBrK-16	Hagerman Valley, ID	2016	*O. mykiss*	M	MB	mG331M
15	Ht134-17	Hagerman Valley, ID	2017	*O. mykiss*	M	MC	mG335M

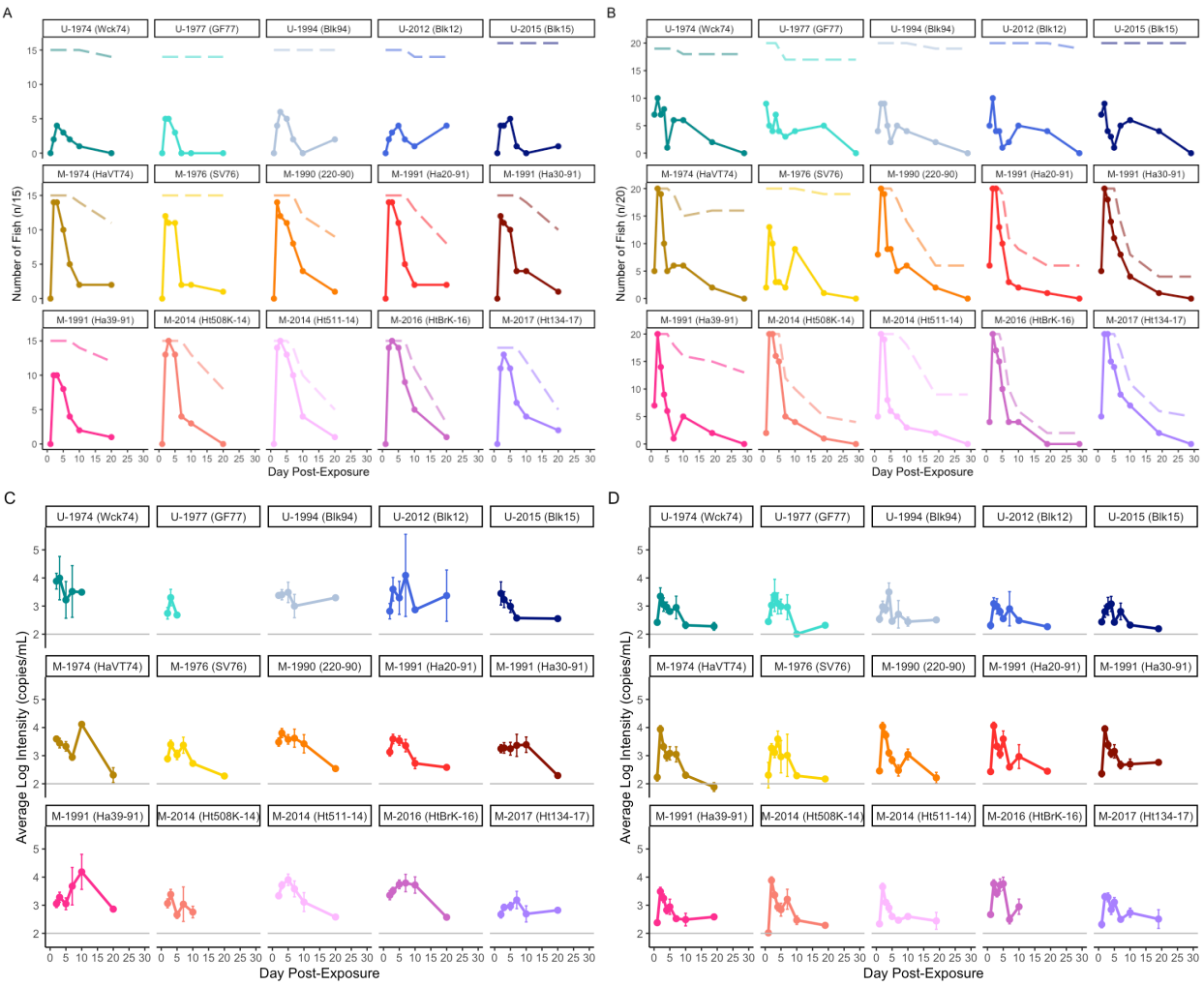

Figure 2.1. Number of fish shedding and surviving post exposure to IHNV (A, B) and mean shedding intensity of IHNV through time (C, D). Solid lines indicate number of living fish shedding IHNV on sampling dates (points). Dashed lines indicate surviving fish through experiment. Panel labels indicate genogroup, collection year, and name of isolate. For experiments 1 (panel A) 15 replicate fish per isolate were held at 10°C, and sampled on days 1-3, 5, 7, and 20. For experiment 2 (panel B) 20 replicate fish per isolate were held at 15°C and sampled on days 1-5, 7, 10, 20, and 29. At each temperature, 5 fish were also included in a Mock treatment (data not shown). Fish continued to be sampled after the time of death, but were not included in the number of fish shedding plots. Survival was checked daily. **For panels C-D,** points indicate mean log quantity (± 1 standard error) of IHNV shedding (viral RNA copies/ml water) for fish exposed to each viral isolate at (C) 10°C and (D) 15°C, on sampling dates. Only live fish positive for virus are included in the mean. Gray lines at y = 2 indicate the minimum threshold of detection for qPCR assays used. Days for which there are no points displayed indicates that no fish shed at detectable levels in the treatment. Panel labels indicate genogroup, collection year, and name of isolate.

Table 2.2. Mortality data by treatment for fish held in individual tanks. For each experimental treatment, the following are listed: Genogroup, Temperature, Viral Isolate, number of replicate fish included at the start of the experiment, number of replicates that died before experiment end, range of days on which fish died, and mean day of death (MDD). No fish died in the following treatments: 10°C Mock, 10°C GF77, 10°C Blk94, 15°C Blk15.

					Range of Death Days		
Genogroup	**Temperature**	**Isolate**	**Replicates**	**Dead**	**First**	**Last**	**MDD**
-	10	Mock	5	0	-	-	-
-	15	Mock	5	1	1	1	1
U	10	WCk74	15	1	11	11	11
U	15	WCk74	19	1	8	8	8
U	10	GF77	14	0	-	-	-
U	15	GF77	20	3	4	6	5.5
U	10	Blk94	15	0	-	-	-
U	15	Blk94	20	1	16	16	16
U	10	Blk12	15	1	8	8	8
U	15	Blk12	20	1	26	26	26
U	10	Blk15	16	2	21	22	21.4
U	15	Blk15	20	0	-	-	-
M	10	HaVT-74	15	4	9	25	15.3
M	15	HaVT-74	20	4	6	8	6.9
M	10	SV76	15	0	22	22	22
M	15	SV76	20	1	15	15	15
M	10	220-90	15	6	8	15	10.7
M	15	220-90	20	14	6	18	12
M	10	Ha20-91	15	7	9	27	14.8
M	15	Ha20-91	20	14	4	16	7.9
M	10	Ha30-91	15	5	7	24	12.5
M	15	Ha30-91	20	16	5	14	8.2
M	10	Ha39-91	15	3	8	23	11.7
M	15	Ha39-91	20	7	6	29	13.6
M	10	Ht508K-14	15	7	8	17	11.7
M	15	Ht508K-14	20	16	5	29	10
M	10	Ht511-14	15	10	6	21	11.3
M	15	Ht511-14	20	11	7	16	12.5
M	10	HtBrK-16	15	12	7	28	12.6
M	15	HtBrK-16	20	18	4	14	7
M	10	Ht134-17	14	9	7	15	10.8
M	15	Ht134-17	20	15	5	19	9.9

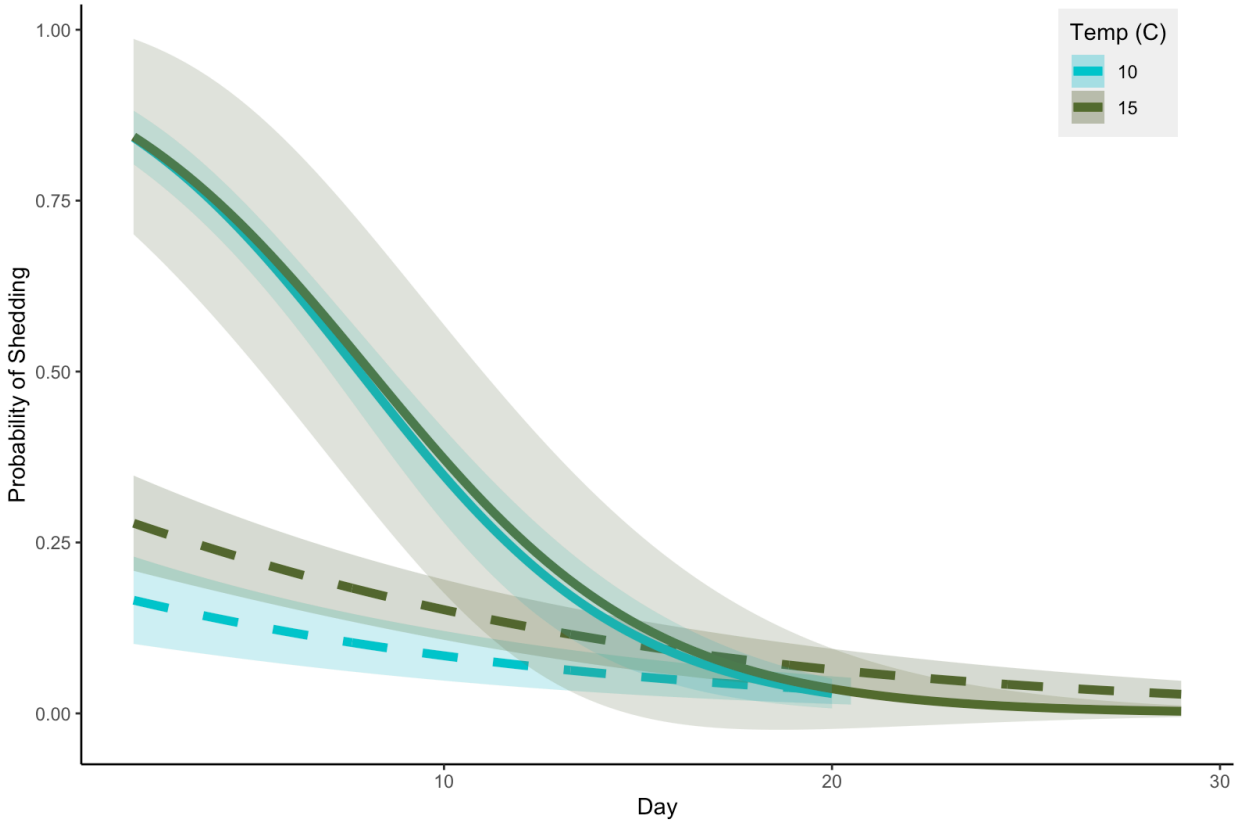

Figure 2.2. Predicted probability of shedding by genogroup and temperature. Lines show predicted probability of individual fish shedding over the sampled course of the experiments, obtained from generalized linear models selected through AICc (Table S1-S4). Since samples were not analyzed past day 20 for the 10°C assay, no predictions are provided beyond the sampled day range. Shading indicates 95% confidence intervals. Genogroups U (dashed lines) and M (solid lines) were analyzed separately. The probability of shedding decreased through the course of the experiment at the same rate for 10°C (blue) 15°C (green). Values are back-transformed from logit values to probability. The M 15°C lines have large confidence intervals because individual isolates differed in their mean probability of shedding and this was dependent on temperature (Figure 2.3), although the rate decrease over the course of the experiments did not differ between isolates or temperatures.

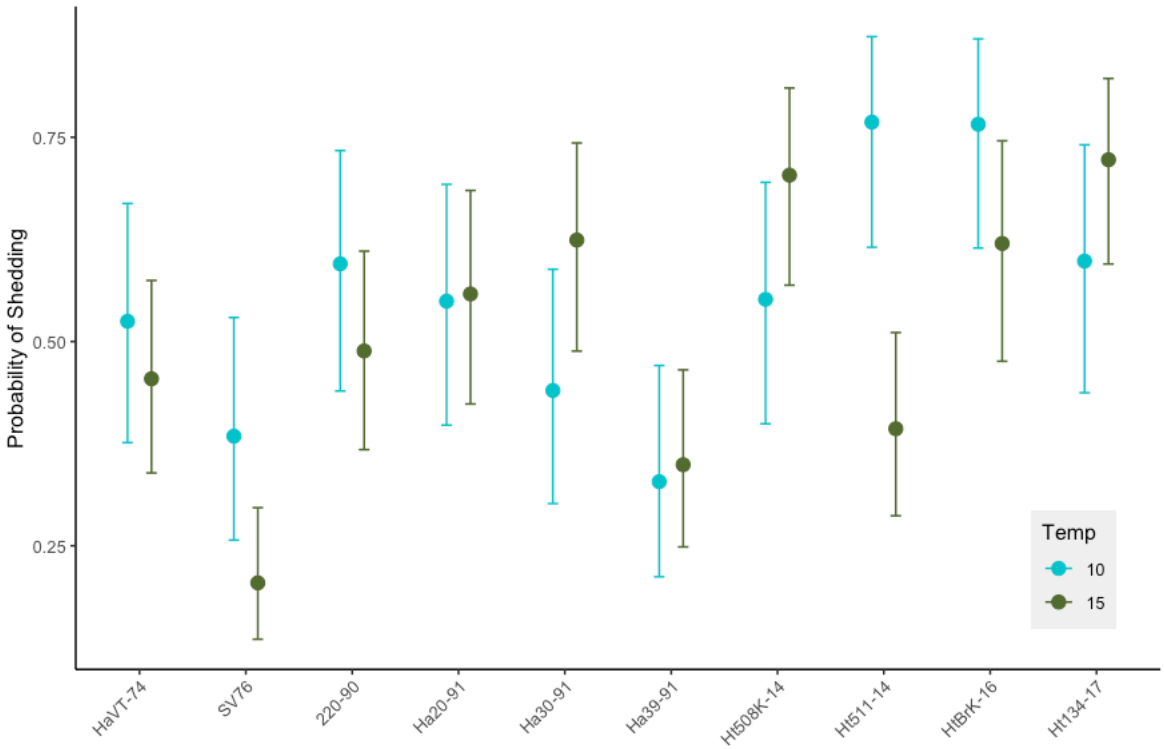

Figure 2.3. Estimated marginal means of probability of shedding by M isolates, averaged over all sampling days of the experiments. Bars indicate 95% confidence intervals. 10°C data is in blue, 15°C data is in dark green. Contrasts which have do not overlapping confidence intervals may be considered significant. See Table S2.4.

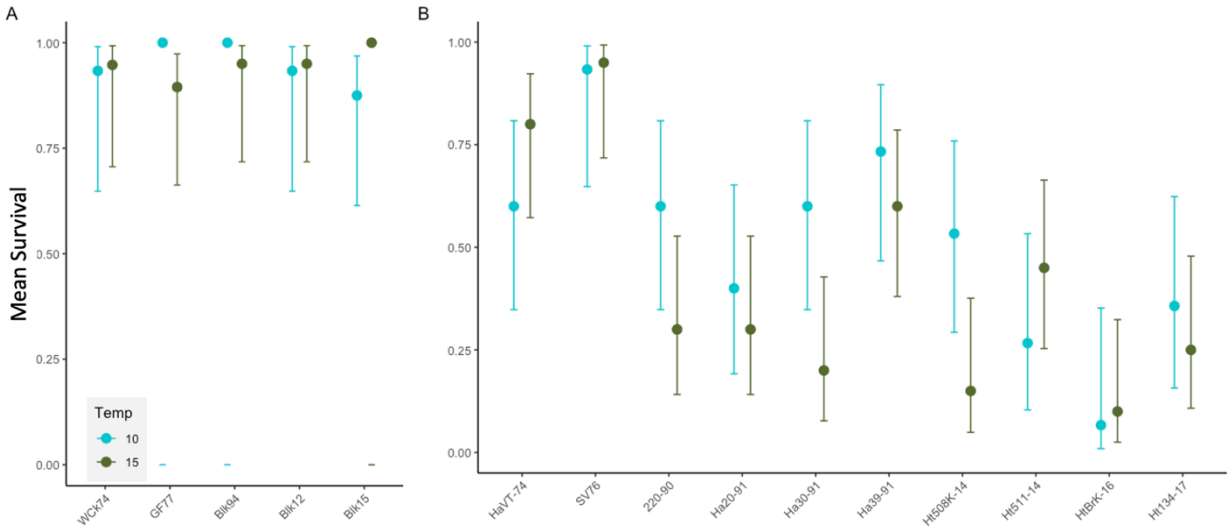

Figure 2.4. Predicted survival. Points show estimated marginal means for survival among U isolates (A) and M isolates (B) at 10°C (blue) or 15°C (green) with 95% confidence intervals (bars), obtained from AICc selected models (Tables S2.5-S2.6). No isolate or temperature levels were significantly different from each other among U isolates. A point without bars indicates that no fish died in the treatment and confidence intervals could not be determined because the error estimate was 0. Select levels of M isolates at different temperatures were significantly different from each other and are indicated by brackets with asterisks. Contrasts which have do not have overlapping confidence intervals may be considered significant.

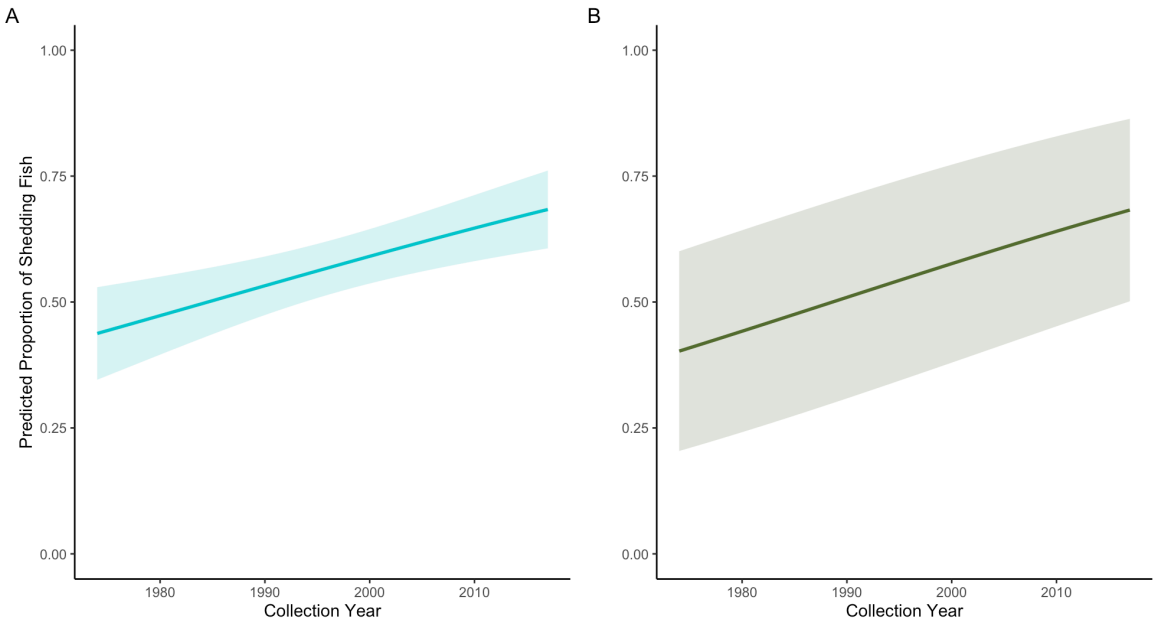

Figure 2.5. The effect of collection year on predicted proportion (frequency) of hosts shedding M isolates at (A) 10°C in blue and (B) 15°C in green, from AICc-selected models (Tables S2.7-S2.8). Shading indicates 95% confidence interval. Temperature data was analyzed separately due to more frequent sampling and subsequently greater quantity of available data in the 15°C experiment. For each model, predictions were made holding Day constant with the mean value of Day for each temperature dataset, respectively.

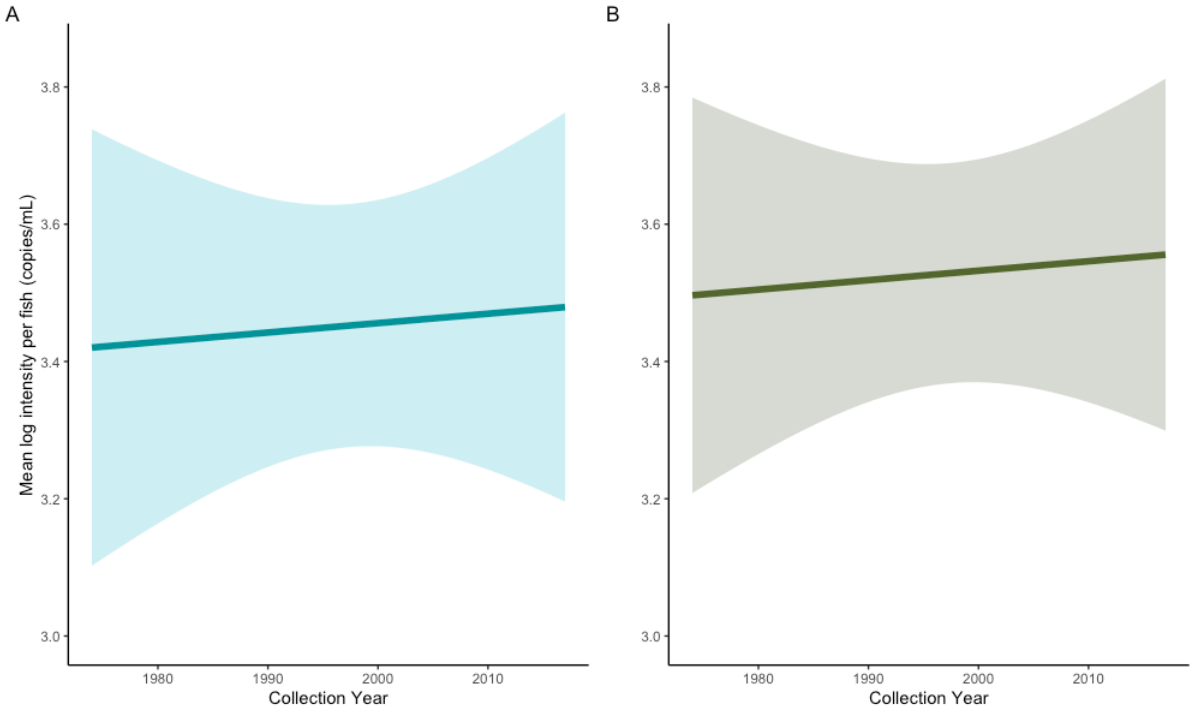

Figure 2.6. The effect of collection year on predicted mean M isolate shedding intensity per fish at (A) 10°C in blue and (B) 15°C in green, from AICc-selected models (Tables S2.9-S2.10). Shading indicates 95% confidence interval. Shedding intensity was estimated to be higher at 15°C than at 10°C, but the increase associated with year was consistent across temperatures. Temperature data was analyzed separately due to more frequent sampling and subsequently greater quantity of available data in the 15°C experiment.

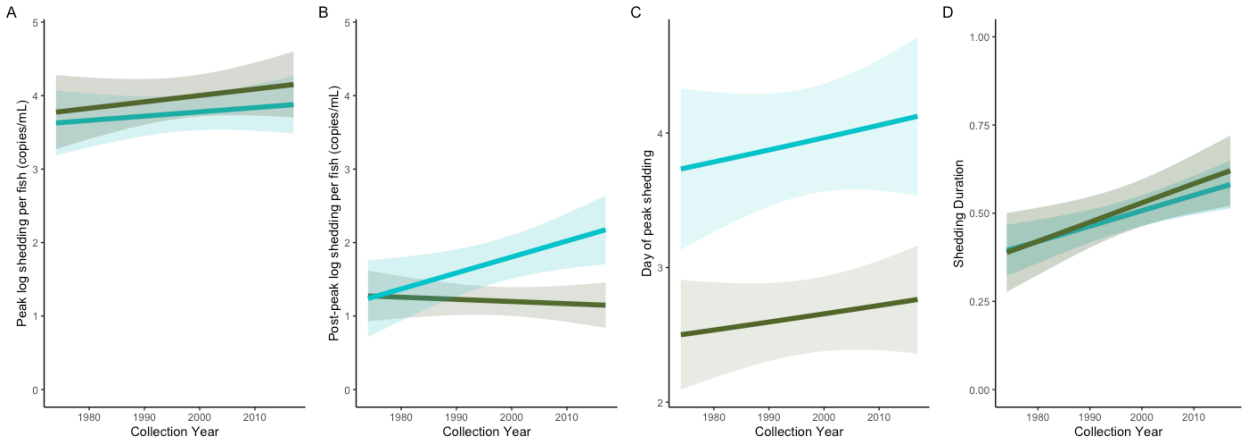

Figure 2.7. Shedding phenotypes of M-genogroup isolates over evolutionary time. Lines show predicted values from AICc selected statistical models (Tables S2.11-S2.17), for shedding parameters as a function of virus isolate collection year. Experiment 1 (10°C- blue line) and 2 (15°C data - green line) were analyzed separately, but compiled in plots for ease of interpretation. Shading indicates 95% confidence interval. (A) Peak period shedding per fish (Tables S2.11-S2.12). (B) Post-peak shedding (Tables S2.13-S2.14). (C) Day of peak intensity (Table S2.15). (D) Predicted proportion of days fish test positive (duration of shedding) (Tables S2.16-S2.17).

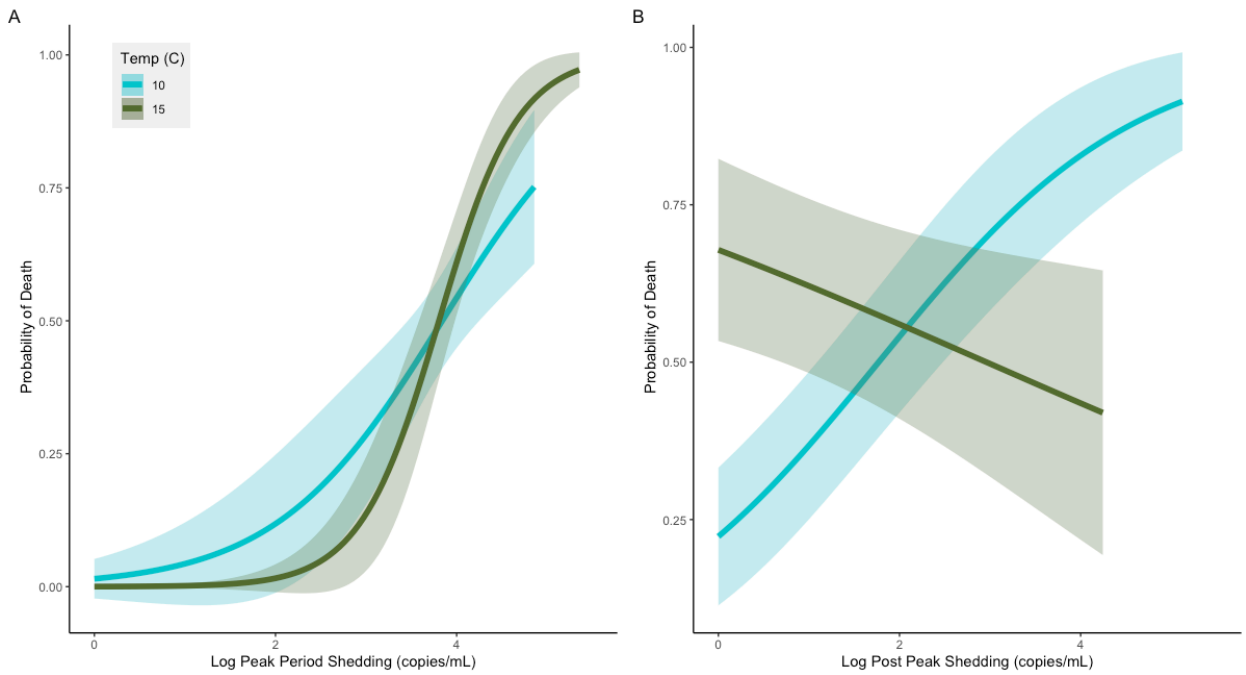

Figure 2.8. Association between predicted probability of death and cumulative shedding for M isolates. Plots show predicted probability of fish death as a function of shedding summed across all days for each individual fish for the peak (days 0-5, panel A) and post-peak (days 7-30, panel B) period, obtained from AICc selected models (Tables S2.18-S2.23). Experiment 1 (10°C- blue line) and 2 (15°C data - green line) were analyzed separately, but compiled in plots for ease of interpretation. These predicted data are averaged across effect of collection year.

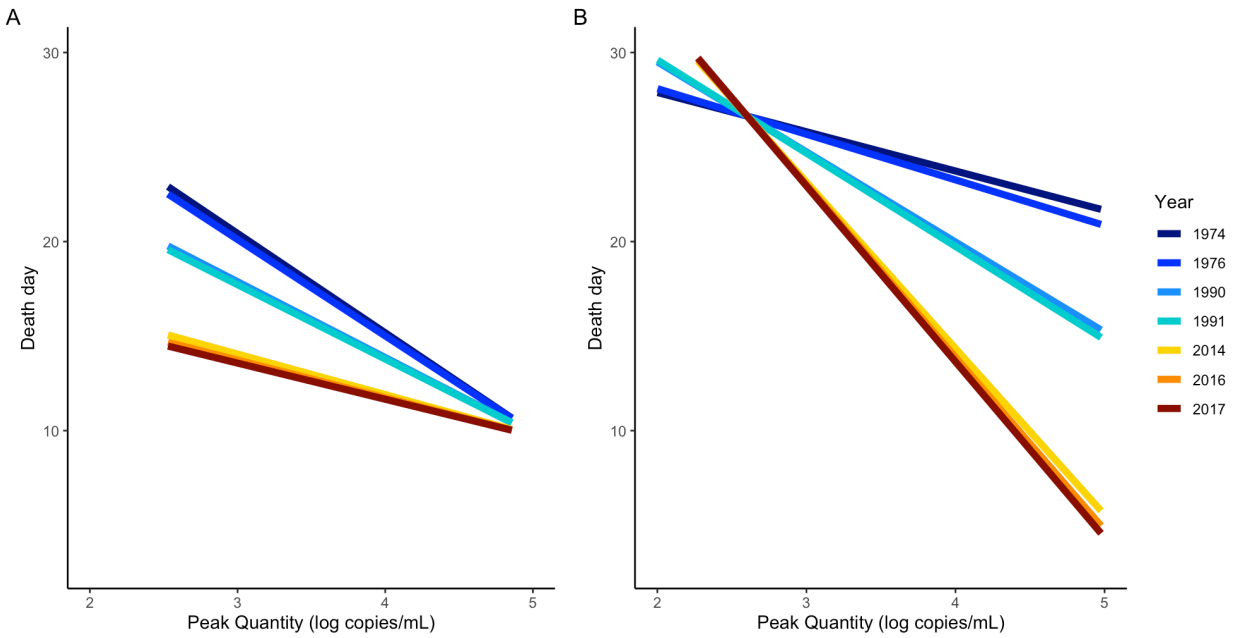

Figure 2.9. Association between day of death and peak period shedding for individual fish exposed to M isolates. Predicted day of death is shown as a function of shedding summed across all days for individual fish during the peak at 10°C (A) and 15°C (B) for different collection years, obtained from AICc selected models (Tables S2.22-S2.25). Predictions were only made across observed ranges of values and days for each experiment respectively.

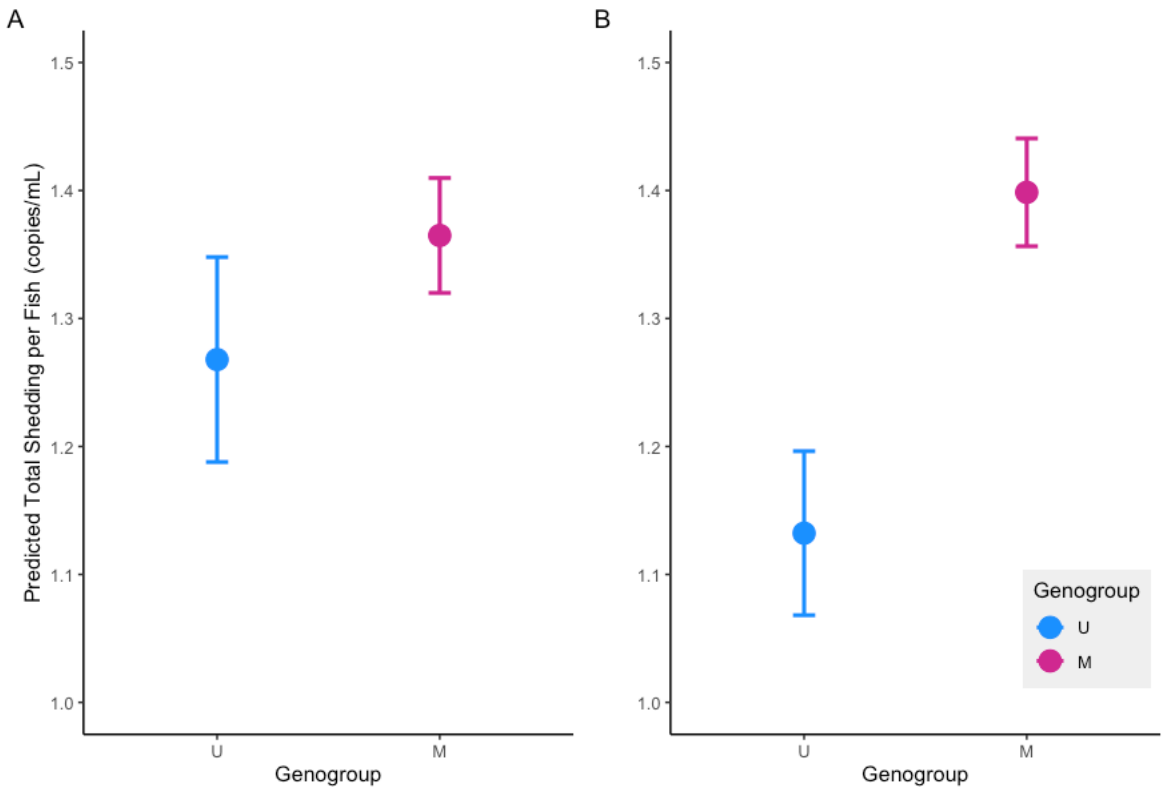

Figure 2.10: Predicted IHNV genogroup differences in shedding phenotypes. Panels show comparisons of M (magenta) and U (blue) genogroup predicted shedding phenotypes with 95% confidence intervals from AICc-selected zero-inflated GLME models (Tables S2.20-S2.21) at (A) 10°C and (B) 15°C, not including random effects (isolate).

Supplemental Materials

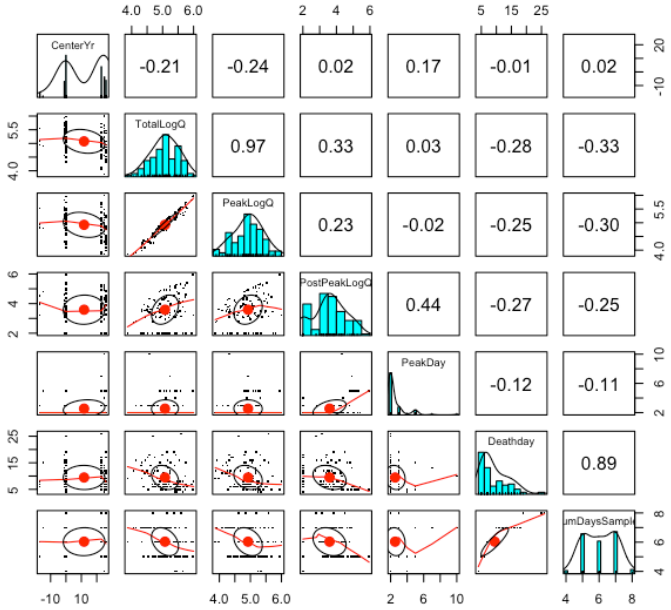

Figure S2.1. Correlation plots generated with pairs.panels() function for M-isolate data at 15°C. Histograms on the diagonal plot the data distributions. Panels below the diagonal are correlation plots where small black dots represent individual fish, red dots are means, and red lines are loess curves. Panels above the lines are Pearson correlation coefficients of the corresponding row and column.

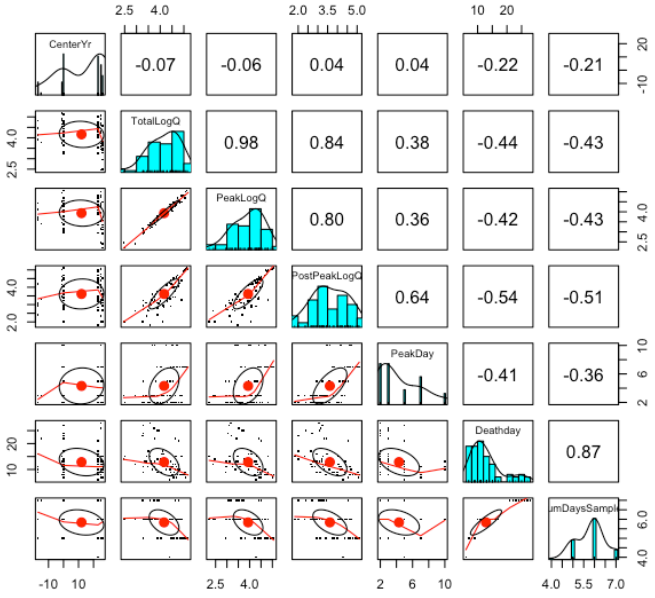

Figure S2.2. Correlation plots generated with pairs.panels() function for M-isolate data at 10°C. Histograms on the diagonal plot the data distributions. Panels below the diagonal are correlation plots where small black dots represent individual fish, red dots are means, and red lines are

loess curves. Panels above the lines are Pearson correlation coefficients of the corresponding row and column.

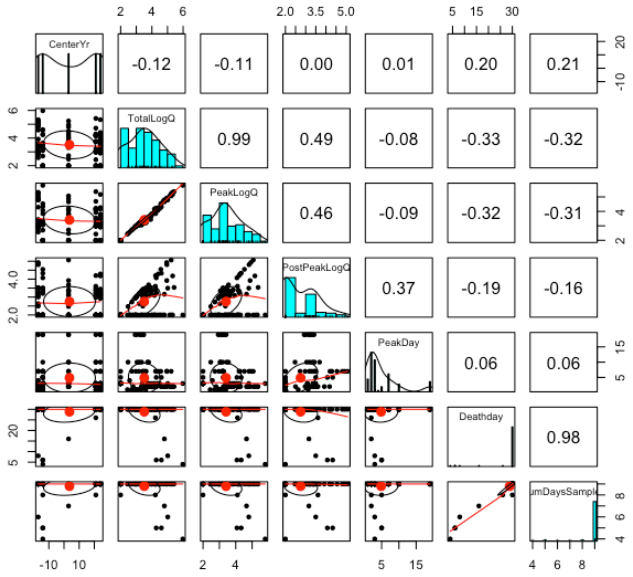

Figure S2.3. Correlation plots generated with pairs.panels() function for U-isolate data at 15°C. Histograms on the diagonal plot the data distributions. Panels below the diagonal are correlation plots where small black dots represent individual fish, red dots are means, and red lines are loess curves. Panels above the lines are Pearson correlation coefficients of the corresponding row and column.

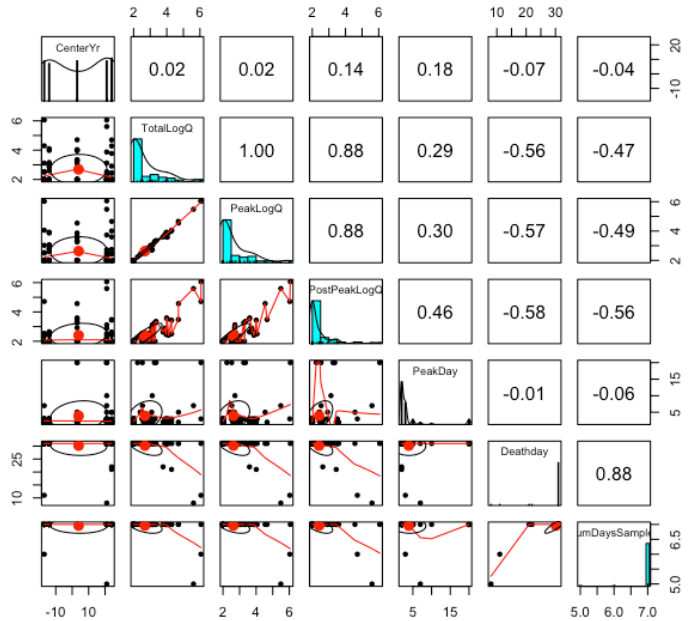

Figure S2.4. Correlation plots generated with pairs.panels() function for U-isolate data at 10°C. Histograms on the diagonal plot the data distributions. Panels below the diagonal are correlation plots where small black dots represent individual fish, red dots are means, and red lines are loess curves. Panels above the lines are Pearson correlation coefficients of the corresponding row and column.

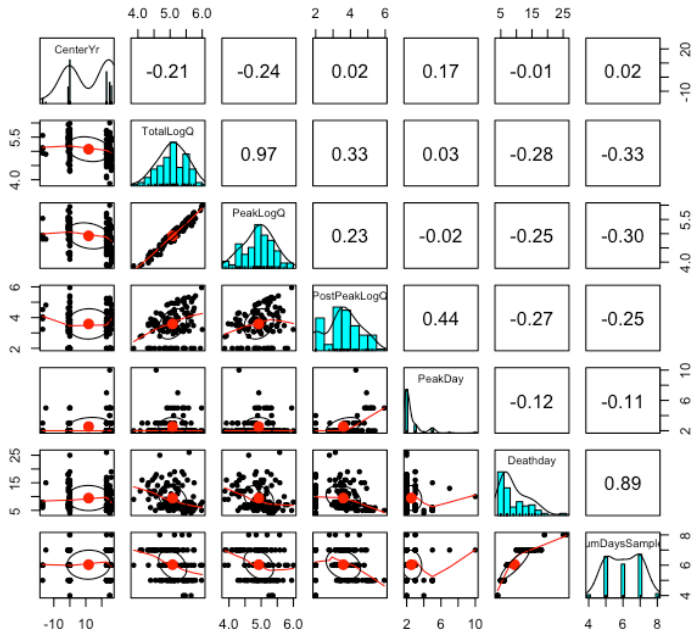

Figure S2.5. Correlation plots generated with pairs.panels() function for subset data: all fish that were exposed to an M-isolate, 15°C, and died during the experiment. Histograms on the diagonal plot the data distributions. Panels below the diagonal are correlation plots where small black dots represent individual fish, red dots are means, and red lines are loess curves. Panels above the lines are Pearson correlation coefficients of the corresponding row and column.

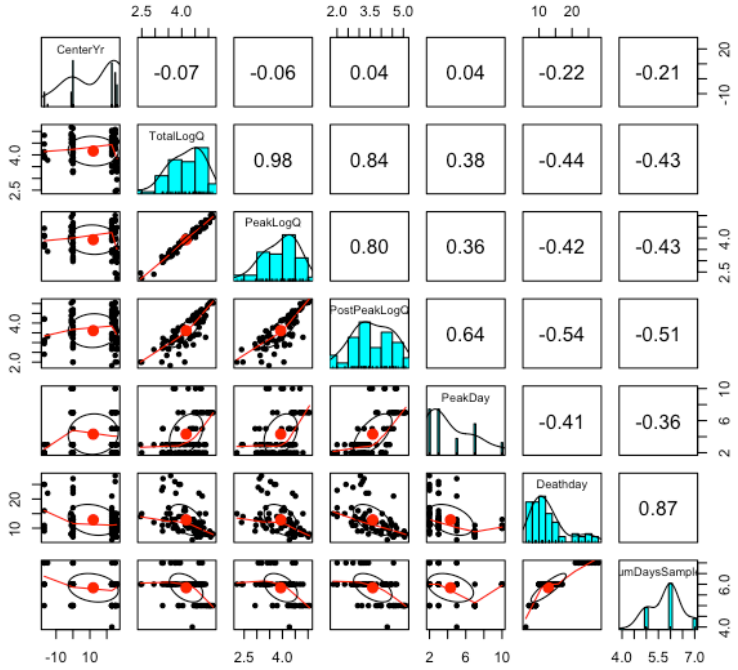

Figure S2.6. Correlation plots generated with pairs.panels() function for subset data: all fish that were exposed to an M-isolate, 10°C, and died during the experiment. Histograms on the diagonal plot the data distributions. Panels below the diagonal are correlation plots where small black dots represent individual fish, red dots are means, and red lines are loess curves. Panels above the lines are Pearson correlation coefficients of the corresponding row and column.

Table S2.1. GLME model selection table for probability of shedding among U isolates. A '+' symbol indicates the predictor was included in the model. Model 1 is the best fit model.

Model	Intercept	Day	Temp	Virus	Day: Temp	Day: Virus	Temp: Virus	Day: Temp: Virus	Df	AICc	ΔAICc	AICc weight
1	-1.421	-0.096	+						4	1110.2	0	0.513
2	-1.287	-0.120	+		+				5	1111.5	1.32	0.265

Table S2.2. GLME model selection table for probability of shedding among M isolates. A '+' symbol indicates the predictor was included in the model. Model 1 is the best fit model.

Model	Intercept	Day	Temp	Virus	Day: Temp	Day: Virus	Temp: Virus	Day: Temp: Virus	Df	AICc	ΔAICc	AICc weight
1	2.448	-0.286	+	+			+		22	2130.2	0	0.570
2	2.534	-0.304	+	+	+		+		23	2131.4	1.21	0.312

Table S2.3. Summary of AICc selected GLME with binomial distribution for estimating probability of shedding of U isolates in rainbow trout over all experiment days.
Estimates and associated error are on logit scale. Residual degrees of freedom = 1214. Model structure is given at the bottom of the table.

Fixed effect	Estimate	Standard error	Z-value	Degrees of freedom
Intercept	-1.42068	0.24269	-5.854	
Day	-0.09625	0.01444	-6.664	8
Temperature	0.66630	0.26876	2.479	1
Shedding Status ~ Day + Temp + (1|Fish)				

Table S2.4. **Summary of AICc selected selected GLME with binomial distribution for estimating probability of shedding M isolates in rainbow trout over all experiment days.** Estimates and associated error are on logit scale. Residual degrees of freedom = 2043. Note on terminology in model output: Virus and Isolate are used interchangeably.

Fixed effect	Estimate	Standard error	Z-value
Intercept	2.17319698	0.32408105	6.70572051
Day	-0.2862849	0.01832318	-15.624191
Temp15	-0.3306261	0.38973329	-0.8483394
Virus220-90	0.28311597	0.43816055	0.64614664
VirusHa20-91	0.09900631	0.43249269	0.22892019
VirusHa30-91	-0.3326851	0.42652475	-0.7799902
VirusHa39-91	-0.7990363	0.42548283	-1.877952
VirusHt134-17	0.29791098	0.44658974	0.66707976
VirusHt508K-14	0.10873809	0.43329894	0.25095396
VirusHt511-14	1.08647337	0.4767472	2.27892975
VirusHtBrK-16	1.07441238	0.47318757	2.27058452
VirusSV76	-0.5624268	0.42330557	-1.3286545
Temp15:Virus220-90	-0.1491289	0.55993069	-0.2663346
Temp15:VirusHa20-91	0.31108872	0.56619769	0.54943481
Temp15:VirusHa30-91	1.01838904	0.56513897	1.80201527
Temp15:VirusHa39-91	0.35396235	0.54649387	0.64769683
Temp15:VirusHt134-17	0.84833931	0.58590569	1.44791103
Temp15:VirusHt508K-14	0.94001747	0.57930287	1.62267014
Temp15:VirusHt511-14	-1.3399863	0.58705537	-2.2825552
Temp15:VirusHtBrK-16	-0.4130864	0.60627502	-0.6813515
Temp15:VirusSV76	-0.6221811	0.5463745	-1.1387447
Status ~ Day + Temp + Virus + Temp*Virus + (1|Fish)			

Table S2.5. Summary of GLM with binomial distribution for estimating probability of mortality across experimental days for fish exposed to U isolates. The reference level for isolate is the earliest collected isolate, Wck74. Residual degrees of freedom = 9.

Fixed effect	Estimate	SE	Z-value
(Intercept)	2.63905733	1.03509834	2.5495716
Temp15	0.25131443	1.45841836	0.17231985
VirusBlk12	1.34E-15	1.46385011	9.14E-16
VirusBlk15	-0.6931472	1.28173989	-0.5407862
VirusBlk94	23.8452758	88268.7529	2.70E-04
VirusGF77	23.7820027	88521.5539	2.69E-04
Temp15:VirusBlk12	0.05406722	2.06180607	0.02622323
Temp15:VirusBlk15	24.5545462	87379.7873	2.81E-04
Temp15:VirusBlk94	-23.791209	88268.7529	-2.70E-04
Temp15:VirusGF77	-24.532308	88521.5539	-2.77E-04

Table S2.6. Summary of GLM with binomial distribution for estimating probability of mortality across experimental days for fish exposed to M isolates. The reference level for isolate is the earliest collected isolate, HaVT-74. Residual degrees of freedom = 19.

Fixed effect	Estimate	SE	z-value
(Intercept)	0.40546511	0.52704628	0.76931595
Temp15	0.98082925	0.76829537	1.27663043
Virus220-90	2.34E-16	0.74535599	3.13E-16
VirusHa20-91	-0.8109302	0.74535599	-1.0879771
VirusHa30-91	-1.11E-15	0.74535599	-1.48E-15
VirusHa39-91	0.6061358	0.78656651	0.77060973
VirusHt134-17	-0.9932518	0.76739096	-1.294323
VirusHt508K-14	-0.2719337	0.73867105	-0.3681391
VirusHt511-14	-1.417066	0.78656651	-1.8015845
VirusHtBrK-16	-3.0445224	1.1615532	-2.6210788
VirusSV76	2.23359222	1.1615532	1.92293579
Temp15:Virus220-90	-2.2335922	1.05173704	-2.1237174
Temp15:VirusHa20-91	-1.422662	1.05173704	-1.3526784
Temp15:VirusHa30-91	-2.7725887	1.08653373	-2.5517742
Temp15:VirusHa39-91	-1.5869651	1.06748312	-1.4866418
Temp15:VirusHt134-17	-1.4916549	1.08076619	-1.3801828
Temp15:VirusHt508K-14	-2.8489617	1.11816447	-2.5478915
Temp15:VirusHt511-14	-0.169899	1.06452199	-0.1596012
Temp15:VirusHtBrK-16	-0.5389965	1.48904714	-0.3619741
Temp15:VirusSV76	-0.6754476	1.64752438	-0.4099773

See Appendix A for individual fish shedding kinetics for all treatments.

Table S2.7. Summary of AICc selected LME for estimating proportion of fish shedding M isolates in rainbow trout at 10°C as a function of isolation year. Residual degrees of freedom = 1250. Model structure is given at the bottom of the table.

Fixed effect	Estimate	Standard error	z-value	
Intercept	2.4222	0.649	3.731	
Collection Year	0.0456	0.0092	4.952	
Day	-0.2863	0.0638	-4.487	
Year * Day	-0.0025	0.0012	-2.145	
Status ~ Year * Day + (1 | Day/Fish)				

Table S2.8. Summary of AICc selected LME for estimating proportion of fish shedding M isolates in rainbow trout at 15°C as a function of isolation year. Residual degrees of freedom = 805. Model structure is given at the bottom of the table.

Fixed effect	Estimate	Standard error	z-value	
Intercept	2.3354	0.1947	11.94	
Collection Year	0.0238	0.0070	3.416	
Day	-0.2882	0.0267	-10.77	
Status ~ CenteredYr + Day + (1 | Day/Fish)				

Table S2.9. LME model summary for estimating mean shedding intensity of M isolates in rainbow trout at 10°C as a function of isolation year. The degrees of freedom for residuals was 146, calculated as the number of observations minus the number of estimated parameters. Model structure is given at the bottom of the table.

Fixed effect	Estimate	Standard error	t-value	Degrees of freedom
Intercept	3.45591	0.09154	37.752	7.93
Collection Year	0.001377	0.00576	0.238	7.96
Log_{10}(intensity) ~ Year + (1|Virus)				

Table S2.10. LME model summary for estimating mean shedding intensity of M isolates in rainbow trout at 15°C as a function of isolation year. The degrees of freedom for residuals was 146, calculated as the number of observations minus the number of estimated parameters. Model structure is given at the bottom of the table.

Fixed effect	Estimate	Standard error	t-value	Degrees of freedom
Intercept	3.532281	0.082908	42.605	7.96
Collection Year	0.001377	0.005214	0.264	7.98
Log_{10}(intensity) ~ Year + (1|Virus)				

Table S2.11. LME model summary for estimating peak shedding quantity of M isolates in rainbow trout as a function of isolation year at 10°C. Residual degrees of freedom =147. Model structure is given at the bottom of the table.

Fixed effect	Estimate	Standard error	t-value	Degrees of freedom
Intercept	3.778713	0.126625	29.842	7.977295
Collection Year	0.005794	0.007958	0.728	7.980072
Log_{10}(sum peak shedding) ~ Year + (1|Virus)				

Table S2.12. LME model summary for estimating peak shedding quantity of M isolates in rainbow trout as a function of isolation year at 15°C. Residual degrees of freedom = 198. Model structure is given at the bottom of the table.

Fixed effect	Estimate	Standard error	t-value	Degrees of freedom
Intercept	4.002219	0.145312	27.542	8.0000
Collection Year	0.008722	0.009132	0.955	8.0000
Log_{10}(sum peak shedding) ~ Year + (1|Virus)				

Table S2.13. LME model summary for post-peak shedding of M isolates through day 29 following exposure in rainbow trout held at 15°C, as a function of isolation year. The degrees of freedom for residuals was 198. Model structure is given at the bottom of the table.

Fixed effect	Estimate	Standard error	t-value	Degrees of freedom
Intercept	1.198051	0.099776	12.007	
Collection Year	-0.002934	0.006270	-0.468	6
Log_{10}(postpeak sum) ~ Year + (1|Virus)				

Table S2.14. LME model summary for post-peak shedding of M isolates through day 20 following exposure in rainbow trout held at 10°C, as a function of isolation year. The degrees of freedom for residuals was 147. Model structure is given at the bottom of the table.

Fixed effect	Estimate	Standard error	t-value	Degrees of freedom
Intercept	1.80428	0.15078	11.966	
Collection Year	0.02177	0.00948	2.297	6
Log_{10}(postpeak sum) ~ Year + (1|Virus)				

Table S2.15. Summary of GLME model with Poisson distribution for timing of peak shedding as a function of isolation year following exposure of rainbow trout to M isolates. The degrees of freedom for residuals was 347. Model structure is given at the bottom of the table.

Fixed effect	Estimate	Standard error	t-value	Degrees of freedom
Intercept	1.3738	0.04977	27.603	
Collection Year	0.002705	0.00257	1.053	6
Temperature	-0.39868	0.05992	-6.653	1
Peak day ~ Year + Temperature + (1|Virus)				

Table S2.16. GLME model selection table for proportion of sample days fish shed M isolates. A '+' symbol indicates the predictor was included in the model. Model 1 is the best fit model.

Model	Intercept	Year	Temp	Year: Temp	Df	AICc	ΔAICc	AICc weight
1	0.07434	0.02011			3	1258.3	0	0.551
2	0.03369	0.02014	+		4	1259.7	1.41	0.272

Table S2.17. Summary of GLME model with binomial distribution for proportion of sampling days fish tested positive for M isolate shedding. Residual degrees of freedom = 1. Model structure is given at the bottom of the table.

Fixed effect	Estimate	Standard error	t-value	Degrees of freedom
Intercept	0.074336	0.092113	0.807	
Collection Year	0.020107	0.005777	3.481	6
cbind(Positive days, Negative days) ~ Year + (1|Virus)				

Table S2.18. GLME model output for association of probability of death at 10°C and peak shedding among M isolates. Binomial error structure. Residual degrees of freedom = 145. Model structure is given at the bottom of the table.

Fixed effect	Estimate	Standard error	t-value	Degrees of freedom
Intercept	-4.05805	1.28748	-3.152	
Peak shedding	1.09151	0.33534	3.255	
Collection Year	0.04920	0.01215	4.049	6

Mortality Status ~ Peak Shedding + Year + (1|Virus)

Table S2.19. GLME model output for association of probability of death at 10°C and postpeak shedding among M isolates. Binomial error structure. Residual degrees of freedom = 145. Model structure is given at the bottom of the table.

Fixed effect	Estimate	Standard error	t-value	Degrees of freedom
Intercept	-1.10577	0.31822	-3.475	
Postpeak shedding	0.70516	0.12785	5.515	
Collection Year	0.05191	0.01648	3.149	6
Mortality Status ~ Postpeak Shedding + Year + (1|Virus)				

Table S2.20. GLME model selection table for probability of death at 15°C among M isolates predicted by peak shedding. Lack of value indicates the predictor was not included in the model. Model 1 is the best fit model.

Model	Intercept	Year	Peak shedding	Year* Peak	df	AICc	ΔAICc	AICc weight
1	- 8.5170	0.07362	2.288		4	191.0	0.00	0.578
2	- 9.0970	-0.06118	2.460	0.034	5	191.6	0.63	0.421

Table S2.21. GLME model output for association of probability of death at 15°C and peak shedding among M isolates. Residual degrees of freedom = 193. Model structure is given at the bottom of the table.

Fixed effect	Estimate	Standard error	t-value	Degrees of freedom
Intercept	-8.51738	1.67417	-5.088	
Peak shedding	2.28829	0.42051	5.442	
Collection Year	0.07362	0.01525	4.828	
Mortality Status ~ Peak shedding + Year + (1|Virus)				

Table S2.22. GLME model selection table for probability of death at 15°C among M isolates predicted by postpeak shedding. Lack of value indicates the predictor was not included in the model. Model 1 is the best fit model.

Model	Intercept	Year	Postpeak shedding	Year*Post peak	df	AICc	ΔAICc	AICc weight
1	0.9287	0.06673	-0.2521		4	226.6	0.00	0.533
2	0.9693	0.07528	-0.2702	-0.006169	5	228.2	1.58	0.242

Table S2.23. GLME model output for association of probability of death at 15°C and postpeak shedding among M isolates. Residual degrees of freedom = 193. Model structure is given at the bottom of the table.

Fixed effect	**Estimate**	**Standard error**	**t-value**	**Degrees of freedom**
Intercept	0.92870	0.34431	2.697	
Postpeak shedding	-0.25213	0.12442	-2.026	
Collection Year	0.06673	0.01966	3.394	
Mortality Status ~ Post peak shedding + Year + (1|Virus)				

Table S2.24. AICc-selected linear model output for day of death as a function of peak shedding parameterized with 10°C data. Model structure is given at the bottom of the table.

Fixed effect	**Estimate**	**Standard error**	**t-value**	**Degrees of freedom**
Intercept	29.26994	3.17963	9.205	180.48
Peak Quantity	-4.32806	0.75185	-5.757	185.42
Year	-0.52490	0.22599	-2.323	178.96
Peak Quantity * Year	0.11288	0.05381	2.098	183.62
Deathday ~ Peak Quantity* Year + (1|Virus)				

Table S2.25. AICc-selected linear model output for day of death as a function of peak shedding parameterized with 15°C data. Model structure is given at the bottom of the table.

Fixed effect	Estimate	Standard error	t-value	Degrees of freedom
Intercept	25.98635	4.68129	5.551	61.17371
Peak Quantity	-3.23421	1.16474	-2.777	61.66993
Year	-0.39279	0.32519	-1.208	56.48419
Peak Quantity * Year	0.07776	0.08101	0.960	56.92368
Deathday ~ Peak Quantity* Year + (1|Virus)				

Table S2.26. Zero-inflated GLME with tweedie distribution comparing total shedding quantity between IHNV-U and IHNV-M in juvenile rainbow trout held at 10°C. The residual degrees of freedom = 218. Model structure is given at the bottom of the table.

Fixed effect	Estimate	Standard error	z-value	Degrees of freedom
Intercept	1.26790	0.04085	31.040	
Genogroup	0.09696	0.04681	2.071	1
Total Shedding per Fish ~ Genogroup + (1|Virus)				

Table S2.27. Zero-inflated GLME with tweedie distribution comparing total shedding quantity between IHNV-U and IHNV-M in juvenile rainbow trout held at 15°C. The residual degrees of freedom = 293. Model structure is given at the bottom of the table.

Fixed effect	Estimate	Standard error	z-value	Degrees of freedom
Intercept	1.13223	0.03270	34.63	
Genogroup	0.26634	0.03912	6.81	1
Total Shedding per Fish ~ Genogroup + (1|Virus)				

Appendix A. Individual fish shedding kinetics.

This appendix includes multi-panel plots depicting the shedding kinetics for individual fish exposed to IHNV isolates at 10°C and 15°C including post-mortem shedding. Isolate panels are color coded for ease of comparing to summary panels in main text Figure 1. Gray horizontal lines indicate detection threshold. Black vertical lines indicate the day of death for individual fish. Panels without vertical lines indicate fish did not die during the experiment. Panel labels denote unique fish identifiers within each experiment. For isolate information refer to main text Table 1.

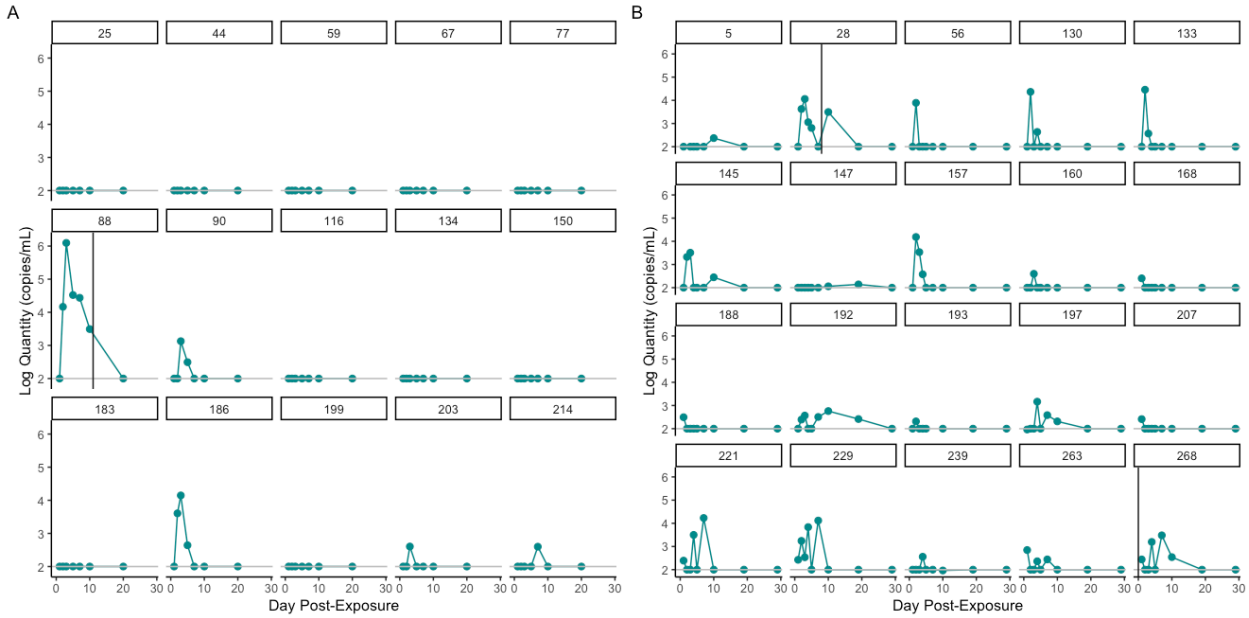

Figure A1. Shedding kinetics of IHNV isolate Wck74 at (A) 10°C and (B) 15°C.

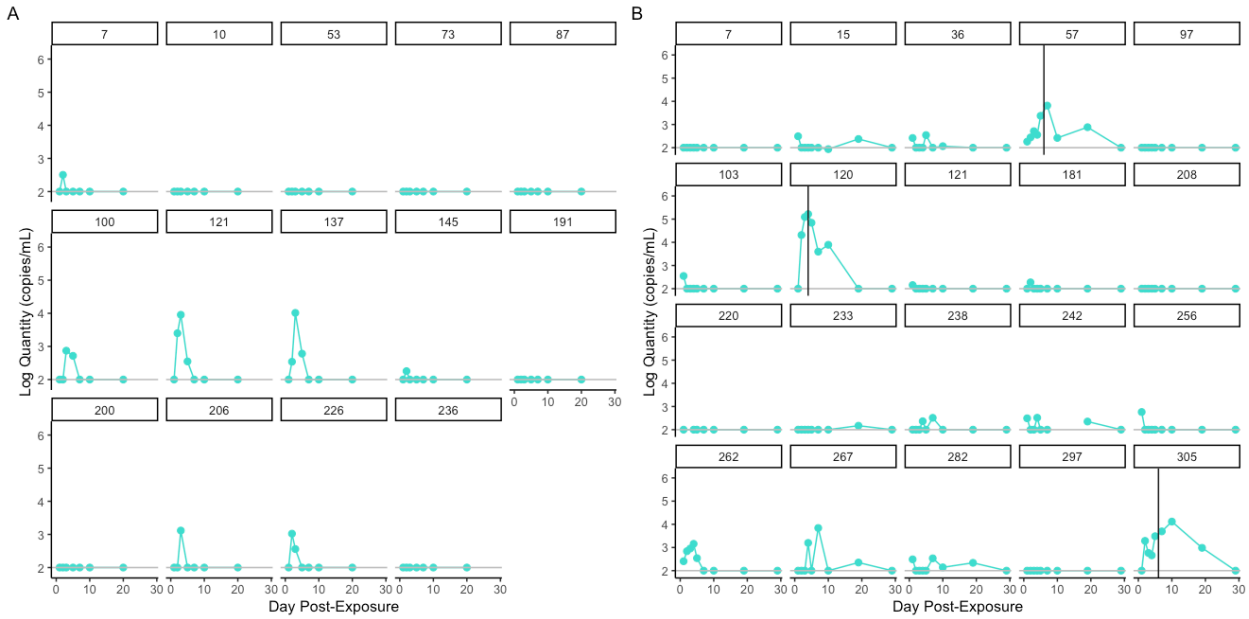

Figure A2. Shedding kinetics of IHNV isolate GF77 at (A) 10°C and (B) 15°C.

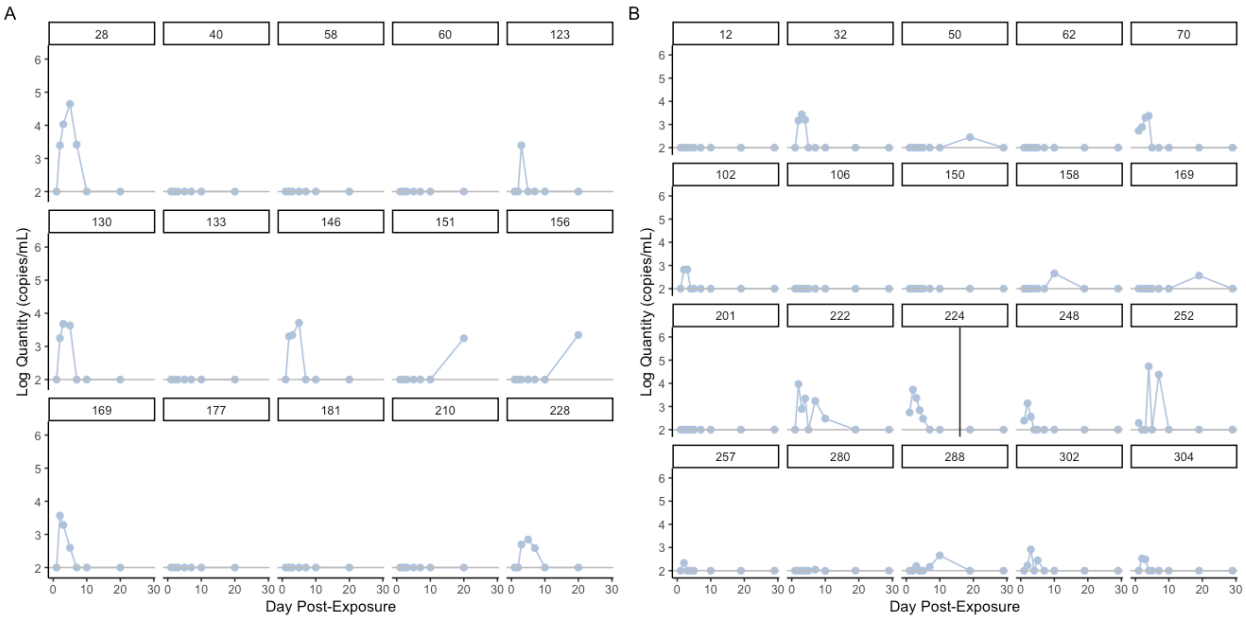

Figure A3. Shedding kinetics of IHNV isolate Blk94 at (A) 10°C and (B) 15°C.

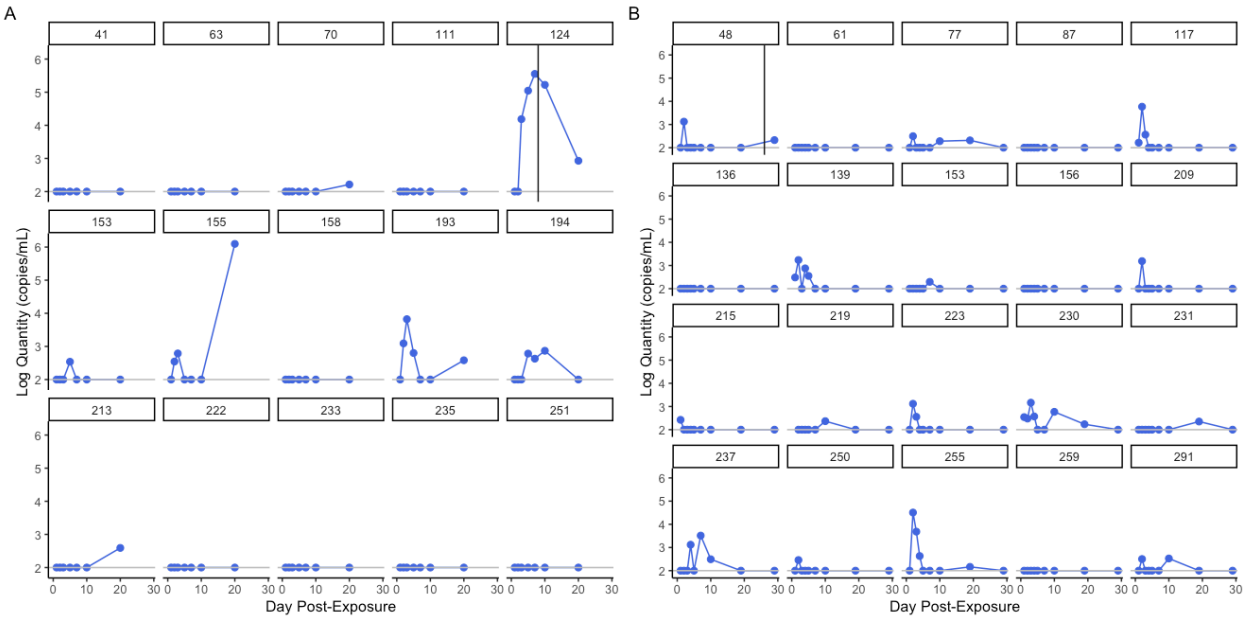

Figure A4. Shedding kinetics of IHNV isolate Blk12 at (A) 10°C and (B) 15°C.

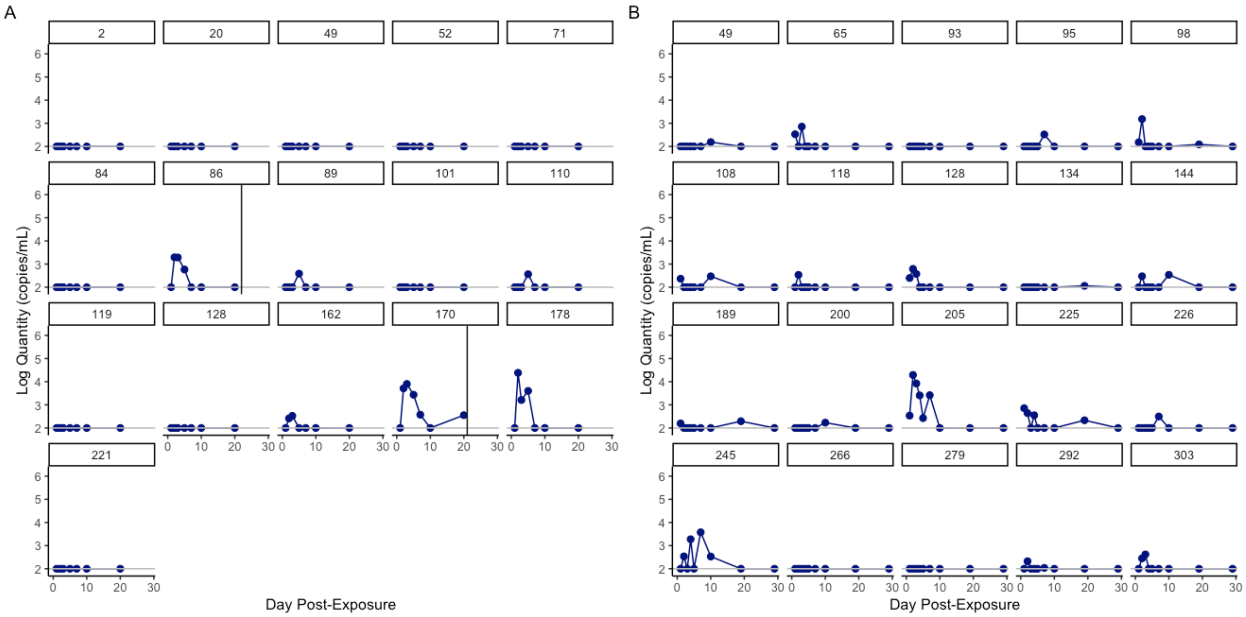

Figure A5. Shedding kinetics of IHNV isolate Blk15 at (A) 10°C and (B) 15°C.

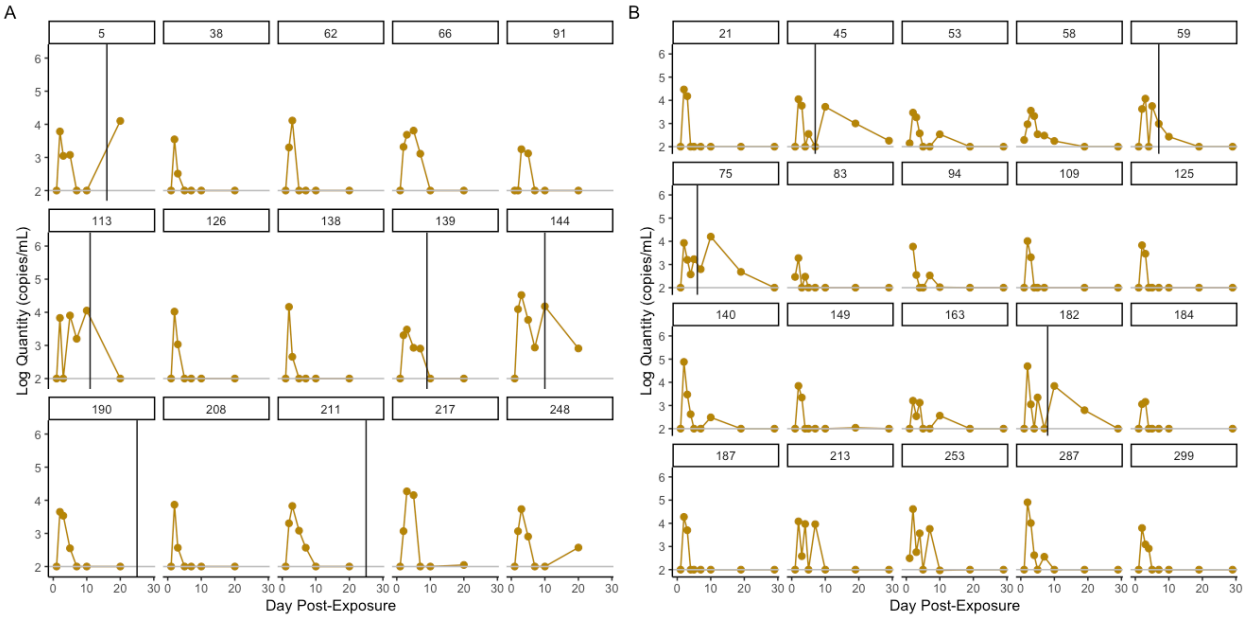

Figure A6. Shedding kinetics of IHNV isolate HaVT74 at (A) 10°C and (B) 15°C.

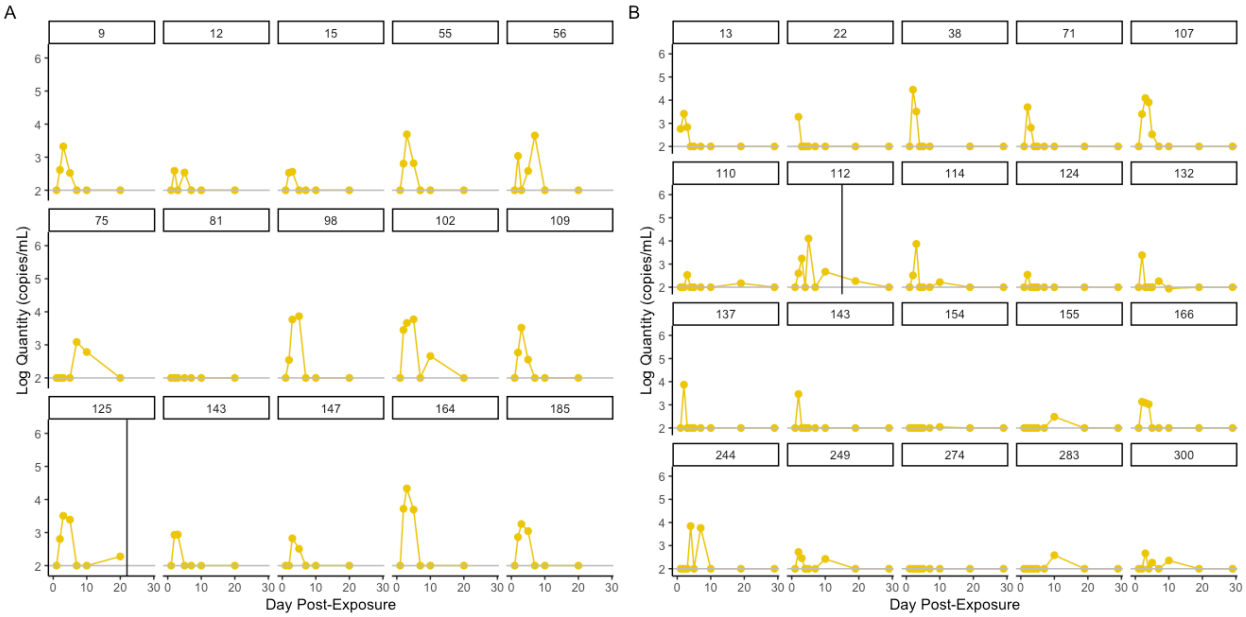

Figure A7. Shedding kinetics of IHNV isolate SV76 at (A) 10°C and (B) 15°C.

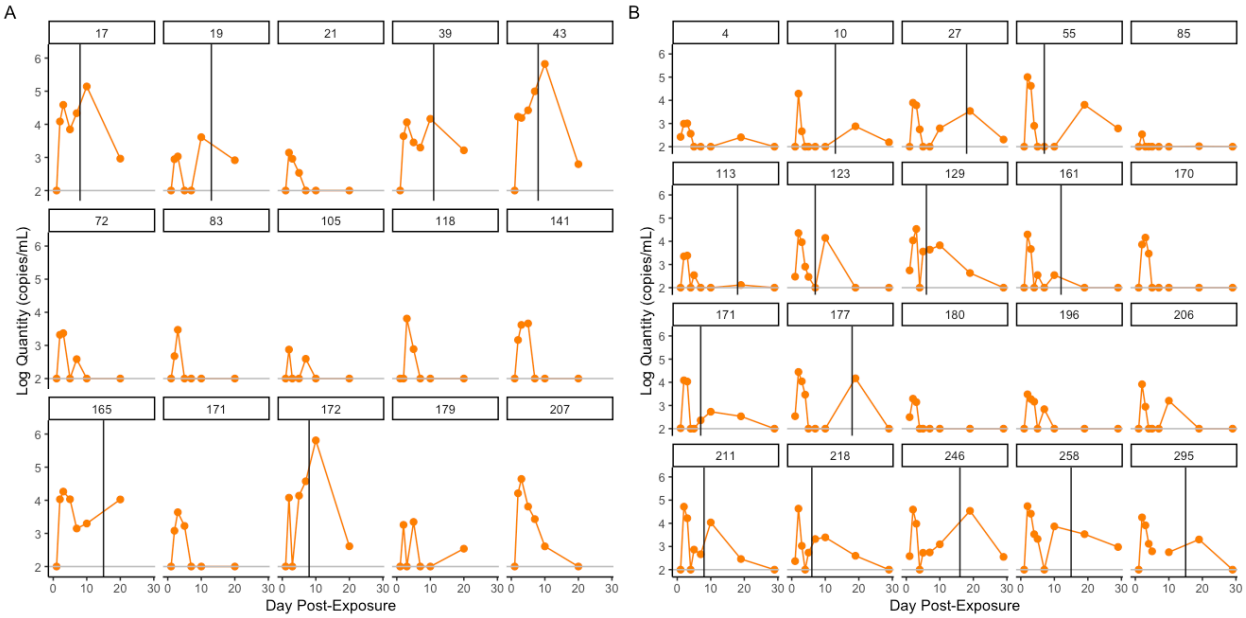

Figure A8. Shedding kinetics of IHNV isolate 220-90 at (A) 10°C and (B) 15°C.

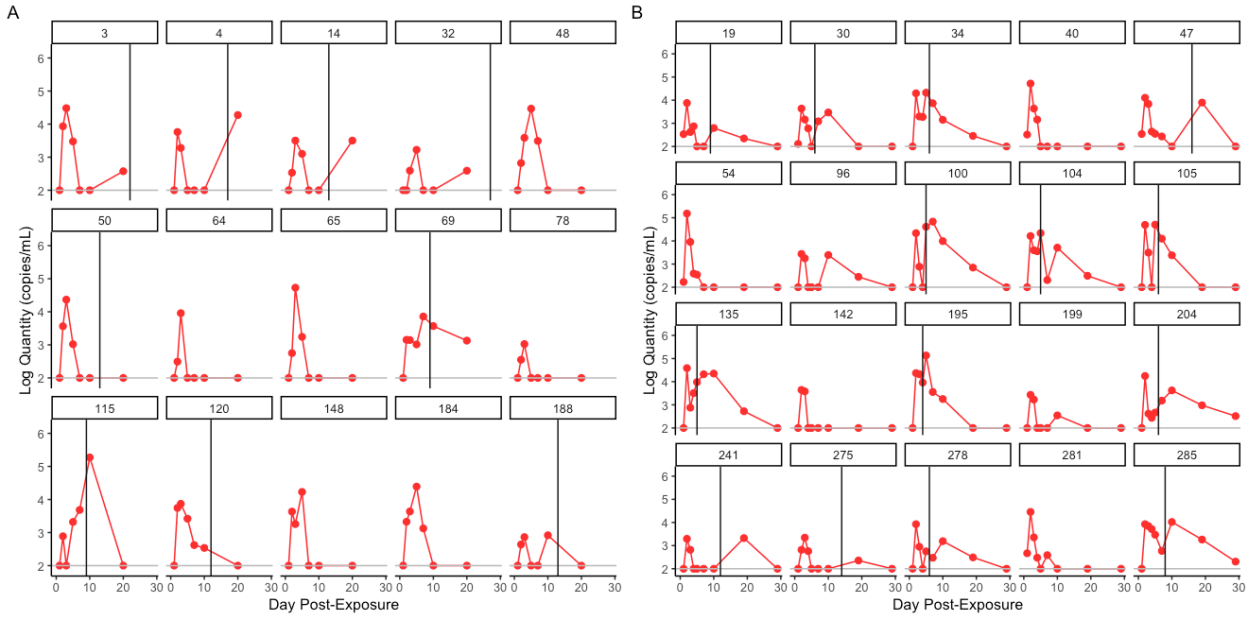

Figure A9. Shedding kinetics of IHNV isolate Ha20-91 at (A) 10°C and (B) 15°C.

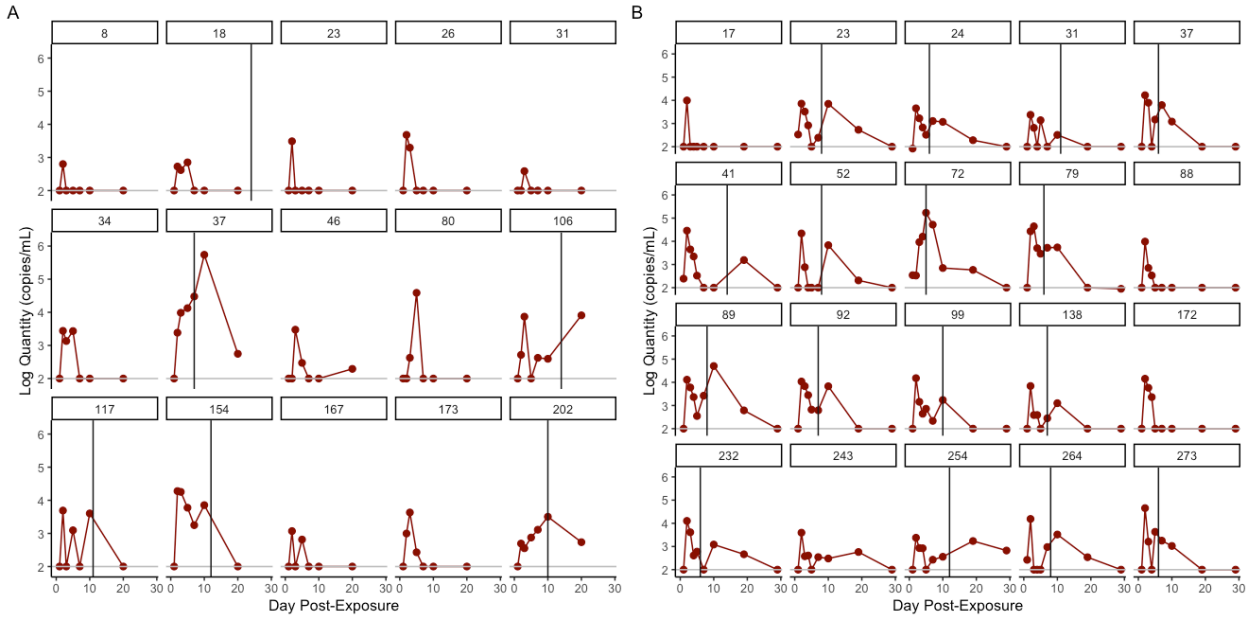

Figure A10. Shedding kinetics of IHNV isolate Ha30-91 at (A) 10°C and (B) 15°C.

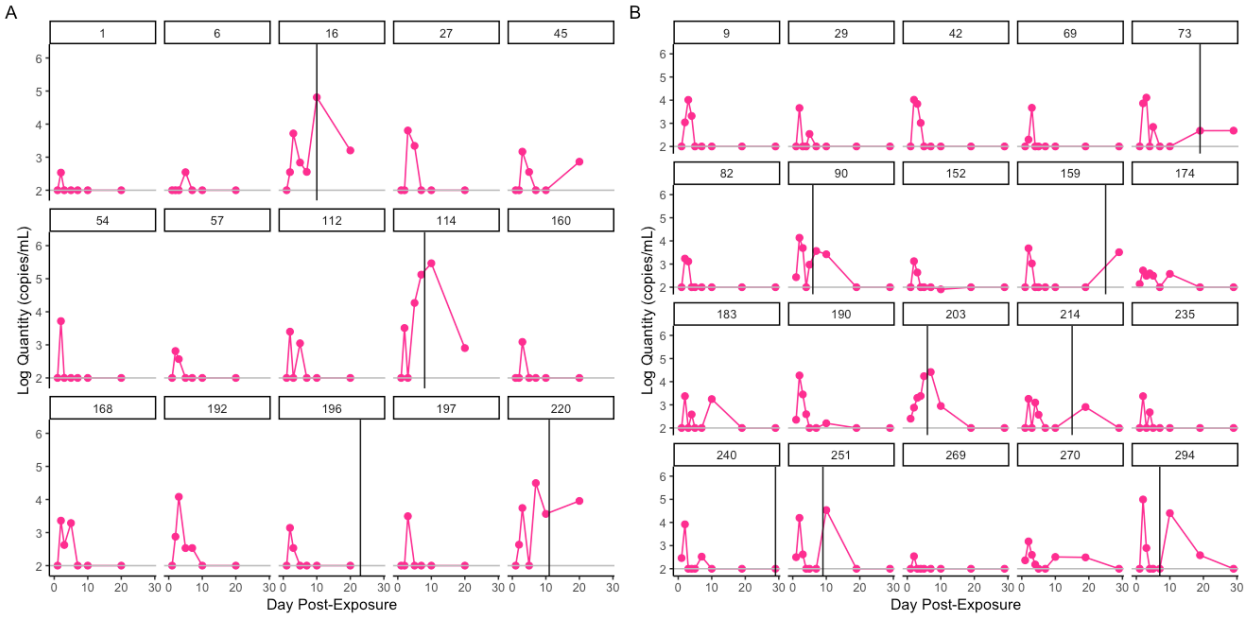

Figure A11. Shedding kinetics of IHNV isolate Ha39-91 at (A) 10°C and (B) 15°C.

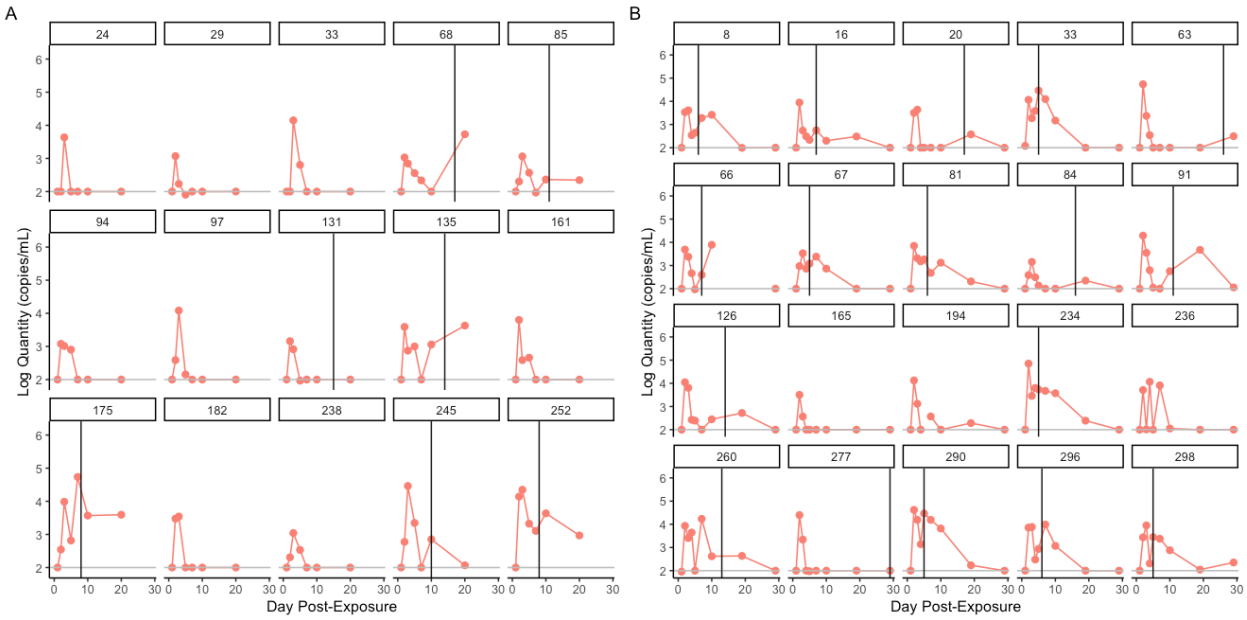

Figure A12. Shedding kinetics of IHNV isolate Ht508k-14 at (A) 10°C and (B) 15°C.

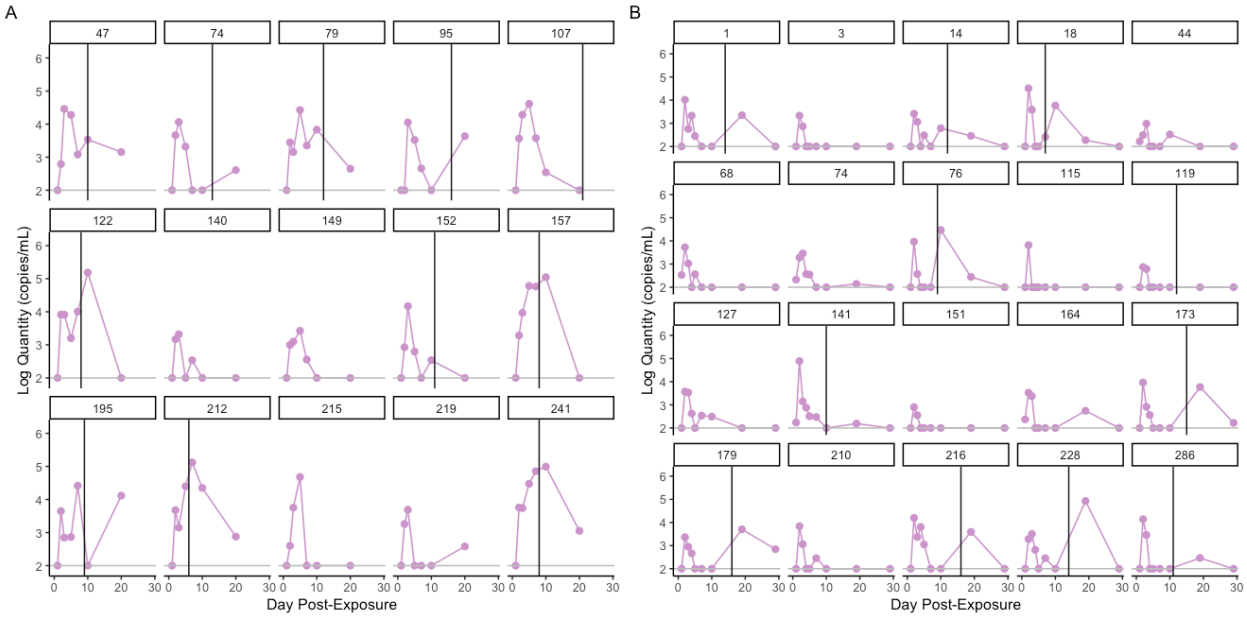

Figure A13. Shedding kinetics of IHNV isolate Ht511-14 at (A) 10°C and (B) 15°C.

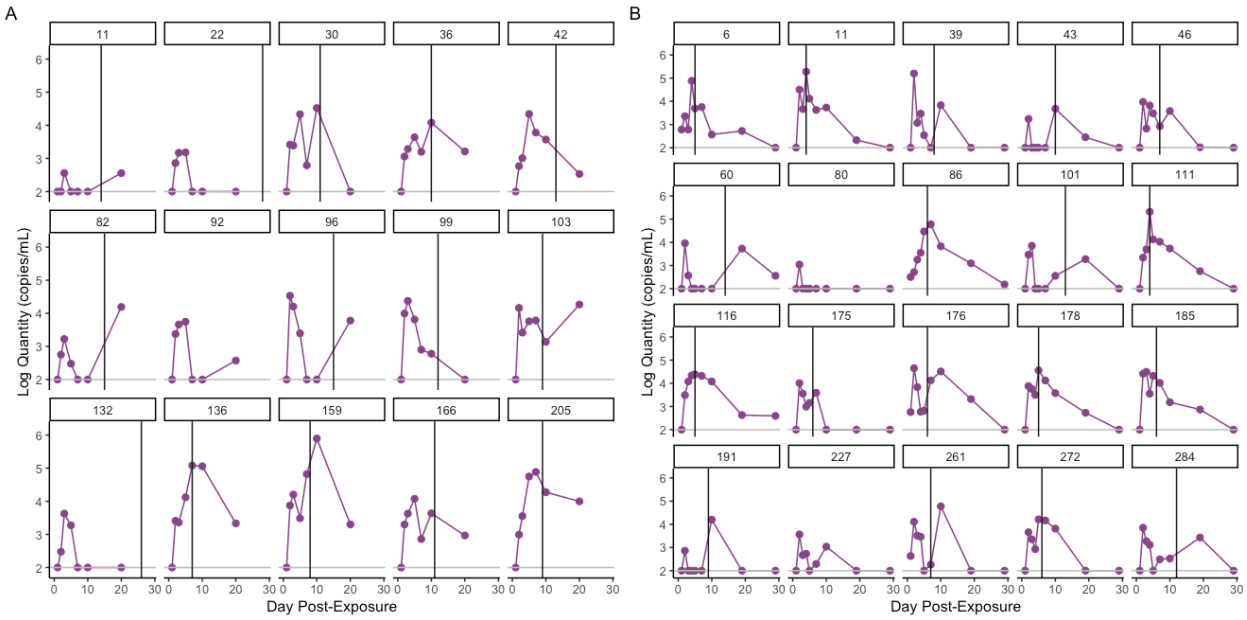

Figure A14. Shedding kinetics of IHNV isolate HtBrK-16 at (A) 10°C and (B) 15°C.

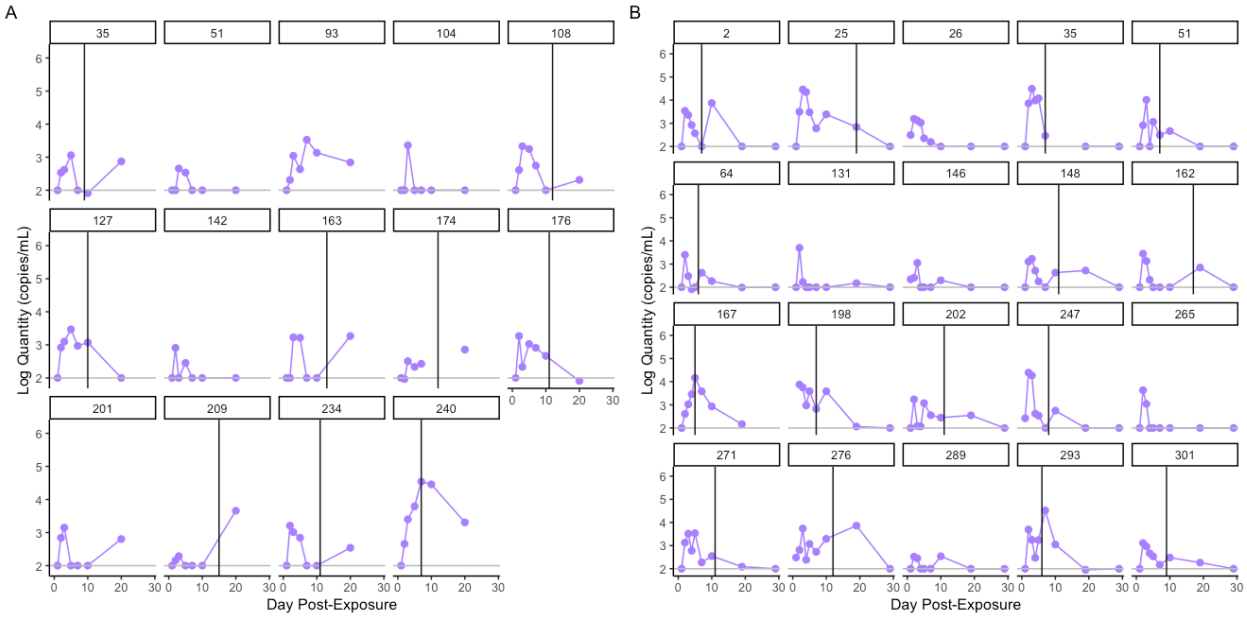

Figure A15. Shedding kinetics of IHNV isolate Ht134-17 at (A) 10°C and (B) 15°C.

CHAPTER 3: Linking virulence and shedding fitness of three sublineages of M-genogroup IHNV following the North American host jump into rainbow trout (*Oncorhynchus mykiss*)

ABSTRACT

The vast commercial rainbow trout industry in North America has witnessed the diversification of infectious hematopoietic necrosis virus (IHNV) in the novel host rainbow trout (*Oncorhynchus mykiss*), in which IHNV poses a significant disease risk. Representative strains of IHNV have demonstrated increasing virulence, shedding intensity, and shedding duration among M-genogroup isolates over time since the host jump, but whether this is a consistent relationship across genetic subgroups has not been tested. The potential interactions between these viral traits are particularly key to untangle for the dense farming region of the Hagerman Valley region of Idaho, where multiple subgroups of IHNV have cocirculated since the 1980s. This chapter explores how virulence (host mortality) and viral shedding phenotypes have changed over time for three subgroups of the M-genogroup which diverged after emergence in the novel host and persist into the present. Results included: selection for higher virulence phenotypes appears to hold across M subgroups, but the relationship between virulence and shedding intensity is not as strong as was expected. Instead, shedding prevalence and duration seem to be greater contributors to fitness.

INTRODUCTION

IHNV is one of the few systems well-equipped to ask key virus evolution questions regarding the relationships between virulence and shedding. Empirical data from the system may be used to make inferences about overall virus fitness and transmission risk across viral genetic variation and host species, from which generalized epidemiological parameters can be constructed for this and other systems. Initial characterization of IHNV documented high and low virulence types as well as the increase in virulence from the time of host jump to rainbow trout to the present (Chapter 1, (1, 2)). Shedding phenotypes exhibited slightly increased shedding intensity and more lengthy shedding durations across time (Chapter 2). Past work examining within-host replication has linked highly virulent genotypes of IHNV with greater body burdens of IHNV, indicating that virus replication and shedding may confer both virulence and fitness advantages to IHNV among emergent isolates (2). Since shedding appears to confer transmission throughout the acute shedding window, it is imperative to investigate how widely these trends vary in the IHNV system (Chapter 3).

A key question in all host-pathogen systems is how strongly pathogen genotypes influence phenotype, especially from a health perspective. Early in the COVID-19 pandemic, genetic haplotype diversity of SARS-coV-2 was linked to shedding duration, inciting specific risk management protocols such as length of quarantine protocols (3). Another study identified varying relationships between shed loads and emergent genotypes of SARS-coV-2, with no consistent relationship with virulence, necessitating comprehensive virus typing to identify additional moderating factors for virulence (4). Among animal study systems, Marek's disease models in poultry farms have linked increasing virulence with continued shedding through recovery times influenced by vaccination practices (5, 6). Whether or not longer shedding durations and increasing virulence are a generalizable model for other systems, such as trout farms, is unknown.

The infectious hematopoietic necrosis virus (IHNV) and salmonid host system is a ready opportunity for the investigation of whether evolutionary trends detected in a subset can be extrapolated across the phylogenetic tree branches or across time. A wealth of data is available on IHNV phylogeny, genetic variation and history of dominance and field displacements, virulence patterns, and described shedding kinetics. Since IHNV isolates have emerged and largely evolved in the fragmented but interconnected landscape of trout aquaculture, it is possible that uniform drivers of virulence or fitness might result in parallel evolutionary trends across different branches of the phylogenetic tree. The expanded isolate selection in this chapter allows for questions about nuances of the phylogenetic tree: is there evidence for a clear driver towards a particular viral virulence and shedding phenotype? Do evolutionary trends remain constant across different viral subgroups?

IHNV phylogeny is organized into genogroups U, M, and L in North America (7, 8). The M-genogroup diversity found in the Hagerman Valley region of Idaho is greater than the U and L-genogroups combined, and possesses a complex and strongly supported phylogenetic substructure (8–10). Following the host jump from sockeye to rainbow trout, the M virus was monophyletic initially and is now termed the MN subgroup, which was primarily detected between the 1970s-1980s. The MN group diverged into multiple new lineages termed MB, MC, MD, which have been detected consistently from the mid-1980s to the present day (9–14). These subgroups co-circulate among the Hagerman Valley region and are occasionally detected outside the area (12). Several other subgroups, (MA, ME, MF) have been sporadically detected in the Hagerman region as well but since they have not been collected in recent decades, they are considered extinct, presumably outcompeted by the extant subgroups MB, MC, MD. Given the density and scale of the commercial trout industry in this area, this system has much to gain from learning how viruses continue to evolve in the region.

Despite the documented evolutionary trends following the IHNV host jump to rainbow trout (increased virulence, Chapter 1; increased shedding quantity and longer shedding

durations, Chapter 2), a variety of both virulence and shedding phenotypes persist among novel isolates. Whether these also represent shedding variation and subsequent transmission risk is unknown. This chapter seeks to understand whether the evolutionary patterns uncovered in Chapters 1 and 2 across IHNV genogroups hold true at the subgroup level, and to what extent. This study is the first large-scale experiment that quantifies and directly compares virulence and viral shedding fitness among 40 IHNV genotypes with replication across subgroups of IHNV.

METHODS

1. Virus selection

Forty-one genetically distinct viral isolates were selected to investigate evolution of M-genogroup viruses following the time of host jump over five decades (Table 3.1). This selection expands upon and fills the temporal gaps between M-isolates used in Chapters 1 and 2, with the specific additions of isolates that span the subgroups of the M-genogroup (MN, MB, MC, MD) (12). Twelve representative strains of the ancestral MN group are included that span the 1970s-80s and are the oldest representations available of early M-genogroup that emerged after the host jump to rainbow trout. Twelve MB isolates, nine MC isolates, and seven MD isolates which span the late 1980s to the late 2010s represent the evolution of the M-genogroup since the ancestral MN group diverged into distinct subgroups. These branches of IHNV represent the dominant branches that have consistently been detected from the field and are extant. One isolate from the U-genogroup was also included to serve as a benchmark for comparison to other studies. As described in Chapter 1, virus stocks were propagated on fish cell lines and titered a minimum of three times prior to *in vivo* challenges to ensure known exposure doses.

2. Host species

Rainbow trout (*O. mykiss*) were obtained from a commercial trout producer as eggs and reared in a freshwater, pathogen-free, UV-irradiated flow-through system at 12.5°C. These trout are from the same genetic line as studied in previous chapters. Eggs were maintained in egg trays under 2 gpm flow until hatching, when they were transferred to 50-gallon flow trout tanks maintained at 1gpm flow. Fry were gradually stepped up to 15°C and fed a daily diet of semi-moist pellets at a rate equivalent to 1.5% biomass until use in experiments. The specific line of trout was chosen as the best available representation of hosts at the time of host jump. The line has not undergone selective breeding and is considered to have similar genetic diversity to wild-type rainbow trout.

3. In vivo shedding assay

Shedding studies were conducted with 41 viral isolates using methods described in Chapter 2, with reduced replicate number (n=13 fish replicates per isolate). Fish were exposed via bath immersion to virus at a dose of 2×10^4 pfu/mL (the same dose as the moderate virulence challenge exposure). Following exposure, replicate fish were separated and assigned to individual flow-through tanks held at 15°C. Water samples were collected on days 2 and 5, then stored at -80°C. These timepoints were selected following examination of Chapter 2 data, which indicated day 2 to be a reliable measure of peak shedding quantity, and day 5 to be a consistent measure of post-peak shedding quantity. Samples were processed via RT-qPCR as previously described (Chapter 2). The shedding assay and all molecular work were conducted at the Virginia Institute of Marine Science (Gloucester Point, USA).

4. In vivo virulence challenge

To quantify virulence phenotypes for all isolates, fish challenges used an exposure design as described in Chapter 1, with the following exceptions: exposure doses were 2 x 10^3 pfu/mL (low) and 2 x 10^4 pfu/mL (moderate), a single temperature was used (15°C), and there were 41 viral isolate treatments. Briefly, a standard *in vivo* batch challenge method was used where triplicate groups of 20 fish were exposed to one of the 41 isolate treatments or a Mock treatment of the diluent used for the virus treatments in 6L tanks (Minimum Essential Media with 10% fetal bovine serum) as previously described (1, 15–17). Fish were held static for 1 hour, then maintained on aerated flow-through water through day 30. Mortality was recorded daily, and dead fish were removed from tanks daily. Both challenges were conducted at the USGS Western Fisheries Research Center (Seattle, USA).

5. Statistical analysis

All analyses were conducted in R (version 3.4.2) (18). The analysis was broken into four parts: (i) evolution of M shedding across collection years, (ii) shedding fitness across subgroups, (iii) virulence among M subgroups, and the (iv) association between virulence and shedding. Linear regression methods were implemented with the lme4 and glmmTMB packages (19, 20). After visually comparing the data from the U isolate to benchmark the experiments, data from the U isolate was dropped from all subsequent analyses. Mock data were also dropped after no shedding in any mock treatments was detected.

5.1 Evolution of M shedding across collection years

The probability of shedding was qualitatively compared using figures of IHNV subgroup shedding frequency over the range of collection years. For shedding intensity, a linear model

was used with Gaussian error distribution. The response variable of shedding intensity (continuous) was modeled with the fixed effects of collection year (continuous) and sampling day (categorical), and the random effects of viral isolate and individual fish, since repeated measures were taken from fish over sampling days. Data from fish that did not shed were dropped from the analysis to better detect differences among shedding fish. Data from dead fish were omitted from the day following death onward.

5.2 Shedding fitness across M subgroups

This section of analysis was conducted separately for each subgroup (MB, MC, MD, MN) to elucidate whether total shedding quantity, peak intensity, or probability of shedding varied across the phylogenetic groups from the 1980s onward. Univariate statistics were calculated to broadly compare subgroups. The analyses investigate whether any evolutionary trend could be identified within the subgroups, and if trends were consistent. Total shedding quantity was analyzed using a zero-inflated LME for each subgroup to account for zero-inflation in the data. The response variable was quantity of virus summed over sample days with a transformation of $\log_{10}(x + 1)$. Predictors included collection year as a fixed effect and isolate as a random effect. Peak intensity (continuous) or status of shedding (binomial) was modeled with the same predictors as previous sections: collection year and day were fixed effects, isolate and fish as random effects. Peak intensity used an LME model with Gaussian distribution; probability of shedding used a GLME model with binomial distribution. Peak intensity was defined as the quantity of virus shed from positive fish during the peak period, defined as day 2 based on shedding kinetics data from Chapter 2.

5.3 Virulence among M subgroups

To compare relative virulence in each subgroup and across time, the total mortality at the end of the virulence assay experiments (day 30) was modeled with a GLME and binomial

distribution, as described in Chapter 1, with the addition of the 'bobyqa' optimizer (20). The response was the number of fish dead or alive in each treatment, with fixed effects of subgroup (categorical), dose (categorical), collection year (continuous), and random effects of isolate and tank.

5.4 Association between virulence and shedding

A qualitative analysis was accomplished through a series of correlation plots to identify possible relationships between virulence and shedding metrics. A GLME analysis was conducted on virulence (cumulative dead and alive fish at experiment end) data from the moderate dose (2 x 10^4 pfu/mL) virulence assay. The predictors in the model were shedding frequency on days 2 and 5 (continuous), subgroup (categorical), and collection year centered around mean year (continuous), with the random effect of isolate. Shedding frequency was also analyzed using GLME with the proportion of fish shedding (from shedding assay experiments) as the response variable, and the predictors listed for the virulence analysis. A second GLME analysis was conducted using mean intensity of shedding on day 2 and day 5 (continuous) as a fixed effects instead of prevalence. Mean intensity data only included fish that shed detectable virus. Each GLME analysis used a binomial error distribution.

RESULTS

1. *Evolution of M shedding across collection years*

Isolates shed more on day 2 than day 5 in terms of both frequency (number of fish shedding) and intensity (quantity of virus) (Figures 3.1-3.3). Probability of shedding did not appear to exhibit any correlation with virus isolate collection date (i.e. evolutionary time) (Figure 3.3). Peak shedding frequency ranged from 6-13 fish of 13 replicates (Figure 3.1), indicating high variability

in isolate infectivity and individual fish susceptibility. From day 2 to day 5 the mean probability of shedding virus decreased from 78% to 22% across all M isolates (Figure 3).

The shedding intensity analysis indicated more recently collected isolates shed less than older isolates. However, the effect was dependent on shedding sample collection day, with day 5 (post peak) shedding decreasing at a faster rate across collection years than day 2 peak shedding (Figures 3.2, 3.4, Table S3.1).

2. Shedding fitness across M subgroups

Among the subgroups, 85% of fish in MB shed during the peak period compared to 74-75% in all other subgroups (Table 3.2). MB isolates also shed slightly more often (28%) than other subgroups during the post peak period (17-24%, Table 3.2). Conversely, MB had the lowest mean peak intensity (3.36 log copies/mL) compared to other subgroups (3.46-3.48 log copies/mL) and the highest mean post-peak intensity (Table 3.2). Mean total quantity across sampling days was comparable for all subgroups, ranging between 1.63-1.86 log copies/mL. Mean comparisons between subgroups in shedding intensity and total shedding were not found to be statistically significant but demonstrate subtle subgroup variation (Table 3.2).

The analysis predicting day 2 (peak) intensity showed a consistent decrease across evolutionary time among all subgroups (Figure 3.5A, Tables S3.2-S3.5). The change in MN across the range of collection years spanning from 1972-1984 was subtle (Figure 3.5A, Table S3.2). Negative trends were more pronounced and consistent for the MB, MC, and MD subgroups, whose intensity during the peak period was predicted to decrease by 0.01 to 0.02 log copies/mL for every increase in collection year (Figure 3.5A, Tables S3.3-S3.5). In contrast to the more moderate changes over evolutionary time observed during the peak period, more dramatic trends were evident during the post-peak period (day 5 data) (Figure 3.5B). Year effect estimates of the decrease in shedding intensity for MN, MB, and MC ranged from 0.06 to 0.03 log viral copies per collection year. The MD subgroup showed an opposite trend, where every

unit increase in collection year resulted in a predicted increase of 0.02 log copies/mL in post-peak shedding intensity (Figure 3.5B, Tables S3.6-S3.9).

3. Virulence among M subgroups

Cumulative percent mortality ranged between 15-73% among tanks in the low dose virulence assay and 13-95% in the moderate dose assay (Figures 3.6A-3.6B). Across evolutionary time from the time of the host jump to present, a positive correlation was detected between recency of collection and virulence (Figures 3.7A-3.7B). As such, more recent isolates were more virulent than older ones at either exposure dosage. However, the rate of increase for virulence through evolutionary time did not depend on subgroup. The overall difference in virulence between subgroups did depend on dose, such that genogroup MB was found to have statistically higher virulence than MN, MD subgroups, but only at the moderate dose treatment. Within subgroups, the virulence of subgroups MB and MC was significantly elevated to 65-75% at the moderate dose, from 40-50% at the low dosage (Figure 3.7) but no difference in mortality was observed among the MN and MD subgroups. No statistically significant differences were detected among the other subgroup pairwise comparisons or among subgroups at the low dose. Qualitatively, MB and MC subgroups generally exhibited higher virulence than MN and MD subgroups, at both exposure dosages.

4. Association between virulence and shedding

Qualitatively, earlier day of death among individual fish in the shedding assay positively correlated with increased shedding quantity (Figure 3.8). When virulence data from the virulence assay was compared against day 2 shedding data, little variation was apparent (binned by collection year; Figures 3.9A, 3.9C). However, day 5 shedding data pointed to a possible positive correlation between high virulence, increased post-peak shedding frequency, and decreased post-peak intensity among most recently collected isolates (pink points, Figures

3.9B, 3.9D). The oldest isolates (all MN) never exceeded 75% mortality, but generally occupied the same ranges as more recent and virulent isolates for all shedding metrics (navy points, Figure 3.9). Among the isolates collected in the intermediate year range, no correlations were apparent.

The analysis of associations between virulence and shedding indicated a positive relationship between the number of fish shedding on day 5 and the probability of death (Figure 3.10A, Tables S3.11 – S3.12). However, this relationship only held true for more recently collected isolates (which fell into the MB, MC, or MD subgroups) (Figure 3.10B, Table S3.12). No relationship was found between shedding frequency on day 2 and mortality (Tables S3.11 – S3.12). Differences among the subgroups also contributed to baseline probability of mortality. Compared to the MN subgroup, the log-odds of mortality increased by 0.04 in the MD subgroup, 0.57 in the MC subgroup, or 0.85 in the MB subgroup (Figure 3.10A, Table S3.12).

A second analysis, which utilized shedding intensity as a predictor instead of frequency, also found no relationship between day 2 shedding intensity and probability of death (Table S3.13). However, the analysis indicated an interaction between day 5 intensity and collection year, such that older isolates displayed a positive relationship between shedding intensity and mortality, but newer isolates showed the opposite relationship (Figure 3.11, Table S3.14). As such, among newer isolates, increased post-peak intensity was instead correlated with a lower probability of death (Figure 3.11, Table S3.14).

DISCUSSION

Our study found that virulence phenotypes demonstrated a clear increase over evolutionary time across all IHNV subgroups. This was exemplified by new isolates causing higher levels of fish mortality, for all subgroups examined. The common trend of increasing

virulence and at similar rates across different viral lineages lends support to the theory that universal selection pressures have driven the M-genogroup towards a more virulent phenotype. The trend of increasing virulence through evolutionary time agrees with other studies in this system (Chapter 1, (21, 22)). Among shedding phenotypes examined, our results indicated that peak shedding intensity decreased over evolutionary time for each subgroup. For three of the four subgroups (MN, MB, MC), there was evidence that post-peak shedding intensity also decreased. Overall, the findings of this study suggest that M viruses are evolving towards a lower peak intensity of shedding in rainbow trout novel hosts, although the rate of change is slow. No significant difference in probability of shedding was seen over evolutionary time for any subgroup. Collectively, these results indicate that although the likelihood of fish shedding after exposure to M-genotype IHNV as not changed since the time of the host jump, the amount of virus shed by those fish which become infected, has decreased. The opposite evolutionary directions of increasing virulence and decreasing shedding intensity indicate that virulence and shedding may be more complex in the IHNV system as previously thought.

A major caveat to these findings is the limited number of sampling points. Since shedding was compared at only two time points, there may be nuances in the relationship of these phenotypic traits that went undetected, such as clearance rate of the infection (shedding duration). Acute shedding within the peak period may be incompletely described, in contrast to the more detailed sampling scheme of Chapter 2. Since the peak shedding period for the initial ten M isolates described in previous chapters was defined with greater statistical power, approximating peak shedding in the present study with data from day 2 was reasonable. However, if the hypothesis of shifting phenotypes towards more acute shedding is realistic for M isolates, additional data points for day 1 and 3 shedding would provide greater resolution. Study design characteristics such as dosage, data subsetting by subgroup, or sampling schema may all contribute to the mismatch of shedding trends identified between the previous and current chapter. At the M-genogroup level, evolution of increased shedding intensity was not evidenced

in this study as observed in the Chapter 2 study. It is possible that among the limited selection of isolates used previously, the full range of shedding phenotypes was not captured. It should be noted that fewer fish per treatment were used in Chapter 3 compared to the Chapter 2 study. Accordingly, it is possible that this resulted in a reduction in statistical power, limiting the ability to resolve nuances between shedding trends, subgroups, and isolate collection times. Another notable difference in study design between this chapter and Chapter 2 was the initial IHNV exposure dosage. Chapter 2 hosts received a 2×10^5 pfu/mL exposure, ten-fold higher than the dosage used in Chapter 3 (2×10^4 pfu/mL). The moderate dose was chosen because chapters 1-2 indicated that it would be more informative for resolving shedding and virulence differences, and this dosage has been used extensively in other studies (1, 2, 12, 16, 23, 24). However, we observed that this moderate dosage was not sufficient to elicit detectable shedding in all fish, and where shedding did occur, peak intensity was highly variable between fish. The reduced pool of replicate data may have contributed to the reduced resolution of shedding and virulence differences between isolates, compared to Chapter 2.

Our results comparing peak to post-peak data indicate that shedding fitness of IHNV may hinge more on the rate of infection clearance, rather than intensity. Anderson and May postulated that rapid adaptation may occur right after a host jump since chances are low that an emergent pathogen would reach equilibrium with a new host environment instantaneously (25). It is possible that the MN subgroup possessed high intensity immediately after emerging in novel trout hosts and the descendent subgroups are still moving towards optimal fitness with reduced shedding intensity, or that hosts can tolerate low to moderate levels of IHNV shedding. In farm environments this would be reasonable, given that new technology and manipulated host populations could easily create a moving target of host factors to which viruses must adapt or go extinct. In the classic case of myxoma virus and rabbits in Australia, slower recovery rates were selected over more acute phenotypes resulting in a tradeoff where the most fit viruses had

only moderate virulence and long shedding durations. In a study of MERS-CoV in rhesus macaques, virulence was correlated both with earlier shedding and dramatically higher intensity, seemingly pointing to higher fitness among more acute infections; however, the same phenotypes also correlated with longer shedding duration (26). A phenomenon may be occurring among IHNV isolates from the Hagerman Valley where viruses that shed in high quantities over long recovery times may elicit too much host damage and burn themselves out, and instead we observe lower-intensity viruses over longer durations. However, the increase in post-peak shedding through time for MD isolates demonstrates that even if MB and MC isolates experience slow recovery and high virulence as a cost, it is not the only phenotype that may produce evolutionarily fit viruses in this environment.

Among hosts that shed in the post-peak period, predicted intensity dramatically decreased for two of the extant subgroups (approximately 1 log difference between oldest and newest isolates in the MB subgroup, 1.2 log copies/mL among MC isolates) but increased almost 0.7 log copies/mL in the MD subgroup. The dramatic decrease in post-peak shedding relative to peak shedding allows the possibility that MB and MC isolates may be shifting towards a phenotype that exhibits early shedding. Lower post-peak shedding may be evidence of selection for faster rates of replication and shedding. This would agree with an earlier study which found more intensely shedding viruses to be more virulent (17, 27). However, fewer than half the fish replicates in most isolate treatments shed in the post-peak period, limiting the inferential power post-peak data. Higher virulence was assumed to be indicative of higher fitness among IHNV isolates, but in this study virulence did not appear tightly linked to either shedding frequency or intensity. It is also possible virulence may simply be a consequence rather than the selected trait.

Earlier day of death was associated with higher individual host shedding, demonstrating that virulence and shedding are correlated on an individual host scale, which is broadly in agreement with findings from Chapter 2. Whether this relationship is under selection by way of

impacting IHNV transmission is unclear. It may be that specific conditions or practices in the Hagerman trout industry such as removal of dead fish may preclude viral isolates from reaping the transmission benefit that early death and high shedding intensity could provide on a population level. As such, the theoretical link between high virulence and shedding may not match the reality of field environments on an evolutionary scale. Instead, IHNV may primarily experience selection in locales where mortality-inducing levels of viral shedding are an evolutionary weakness. Perhaps then magnitude of shedding of IHNV in rainbow trout is not under selection pressure, and instead other traits represent more important evolutionary parameters, such as shedding duration and clearance of infection.

In 2000, Troyer et al. began to describe the subgroup evolution and diversity in the Hagerman Valley (9). MB and MC were described as possibly being under directional selection whereas the MD trajectory was less clear. The same study identified the possible mechanisms of trout farms capable of selecting on viral fitness; exact mechanisms are yet unknown. In 2003, Kurath et al. described the total phylogeography known in North America for IHNV but specific mechanisms for directing virulence or shedding kinetics remained undetermined (11). A follow up study by Troyer et al. in 2008 found no difference in relative virulence among isolates determined to be MB, MC, MD (12). The isolates Ha20-91, Ha30-91, Ha39-91 respectively correspond to the representative isolates used in the 2008 study. Virulence measures from Chapter 1 indicated that Ha30-91 tended to produce highest virulence among these, but the difference was not significant, fundamentally agreeing with the 2008 study (Chapter 1, (20)). Shedding metrics from Chapter 2 showed that Ha20-91 and Ha30-91 were similarly likely to shed at 15°C (56-63%) and demonstrated similar peak intensity (4 log copies/mL) but Ha39-91 was significantly less likely to shed (30%) compared to Ha30-91 and peaked at lower intensity (3.6 log copies/mL) (Chapter 2 data). These variable shedding metrics showed that virulence and shedding are not ubiquitously linked but given the low replication of subgroup among the Chapter 2 dataset, generalizations could not be made past the isolate. The present study

demonstrates that while the earliest comparisons were valuable for producing a benchmark, the diverse phenotypes and evolutionary trends of each subgroup may not be encapsulated by the smaller number of representative isolates.

While the present study focuses on parallels or lack thereof among divergent subgroups which cocirculate in aquaculture, it is also worth considering possible evolutionary factors outside the Hagerman region. The MD subgroup is a special case in that this subgroup has undergone at least one set of spillover and spillback events between the Hagerman Valley and the Columbia River Basin system, an adjacent watershed to the Hagerman region and Snake River in the Pacific Northwest (14, 28–30). Among MB, MC, and MD isolates detected outside of the Hagerman Valley region, the MD subgroup is unique in that it has become the dominant type detected in Columbia River Basin steelhead (14, 28).The lower Columbia River is home to several salmonid species as well as intraspecies populations with distinct life histories, compared to the Hagerman Valley and Snake River region of Idaho which has a much higher density of industrialized trout farming activity. Heterogeneity in host susceptibility has been linked to IHNV emergence in the Columbia (28, 29). While geographically separate, these events have the potential to shape evolution where host genetics overlap or where contact is possible between aquaculture origin hosts and wild hosts. An example is hatchery populations, which are released to natural environments to complete their anadromous life cycles but return to heavily managed aquaculture environments for spawning (31). The MD subgroup may exhibit different patterns, like longer shedding durations, that may facilitate its wider prevalence across the field landscape beyond the environmental selection pressures of the Hagerman Valley.

Sub-optimally fit phenotypes for shedding duration or virulence may persist in the region if isolates co-circulate among both wild and captive populations and continue to evolve in competition with IHNV strains that embody alternative fitness tradeoffs. A specific example of this could be applied to the role of post-mortem fish shedding. In commercial farms, health practices include regular (multiple daily) removal of dead fish, which would introduce an earlier

shedding and transmission truncation than in natural environments. If duration of transmission potential is the trait selected for in aquaculture environments, a shift in the shedding rate towards earlier shedding or more intense shedding prior to host mortality might be expected. However, if dead hosts which have succumbed to disease are allowed to remain in contact with naïve individuals, either through less frequent removal in aquaculture or the process of decay in natural environments, the virus would experience less selection pressure for early shedding.

The variation among IHNV phenotypes documented in this study engender further questions about the diversity of evolutionary trajectories in aquaculture environments. Increased virulence has also been documented among IHNV lineages from Europe and Asia, but recent studies have not reported corresponding shedding phenotypes. This leads to the question of whether IHNV isolates with increased virulence may follow one of the two general shedding phenotypes identified in the present study; (i) decreased peak shedding and faster recovery (evidenced by MB and MC subgroups) or (ii) decreased peak and extended post-peak shedding duration (MD subgroup). Furthermore, additional fitness metrics may be at play for IHNV. For example, in the Columbia River watershed system, increasing virulence but not infectivity was documented among IHNV strains (23), demonstrating that IHNV competition fitness does not necessarily track with virulence. Transmission fitness would logically correlate with shedding fitness but was beyond the scope of this study to directly measure.

Few empirical examples are available from other study systems from which we may draw perfect parallels for both evolving virulence and shedding fitness, but there are instances where virulence and shedding explicitly differ. Avian influenza, which has been studied in multiple poultry species, appears to have variable shedding phenotypes, where high-virulence and low-virulence strains have been shown to have different shedding intensity as well as shedding durations, but the relationships are inconsistent across host species, exposure route, and shedding route (i.e., via respiratory tract or cloaca) (32). In Marek's disease and boiler chickens, vaccination has been linked to increased virulence evolution, as shedding fitness

appears unaffected by vaccination and subsequently pathogen particles exhibit longer recovery times, coupled with dust particulates in the environment that facilitate repeated exposure (33). Certainly COVID-19 studies have launched the phenomenon of ‘super-shedders’ into public view, where low or moderately virulent strains of SARS-coV-2 sometimes corresponded to enormous shed loads and thus transmission opportunities that did not match more obvious virulence metrics such as symptoms (34). Ebola virus has repeatedly produced more virulent outbreaks in recent decades, associated with different genetic strains of virus but poorly understood shedding phenotypes and health risks (35).

IHNV may be selected on to produce certain fitness types commensurate with the Hagerman Valley environment; increased virulence is common across subgroups. The variety of relationships between virulence and shedding phenotypes suggest that there are multiple pathways to superlative fitness. However, the fact that not all subgroups follow the same post-peak shedding could just as easily suggest that evolution is neutral and trends we observe are artifacts of stochastic processes. As an RNA virus, IHNV is subject to short generation times and relatively high rates of mutation. Neutral theory predicts most genetic changes in viral genomes yield little functional change (36). Yet since largely consistent virulence and peak shedding phenotypes have been documented and described here, it seems more likely that IHNV is under consistent directional selection in the Hagerman Valley. The M-genogroup nucleotide diversity is estimated at 7.6% which is relatively low for an RNA virus but comprises the majority of genetic diversity of IHNV in North America, where the U and L-genogroups are less than half as much diverse (8). While the majority of mutations for RNA viruses may be neutral, diversity among isolates is important to understand since there is also evidence that even small genetic differences may result in marked phenotypic difference, such as point mutations that resulted in increased virulence in Zika virus (37). The isolates included in this project are genetically distinct and have been typed to subgroup, but full genome analysis and inference of rate of change over evolutionary time will be necessary to conduct a deep

examination of IHNV evolution in the Hagerman. With the myriad viral generations that have undergone selection from the time of host jump to present, evolution of IHNV phenotypes may be occurring at the genogroup rather than subgroup level.

The present system of salmonid fish and IHNV lacks a clear mechanism for directional selection toward increased virulence. Certainly many possibilities exist depending on host factors, environmental factors, and management methods (9, 16, 38). Patterns seem to point towards a general shift towards the acute shedding window without much change in shedding magnitude. This study assumes that shedding is an accurate proxy for transmission, however if the quality of shed virion particles changes over the recovery period (infectivity), transmission duration would require further investigation. How shedding fitness translates to transmission fitness presents a logical next avenue of investigation aquatic pathogen research. One of the most relevant systems to aquatic viral transmission and coldwater fish health in particular is viral hemorrhagic septicemia in Pacific herring, which has demonstrated that slow recovery rate and high shedding rates perpetuate transmission in the wild and play a role in modulating the occurrence of disease events (39, 40). Whether a similar mechanism holds true for IHNV and rainbow trout is unknown.

Since field isolates are nearly all from sites associated with rainbow trout farm sources, these findings are particularly relevant to the rainbow trout aquaculture industry, North American salmonid conservation, and of special interest to the disease ecology discipline as it relates to domestic food production systems. Disentangling the complexity of viral fitness and individual traits is crucial to understanding the selection pressures driving viral evolution and ultimately developing effective disease management strategies for sustainable aquaculture, safeguarding conservation of natural resources, and informing aquatic epidemiology.

References

1. A. R. Wargo, K. A. Garver, G. Kurath, Virulence correlates with fitness in vivo for two M group genotypes of Infectious hematopoietic necrosis virus (IHNV). *Virology* **404**, 51–58 (2010).

2. M. M. D. Peñaranda, A. R. Wargo, G. Kurath, In vivo fitness correlates with host-specific virulence of Infectious hematopoietic necrosis virus (IHNV) in sockeye salmon and rainbow trout. *Virology* **417**, 312–319 (2011).

3. J. T. Wu, *et al.*, Estimating clinical severity of COVID-19 from the transmission dynamics in Wuhan, China. *Nat Med* **26**, 506–510 (2020).

4. Tang, Haijun, et al., Characterization of SARS-CoV-2 Variants N501Y.V1 and N501Y.V2 Spike on Viral Infectivity. *Frontiers in Cellular Infection and Microbiology* **11** (2021).

5. A phylogenomic analysis of Marek's disease virus reveals independent paths to virulence in Eurasia and North America - Trimpert - 2017 - Evolutionary Applications - Wiley Online Library. Available at: https://onlinelibrary.wiley.com/doi/10.1111/eva.12515 [Accessed 7 June 2024].

6. K. E. Atkins, *et al.*, Vaccination and reduced cohort duration can drive virulence evolution: Marek's disease virus and industrialized agriculture. *Evolution* **67**, 851–860 (2013).

7. G. Kurath, "Molecular Epidemiology and Evolution of Fish Novirhabdoviruses" in *Rhabdoviruses: Molecular Taxonomy, Evolution, Genomics, Ecology, Host-Vector Interactions, Cytopathology and Control*, R. G. Dietzgen, I. V. Kuzmin, Eds. (Caister Academic Press, 2012), pp. 423–445.

8. G. Kurath, *et al.*, Phylogeography of infectious haematopoietic necrosis virus in North America. *Journal of General Virology* **84**, 803–814 (2003).

9. R. M. Troyer, S. E. LaPatra, G. Kurath, Genetic analyses reveal unusually high diversity of infectious haematopoietic necrosis virus in rainbow trout aquaculture. *Journal of General Virology* **81**, 2823–2832 (2000).

10. E. J. Emmenegger, T. R. Meyers, T. O. Burton, G. Kurath, Genetic diversity and epidemiology of infectious hematopoietic necrosis virus in Alaska. *Diseases of Aquatic Organisms* **40**, 163–176 (2000).

11. R. M. Troyer, G. Kurath, Molecular epidemiology of infectious hematopoietic necrosis virus reveals complex virus traffic and evolution within southern Idaho aquaculture. *Diseases of Aquatic Organisms* **55**, 175–185 (2003).

12. R. M. Troyer, K. A. Garver, J. C. Ranson, A. R. Wargo, G. Kurath, In vivo virus growth competition assays demonstrate equal fitness of fish rhabdovirus strains that co-circulate in aquaculture. *Virus Research* **137**, 179–188 (2008).

13. R. Breyta, A. Black, J. Kaufman, G. Kurath, Spatial and temporal heterogeneity of infectious hematopoietic necrosis virus in Pacific Northwest salmonids. *Infection, Genetics and Evolution* **45**, 347–358 (2016).

14. R. Breyta, *et al.*, Emergence of MD type infectious hematopoietic necrosis virus in Washington State coastal steelhead trout. *Diseases of Aquatic Organisms* **104**, 179–195 (2013).

15. R. Breyta, I. Brito, G. Kurath, S. Ladeau, “Infectious hematopoietic necrosis virus virological and genetic surveillance 2000-2012” (2017).

16. K. A. Garver, W. N. Batts, G. Kurath, Virulence comparisons of infectious hematopoietic necrosis virus U and M-genogroups in sockeye salmon and rainbow trout. *Journal of Aquatic Animal Health* **18**, 232–243 (2006).

17. M. M. D. Peñaranda, M. K. Purcell, G. Kurath, Differential virulence mechanisms of infectious hematopoietic necrosis virus in rainbow trout (Oncorhynchus mykiss) include host entry and virus replication kinetics. *Journal of General Virology* **90**, 2172–2182 (2009).

18. A. R. Wargo, G. Kurath, In Vivo Fitness Associated with High Virulence in a Vertebrate Virus Is a Complex Trait Regulated by Host Entry, Replication, and Shedding. *Journal of Virology* **85**, 3959–3967 (2011).

19. Posit team, RStudio: Integrated Development Environment for R. (2024). Deposited 2024.

20. D. Bates, M. Mächler, B. Bolker, S. Walker, Fitting Linear Mixed-Effects Models Using {lme4}. *Journal of Statistical Software* **67**, 1–48 (2015).

21. M. Abbadi, *et al.*, Increased virulence of Italian infectious hematopoietic necrosis virus (IHNV) associated with the emergence of new strains. *Virus Evolution* **7**, 1–14 (2021).

22. M. Mochizuki, H. J. Kim, H. Kasai, T. Nishizawa, M. Yoshimizu, Virulence Change of Infectious Hematopoietic Necrosis Virus against Rainbow Trout Oncorhynchus mykiss with Viral Molecular Evolution. *Fish Pathology* **44**, 159–165 (2009).

23. R. Breyta, D. Mckenney, T. Tesfaye, K. Ono, G. Kurath, Increasing virulence, but not infectivity, associated with serially emergent virus strains of a fish rhabdovirus. *Virus Evolution* **2**, 1–14 (2016).

24. D. G. McKenney, G. Kurath, A. R. Wargo, Characterization of infectious dose and lethal dose of two strains of infectious hematopoietic necrosis virus (IHNV). *Virus Research* **214**, 80–89 (2016).

25. R. M. Anderson, R. M. May, “Coevolution of hosts and parasites” (1982).

26. J. Prescott, *et al.*, Pathogenicity and Viral Shedding of MERS-CoV in Immunocompromised Rhesus Macaques. *Front. Immunol.* **9** (2018).

27. M. K. Purcell, S. E. LaPatra, J. C. Woodson, G. Kurath, J. R. Winton, Early viral replication and induced or constitutive immunity in rainbow trout families with differential resistance to Infectious hematopoietic necrosis virus (IHNV). *Fish and Shellfish Immunology* **28**, 98–105 (2010).

28. R. Breyta, A. Jones, G. Kurath, Differential susceptibility in steelhead trout populations to an emergent MD strain of infectious hematopoietic necrosis virus. *Diseases of Aquatic Organisms* **112**, 17–28 (2014).

29. D. G. Hernandez, W. Brown, K. A. Naish, G. Kurath, Virulence and infectivity of UC, MD, and L strains of infectious hematopoietic necrosis virus (IHNV) in four populations of Columbia River Basin chinook salmon. *Viruses* **13** (2021).

30. K. Garver, R. Troyer, G. Kurath, Two distinct phylogenetic clades of infectious hematopoietic necrosis virus overlap within the Columbia River basin. *Dis. Aquat. Org.* **55**, 187–203 (2003).

31. R. Behnke, J. Tomelleri, *Trout and Salmon of North America*, G. Scott, Ed. (The Free Press, 2002).

32. E. A. Germeraad, *et al.*, Virus Shedding of Avian Influenza in Poultry: A Systematic Review and Meta-Analysis. *Viruses* **11**, 812 (2019).

33. D. A. Kennedy, P. A. Dunn, A. F. Read, Modeling Marek's disease virus transmission: A framework for evaluating the impact of farming practices and evolution. *Epidemics* **23**, 85–95 (2018).

34. Á. Kun, *et al.*, Do pathogens always evolve to be less virulent? The virulence–transmission trade-off in light of the COVID-19 pandemic. *Biologia Futura* **74**, 69–80 (2023).

35. M. T. Sofonea, L. Aldakak, L. F. V. . V. Boullosa, S. Alizon, Can Ebola virus evolve to be less virulent in humans? *Journal of Evolutionary Biology* **31**, 382–392 (2018).

36. S. D. W. Frost, B. R. Magalis, S. L. Kosakovsky Pond, Neutral theory and rapidly evolving viral pathogens. *Molecular Biology and Evolution* **35**, 1348–1354 (2018).

37. A. Young, *et al.*, A platform technology for generating subunit vaccines against diverse viral pathogens. *Front. Immunol.* **13** (2022).

38. D. A. Kennedy, *et al.*, Potential drivers of virulence evolution in aquaculture. *Evolutionary Applications* **9**, 344–354 (2016).

39. P. K. Hershberger, *et al.*, Long-term shedding from fully convalesced individuals indicates that Pacific herring are a reservoir for viral hemorrhagic septicemia virus. *Diseases of Aquatic Organisms* **144**, 245–252 (2021).

40. P. K. Hershberger, J. L. Gregg, C. A. Grady, L. Taylor, J. R. Winton, Chronic and persistent viral hemorrhagic septicemia virus infections in Pacific herring. *Diseases of Aquatic Organisms* **93**, 43–49 (2010).

Table 3.1. Isolate information. For each isolate included in this study, the following information is provided: name, location of original collection, collection year, subgroup, and genotype based on mid-G gene sequencing (13, 15).

Isolate #	Isolate name	Collection Location	Year Isolated	Genogroup	mGUSD
1	Wck74	Weaver Creek, B.C.	1974	UP	mG004U
2	Ha1000-72	1000 Spring Trout Farm, Idaho	1972	MN	mG129M
3	HaVT-74	Hagerman Valley, Idaho	1974	MN	mG400MN
4	SV76	Sun Valley Trout Farm BC	1976	MN	mG401MN
5	NY1-78	New York trout farm	1978	MN	mG129M
6	Ha051-78	Hagerman Valley, Idaho	1978	MN	mG125M
7	Hg201-78	Farm site 10, Idaho	1978	MN	mG123M
8	Hg203-80	American Falls, ID, Idaho	1980	MN	mG096M
9	Hg204-81	Hagerman Valley, Idaho	1981	MN	mG097M
10	Ha090-82	Hagerman Valley, Idaho	1982	MN	mG100M
11	Ha053-83	Hagerman Valley, Idaho	1983	MN	mG101M
12	Hg210-83	Farm site 12, Idaho	1983	MN	mG126M
13	Hg211-84	Farm site 4, Idaho	1984	MN	mG126M
14	Ha085-88	Hagerman Valley, Idaho	1988	MB	mG080M
15	Hg002-89	Magic Valley State Hatchery, Idaho	1989	MB	mG090M
16	220-90	Hagerman Valley, Idaho	1990	MB	mG009M
17	Ha20-91	Hagerman Valley, Idaho	1991	MB	mG079M
18	Hg146-97	Farm site 7, Idaho	1997	MB	mG091M
19	HtMa02	Magic Valley State Hatchery, Idaho	2002	MB	mG091M
20	Ht067-08	Farm site A, Idaho	2008	MB	mG348M
21	HtSt004-11	Hagerman State Hatchery	2011	MB	mG246M
22	HtNi743-11	Niagara Springs Hatchery	2011	MB	mG154M
23	Ht508K-14	Hagerman Valley, Idaho	2014	MB	mG296M
24	HtBrK-16	Hagerman Valley, Idaho	2016	MB	mG331M
25	HtBrG-16	Hagerman Valley, Idaho	2016	MB	mG342M
26	Hg113-89	Farm site 9, Idaho	1989	MC	mG119M
27	Ha30-91	Hagerman Valley, Idaho	1991	MC	mG119M
28	Hg139-93	Farm site 1, Idaho	1993	MC	mG008M
29	Ht051-99	Farm site B, Idaho	1999	MC	mG344M
30	Ht060-00	Farm site B, Idaho	2000	MC	mG071M
31	Ht066-08	Farm site A, Idaho	2008	MC	mG306M
32	HtNi-12	Niagara Springs Hatchery	2012	MC	mG248M
33	Ht087-15	Farm site D, Idaho	2015	MC	mG325M
34	Ht134-17	Hagerman Valley, Idaho	2017	MC	mG335M
35	Hg147-89	Farm site 1, Idaho	1989	MD	mG106M
36	Hg115-90	Farm site 4, Idaho	1990	MD	mG106M
37	Ha39-91	Hagerman Valley, Idaho	1991	MD	mG107M

38	Ht056-99	Farm site B, Idaho	1999	MD	mG107M
39	Ht071-09	Farm site A, Idaho	2009	MD	mG350M
40	Ht113-16	Farm site C, Idaho	2016	MD	mG338M
41	Ht511-14	Hagerman Valley, Idaho	2014	MD	mG298M

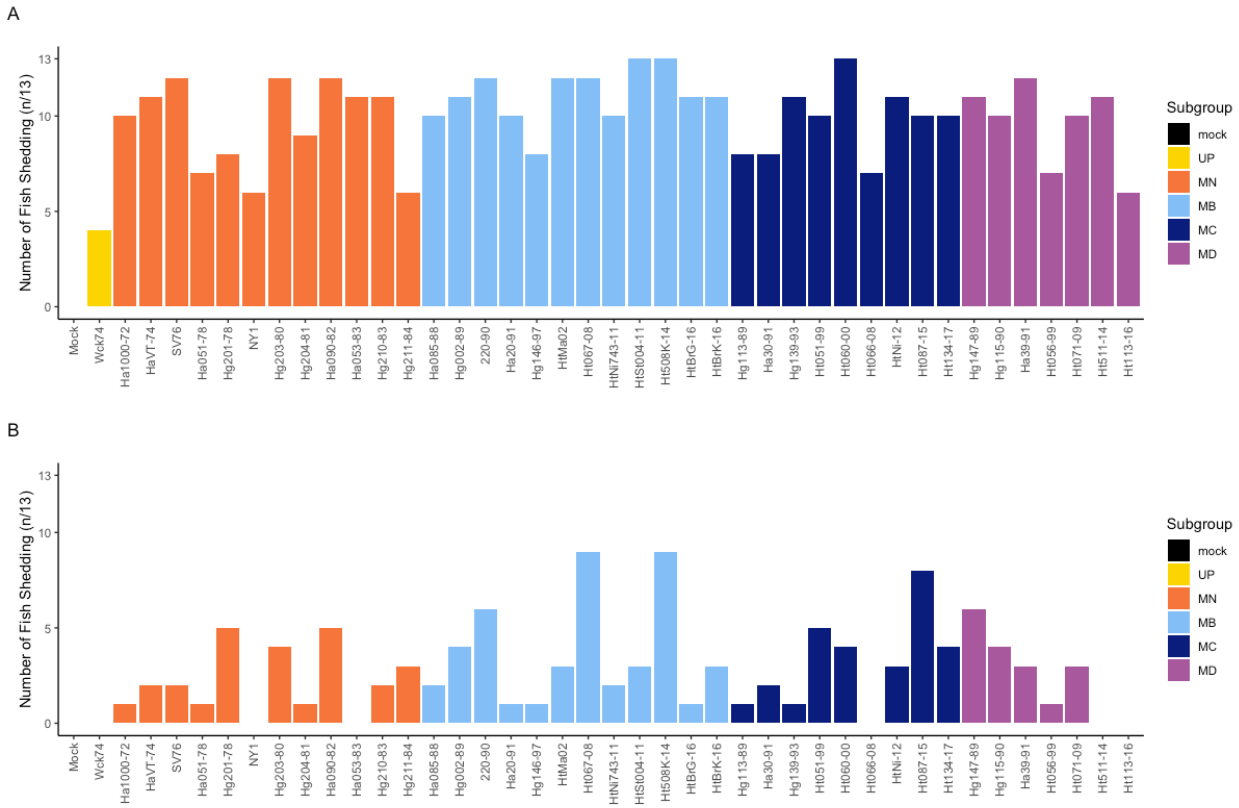

Figure 3.1. Number of fish shedding detectable virus on day 2 (A) and day 5 (B), out of the 13 replicates. The bars are ordered by subgroup classification and then by collection year. A lack of bar indicates no fish shed in that treatment. No virus was detected from Mocks on either day.

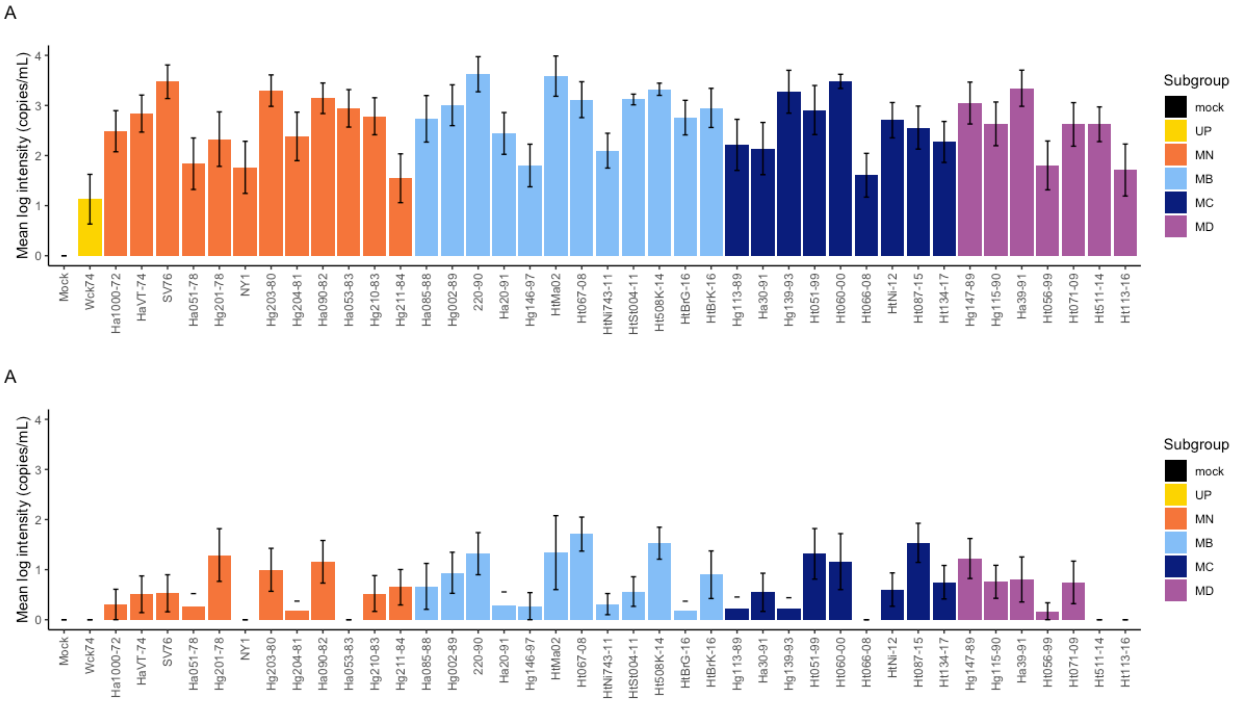

Figure 3.2. Mean shedding intensity with standard error on day 2 (A) and day 5 (B), out of the 13 replicates. Intensity refers only to positive fish; number of fish contributing to mean values is shown in Figure 3.1. The bars are ordered by subgroup classification and then by collection year. A lack of bar indicates no fish shed in that treatment. No virus was detected from Mocks on either day.

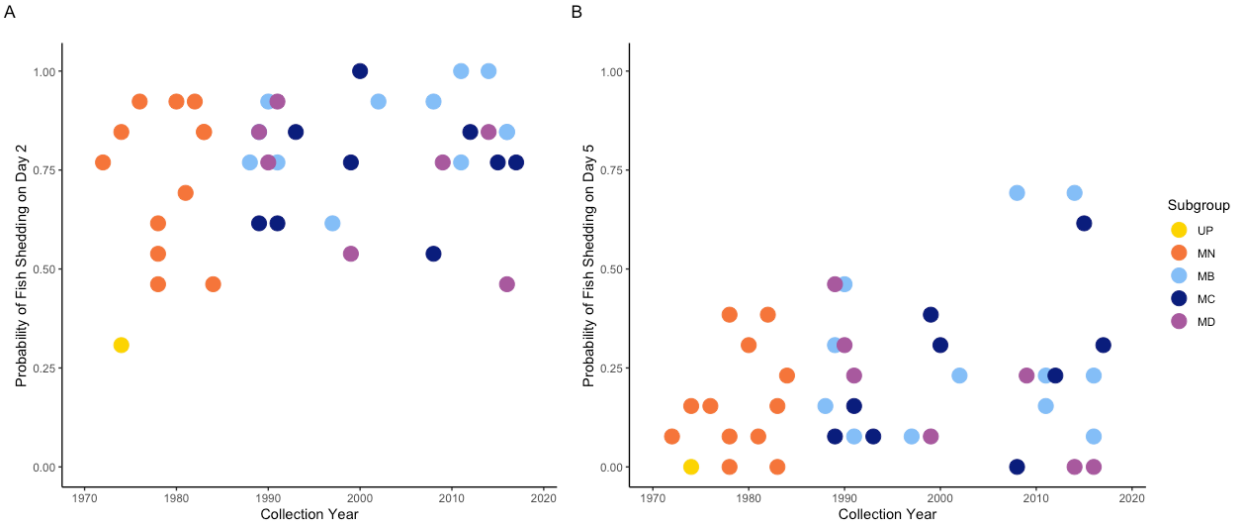

Figure 3.3. Probability of shedding on Day 2 or 5, represented by the proportion of fish replicates(n/13) shedding on Day 2 or 5, respectively. No mock fish shed detectable virus on either day (data not shown).

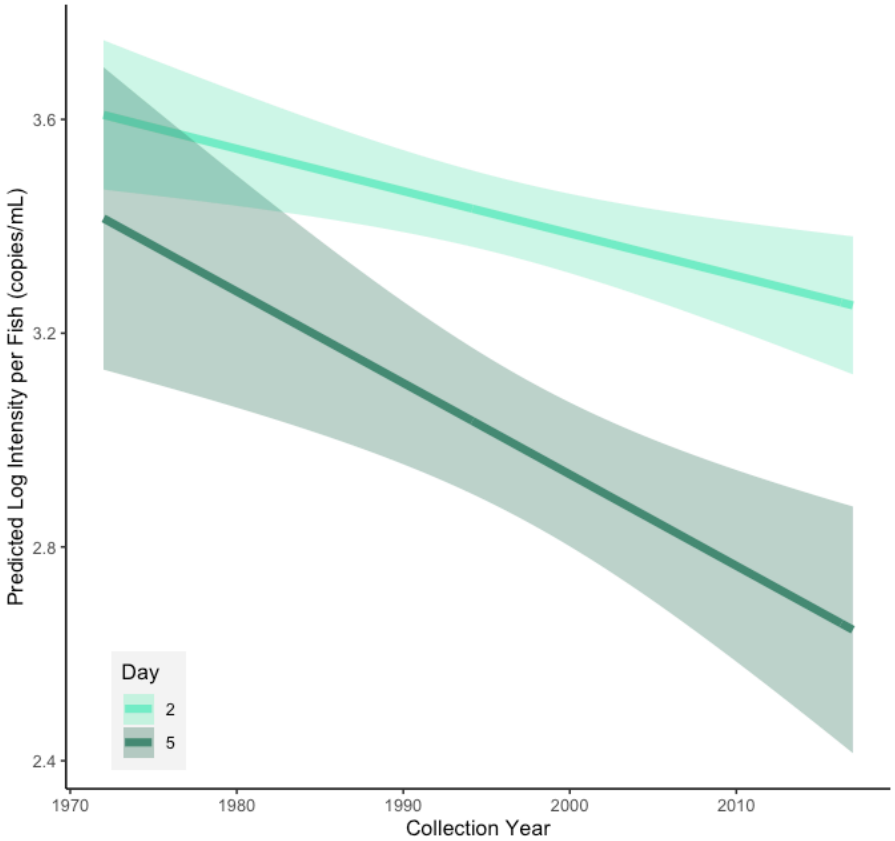

Figure 3.4. Predicted shedding intensity over range of collection years, as output from AICc-selected linear model. Day 2 intensity is shown in light green and day 5 intensity in dark green with 95% confidence intervals. See Table S3.1 for model parameter estimates.

Table 3.2. Univariate statistics for M subgroup phenotype metrics. All shedding metrics are from the shedding assay where isolate treatments had 13 replicate fish. Peak period data were from day 2 post-exposure; post-peak period data were from day 5. Percent shedding refers to the mean number of fish shedding per isolate (there were 13 replicate fish in each isolate treatment). Shedding quantity is reported on a $\log_{10}$ scale with $\log_{10}$ (x+1) transformation; units for quantity and intensity data are copies per mL. Virulence metrics are mean values across isolates from virulence assays where triplicate tanks per isolate had 20 fish each. Low dose was 2000 pfu/mL. Moderate dose was 20000 pfu/mL. Standard error is reported with quantity, intensity, and virulence data.

Subgroup	Number of Isolates Included	Percent shedding: peak ± SE	Percent shedding: post-peak ± SE	Mean Total Quantity ± SE	Mean Peak Intensity ± SE	Mean Post-peak Intensity ± SE	Mean Cumulative Percent Mortality at Low Dose ± SE	Mean Cumulative Percent Mortality at Moderate Dose ± SE
MN	12	74.0 ± 5.0	16.9 ± 4.0	1.63 ± 0.13	3.46 ± 0.06	3.121± 0.13	40.6 ± 4.4	50.7 ± 3.0
MB	12	85.3 ± 3.2	28.4 ± 6.4	1.86 ± 0.15	3.36 ± 0.10	3.20 ± 0.32	48.5 ± 2.9	77.5 ± 3.2
MC	9	75.2 ± 4.8	23.9 ± 6.3	1.74 ± 0.14	3.46 ± 0.11	3.01 ± 0.18	52.3 ± 3.4	72.1 ± 3.5
MD	7	74.2 ± 6.1	18.9 ± 6.5	1.71 ± 0.20	3.48 ± 0.06	2.81 ± 0.24	40.2 ± 5.2	54.6 ± 4.1

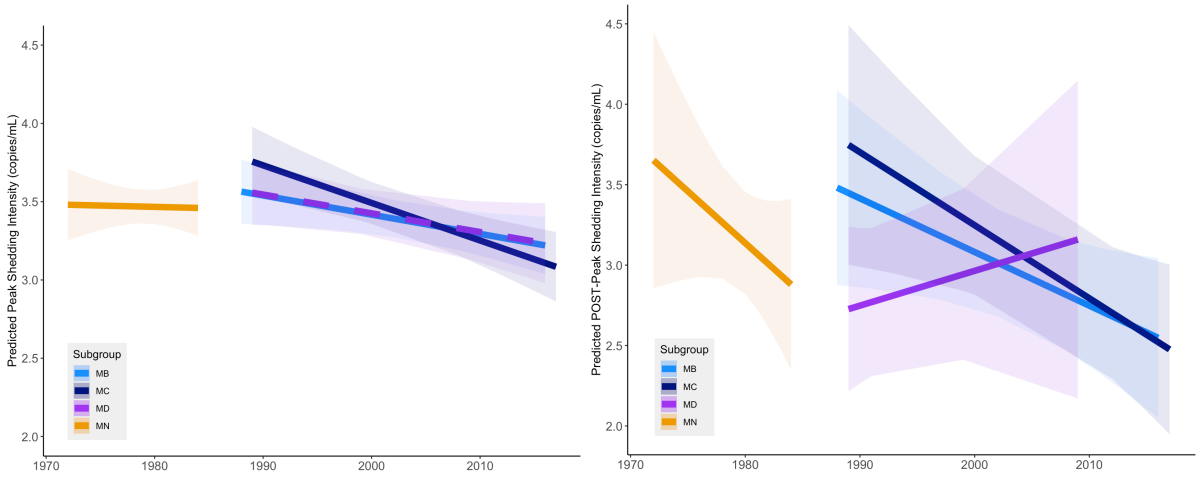

Figure 3.5. Predicted shedding intensity from AICc-selected GLME models on (A) day 2 or (B) day 5, color coded by M subgroup. Subgroups were analyzed separately but are presented on the same plot for ease of comparison. See Tables S3.2-S3.5 for model parameter estimates.

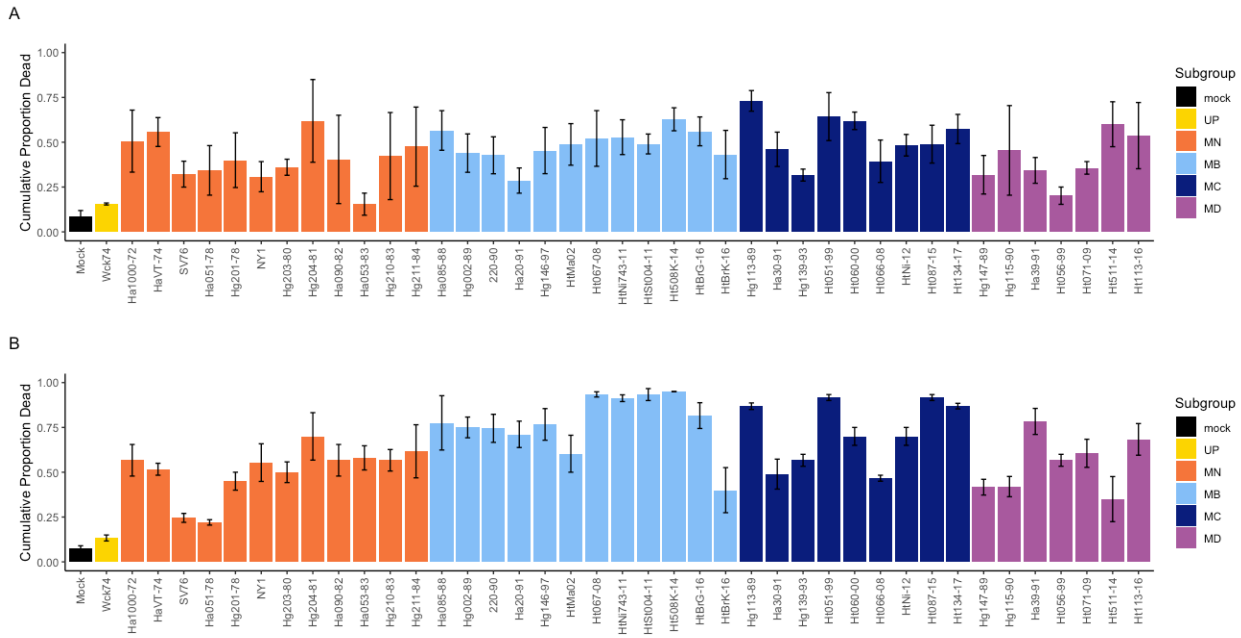

Figure 3.6. Mean cumulative percent mortality on day 30 with standard error bars from low dose (A) and moderate dose (B) experiments. Low dose = $2x10^3$ pfu/mL; moderate dose = $2x10^4$ pfu/mL. Subgroup is denoted by color.

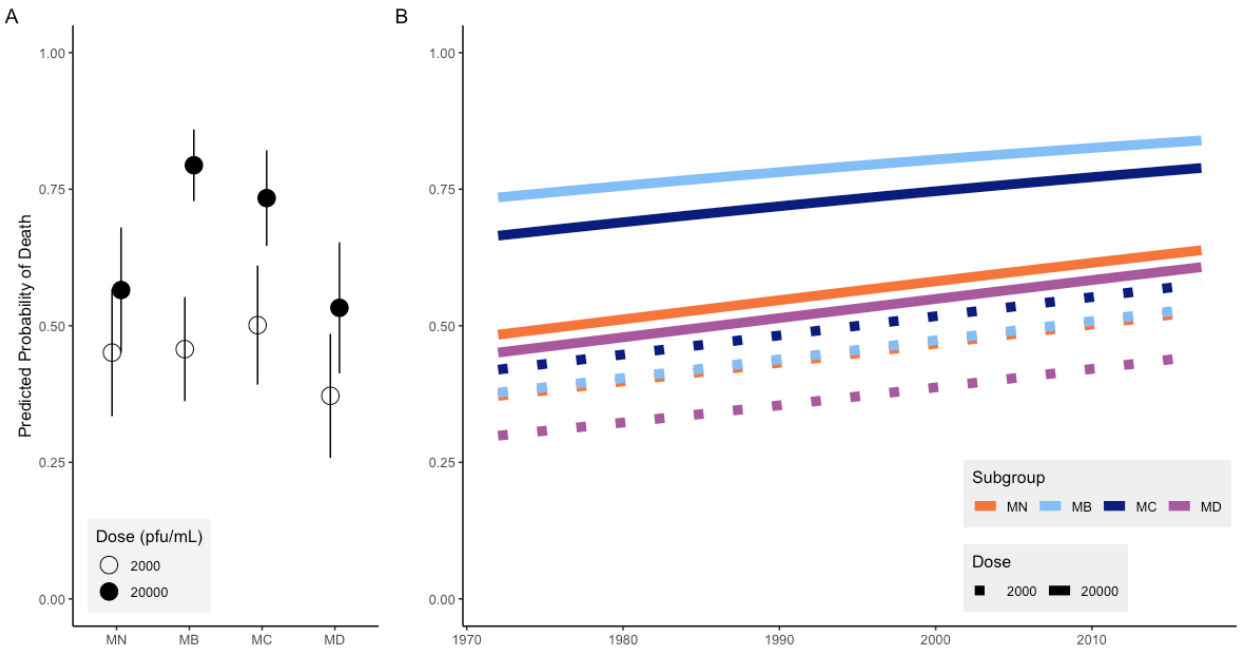

Figure 3.7. Predicted probability of death for M isolates by subgroup with 95% confidence intervals (A) and over evolutionary time (B). Low and moderate doses are indicated respectively by open or solid circles (A) and dotted or solid lines (B). An interaction between dose and subgroup yielded dramatically increasing probability of death for subgroups MB and MC relative to others. Confidence intervals are not displayed on panel B for clarity. Post-hoc Tukey tests yielded the only significant differences among pairwise comparisons for the moderate dose were between MB-MN, and MB-MD, which can be visualized in panel A. No comparisons between low dose data were significant. See Table S3.10 for model parameter estimates.

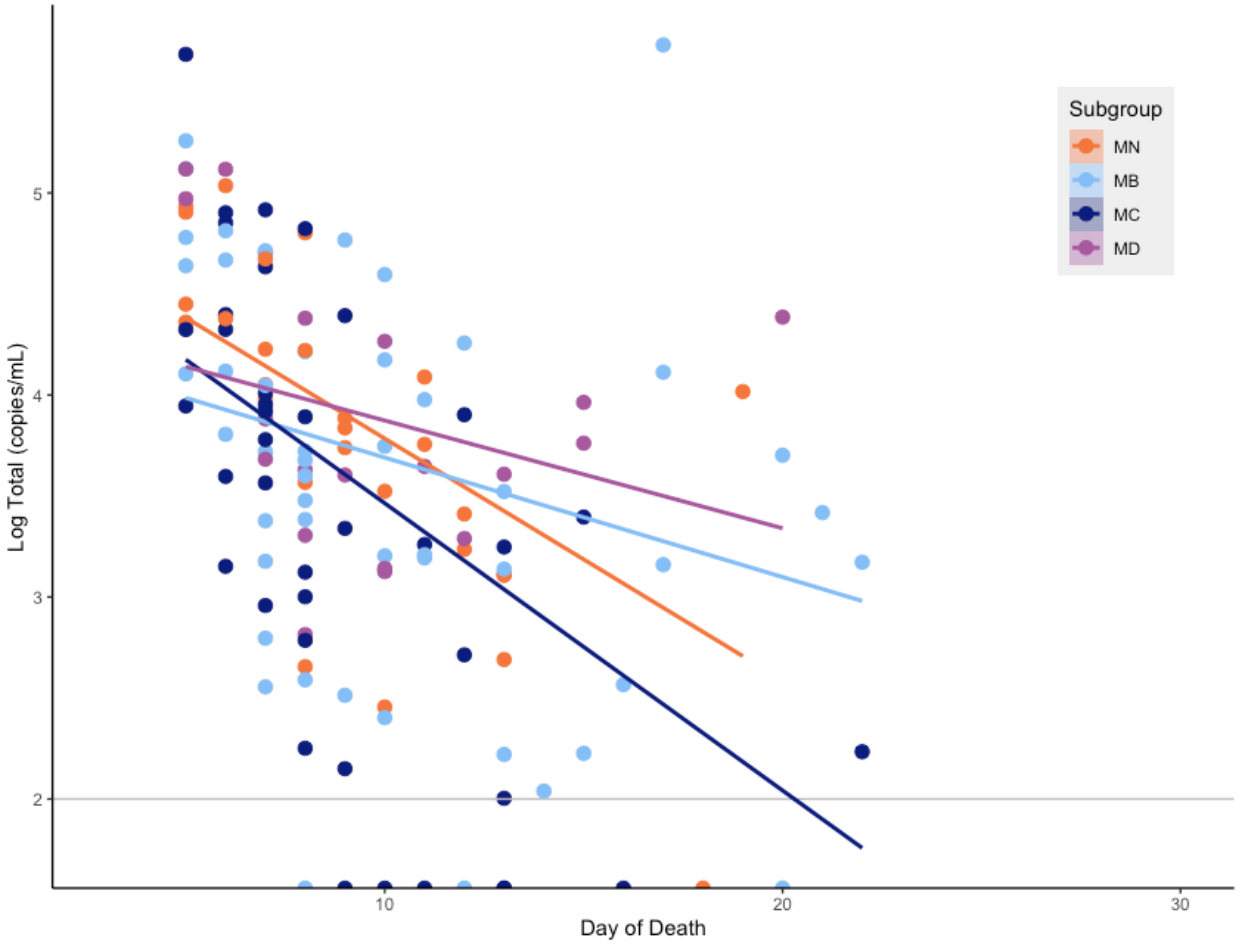

Figure 3.8. Relationship between day of death and log total virus shed for all fish that died over the course of the shedding experiment (n=141). Every dot represents an individual fish, color coded by subgroup. Dots that appear on the x-axis denote fish that died but did not shed detectable virus. Lines are the trendline for each subgroup (y~x).

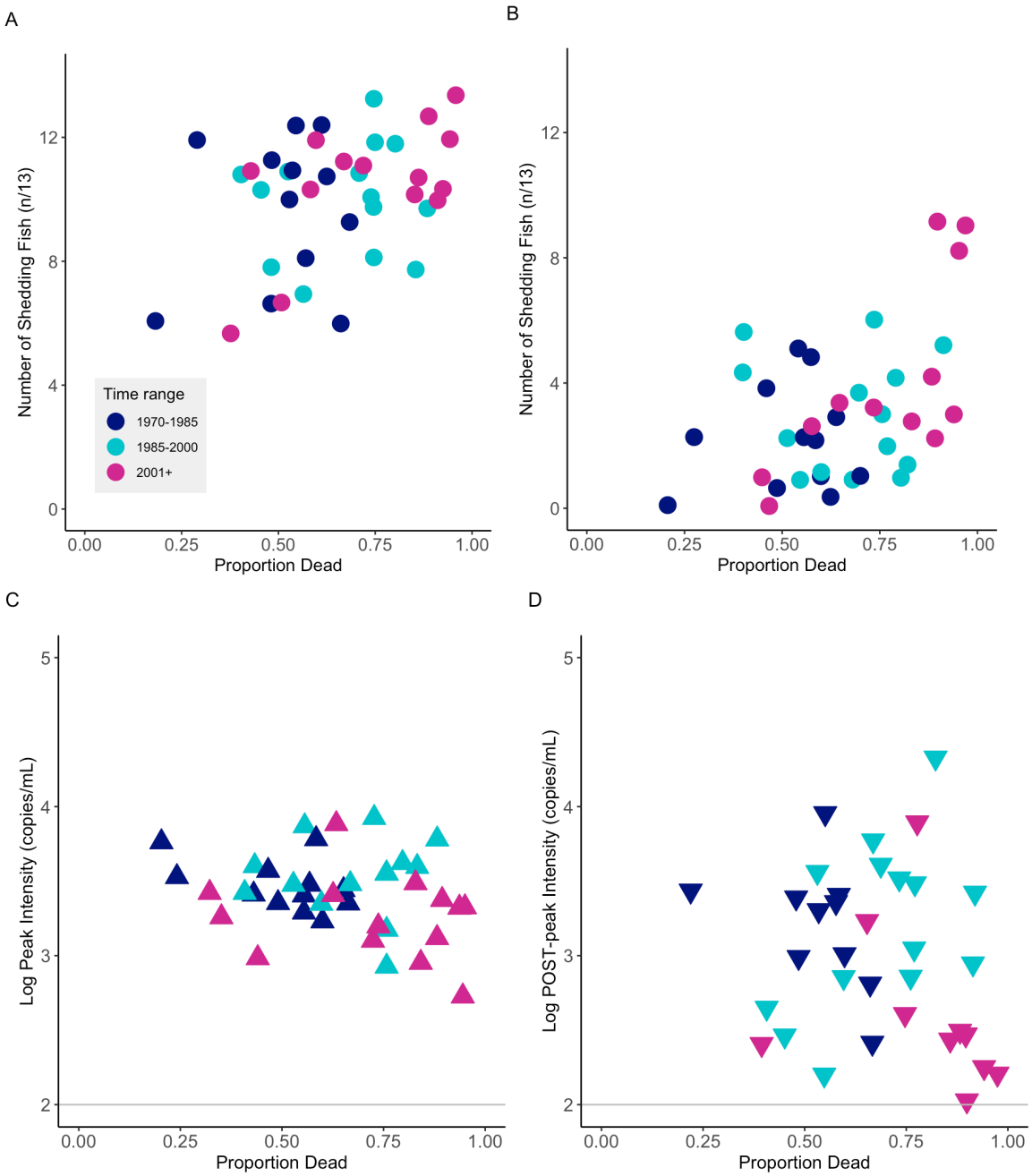

Figure 3.9. Correlation plots relating virulence and shedding metrics for isolates binned by relative time of collection. The x-axis is the same virulence metric for all panels, indicating mean mortality per isolate, as measured in the moderate dose (2 x 10^4 pfu/mL) virulence assay. The y-axis represents different shedding metrics as measured in the shedding assay, including (A) number of fish shedding during peak period (day 2); (B) number of fish shedding during post-peak period (day 5); (C) peak intensity; and (D) post-peak intensity. Points represent mean values for each isolate, where circles indicate shedding numbers and triangles indicate shedding intensity. Gray lines indicate the detection threshold via RT-qPCR. Due to its ancestral age, the MN subgroup and oldest time period are synonymous.

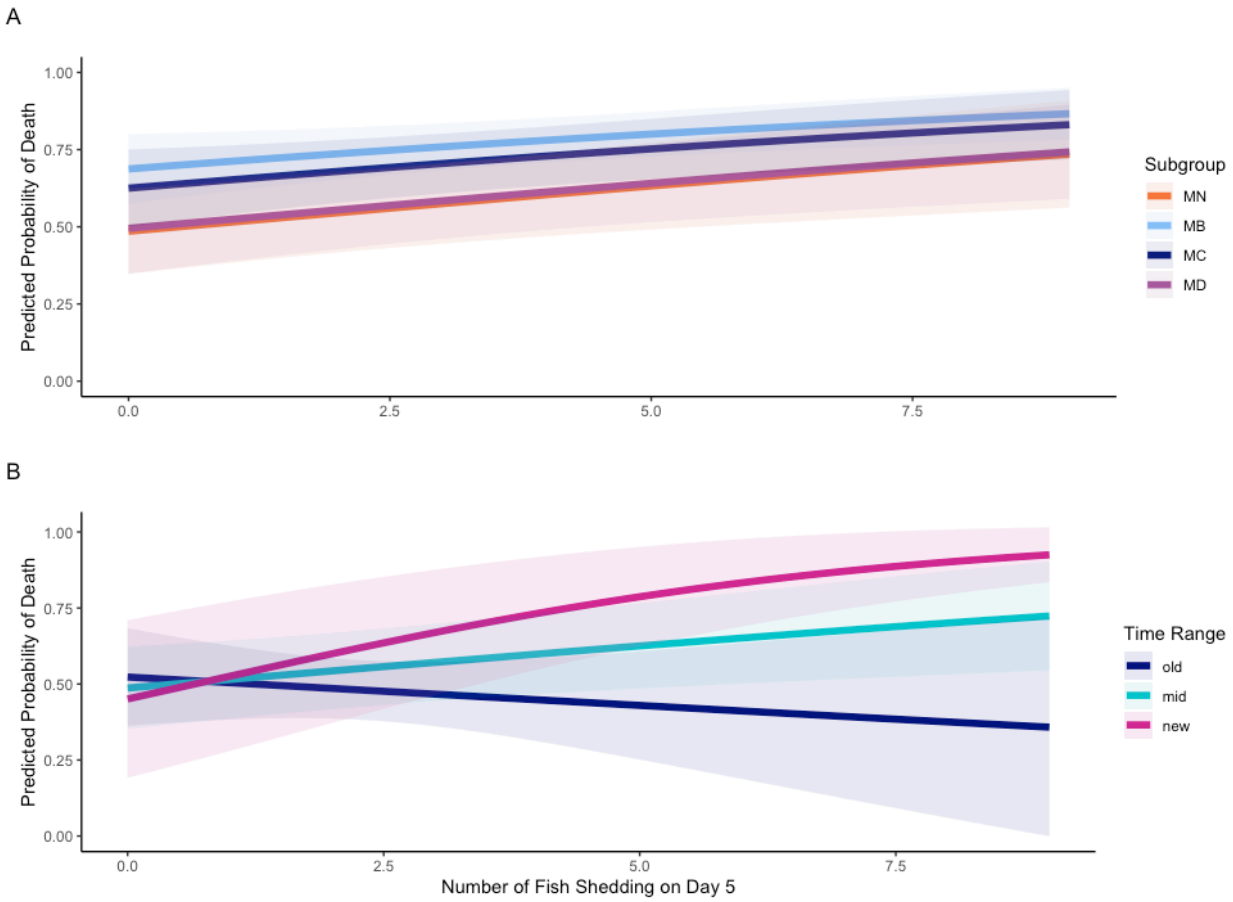

Figure 3.10. Predicted probability of death over range of shedding frequency data from Day 5 shedding assay data with 95% confidence intervals, shown by subgroup (A) and binned collection year (B). To visualize predicted data more easily, output was averaged over collection year (A) and predicted using subgroup constant (B). The trends of probability were consistent regardless of which subgroup subset was used to generate predicted data; data shown were predicted using the most conservative estimate from the MN subset. Data are from AICc-selected model (see Tables S3.11-S3.12).

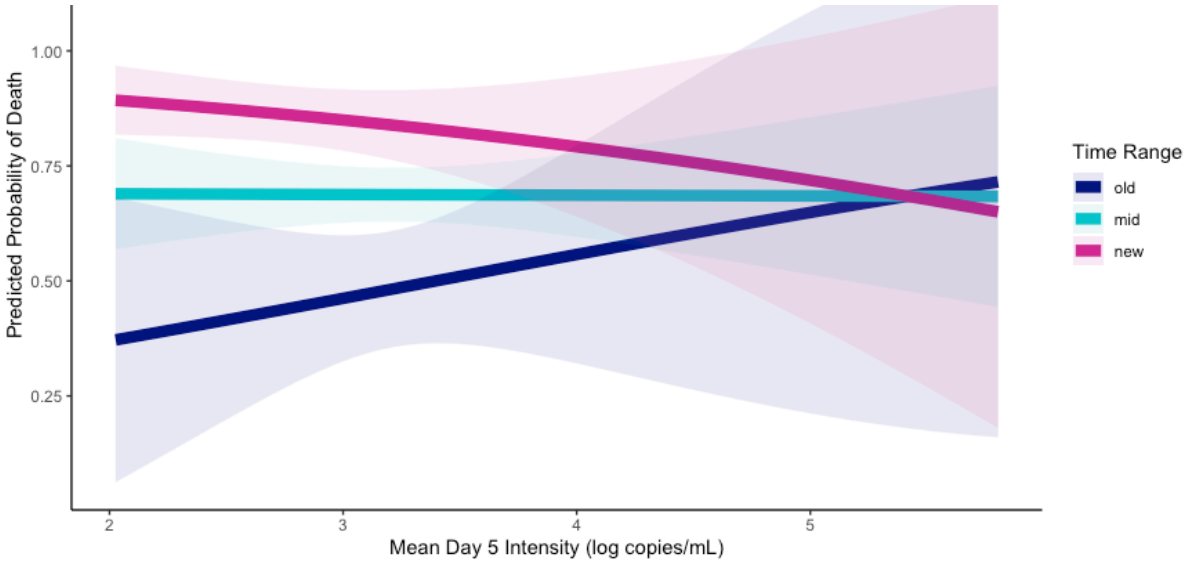

Figure 3.11. Predicted probability of death over range of shedding intensity data from Day 5 shedding assay data with 95% confidence intervals. Collection year is binned into a categorical variable (old = 1970-1985, mid = 1986-2000, new = 2001-2017), to clarify trends**.** Only data from treatments with fish that shed detectable virus on Day 5 were used to parameterize the model; as such, data were dropped from treatments that included isolates Ht511-14, NY1, Ht113-16, Ht066-08, Ha053-83. Very few data were available to parameterize the model for intensity values exceeding 4 log copies/mL, contributing to large confidence intervals. Data are from AICc-selected model (see Table S3.13-S14).

Supplemental Materials

Table S3.1. Summary of AICc selected linear model with Gaussian distribution for estimating intensity of shedding across experimental days for all M isolates. Residual degrees of freedom = 514.

Fixed effect	Estimate	SE	t-value
Intercept	3.386671	0.037771	89.663
Year	0.007919	0.002586	-3.062
Day	-0.450890	0.078356	-5.754
Day*Year	-0.009189	0.005607	-1.639
Intensity ~ Collection Year * Day			

Table S3.2. Summary of AICc selected linear model with Gaussian distribution for estimating peak intensity of shedding for MN isolates (parameterized with day 2 data only). Residual degrees of freedom = 113. Model structure is given at the bottom of the table.

Fixed effect	Estimate	SE	t-value
Intercept	3.432791	0.311136	11.033
Collection Year	-0.001702	0.014606	-0.117
Intensity ~ Collection Year			

Table S3.3. Summary of AICc selected linear model with Gaussian distribution for estimating peak intensity of shedding for MB isolates (parameterized with day 2 data only). Residual degrees of freedom = 131. Model structure is given at the bottom of the table.

Fixed effect	Estimate	SE	t-value
Intercept	3.41707	0.06263	54.56
Collection Year	-0.01226	0.00560	-2.19
Intensity ~ Collection Year			

Table S3.4. Summary of AICc selected linear model with Gaussian distribution for estimating peak intensity of shedding for MC isolates (parameterized with day 2 data only). Residual degrees of freedom = 86. Model structure is given at the bottom of the table.

Fixed effect	Estimate	SE	t-value
Intercept	3.49211	0.06809	51.29
Collection Year	-0.02400	0.00661	-3.63
Intensity ~ Collection Year			

Table S3.5. Summary of AICc selected linear model with Gaussian distribution for estimating peak intensity of shedding for MD isolates (parameterized with day 2 data only). Residual degrees of freedom = 65. Model structure is given at the bottom of the table.

Fixed effect	Estimate	SE	t-value
Intercept	3.425825	0.073240	46.776
Collection Year	-0.011976	0.006783	-1.766
Intensity ~ Collection Year			

Table S3.6. Summary of AICc selected linear model with Gaussian distribution for estimating post-peak intensity of shedding for MN isolates (parameterized with day 5 data only). Residual degrees of freedom = 24. Model structure is given at the bottom of the table.

Fixed effect	Estimate	SE	t-value
Intercept	1.85085	1.01864	1.817
Collection Year	-0.06431	0.04926	-1.306
Intensity ~ Collection Year			

Table S3.7. Summary of AICc selected linear model with Gaussian distribution for estimating post-peak intensity of shedding for MB isolates (parameterized with day 5 data only). Residual degrees of freedom = 42. Model structure is given at the bottom of the table.

Fixed effect	Estimate	SE	t-value
Intercept	3.08142	0.17915	17.20
Collection Year	-0.03335	0.01611	-2.07
Intensity ~ Collection Year			

Table S3.8. Summary of AICc selected linear model with Gaussian distribution for estimating post-peak intensity of shedding for MC isolates (parameterized with day 5 data only). Residual degrees of freedom = 26. Model structure is given at the bottom of the table.

Fixed effect	**Estimate**	**SE**	**t-value**
Intercept	3.24788	0.21981	14.776
Collection Year	-0.04540	0.01906	-2.382
Intensity ~ Collection Year			

Table S3.9. Summary of AICc selected linear model with Gaussian distribution for estimating post-peak intensity of shedding for MD isolates (parameterized with day 5 data only). Residual degrees of freedom = 15. Model structure is given at the bottom of the table.

Fixed effect	**Estimate**	**SE**	**t-value**
Intercept	2.96450	0.28878	10.27
Collection Year	0.02164	0.02965	0.73
Intensity ~ Collection Year			

Table S3.10. Summary of AICc-selected GLME model with binomial distribution for estimating probability of death using data from the virulence assay. Residual degrees of freedom = 229. The reference level for Subgroup was set to MN. Model structure is given at the bottom of the table.

Fixed effect	Estimate	Std.Error	z-value
(Intercept)	-0.1317	0.2697	-0.4884
SubgroupMB	0.0254	0.3422	0.0743
SubgroupMC	0.2018	0.3579	0.5639
SubgroupMD	-0.3274	0.3687	-0.8882
Dose20000	0.4604	0.2055	2.2410
Year	0.0141	0.0093	1.5069
SubgroupMB:Dose20000	1.0597	0.2959	3.5819
SubgroupMC:Dose20000	0.5487	0.3166	1.7333
SubgroupMD:Dose20000	0.1958	0.3378	0.5796
cbind(NumberDead, NumberAlive) ~ Subgroup * Dose + Collection Year + (1|Isolate) + (1|Tank)			

Table S3.11. GLME model selection table for modeling predicted probability of death over range of shedding frequency data. Model 1 is the best fit model reported in Results. Global model structure tested is reported at bottom of table. Abbreviated results are reported here after initial model selection determined Day 2 Frequency was not a meaningful predictor and no other interaction terms were meaningful.

Model	Intercept	Year	Sub group	D5 Freq	D2 Freq	Year* D5	df	loglik	AICc	ΔAICc	AICc weight
1	0.7876	-0.006	+	0.11990		0.0084	8	-298.7	614.7	0.0	0.255
2	0.2721	0.004		0.13750		0.0098	5	-302.7	615.9	1.19	0.141

cbind(NumberDead, NumberAlive) ~ CollectionYear * Subgroup * Day5 Frequency + Day2 Frequency + (1|Isolate)

Table S3.12. Summary of GLME with binomial distribution for estimating predicted probability of mortality with shedding frequency data. Residual degrees of freedom = 112. Reference level for subgroup predictor is MN. Model structure is given at the bottom of the table.

Fixed effect	**Estimate**	**SE**	**z-value**
(Intercept)	-0.058211	0.281708	-0.207
Collection Year	-0.006434	0.015403	-0.418
Day5 Frequency	0.119946	0.051823	2.315
Subgroup MB	0.845799	0.381072	2.220
Subgroup MC	0.569130	0.391950	1.452
Subgroup MD	0.038050	0.411743	0.092
Collection Year* Day5 Frequency	0.008354	0.003660	2.283

cbind(NumberDead, NumberAlive) ~ CollectionYear * NumSheddingDay5 + Subgroup + (1|Isolate)

Table S3.13. GLME model selection table for modeling predicted probability of death from shedding intensity data. Model 1 is the best fit model reported in Results. Global model structure tested is reported at bottom of table. Abbreviated results are reported here after initial model selection determined Day 2 Intensity and Subgroup were found not to be meaningful predictors.

Model	Intercept	Year	Sub group	D5 Intensity	D2 Intensity	Year* D5 Intensity	df	loglik	AICc	Δ AICc	AICc weight
1	0.260	0.004		0.646		0.047	5	-303.9	618.2	0.0	0.27
2	0.019	-0.003	+	0.520		0.038	8	-300.6	618.5	0.25	0.24

cbind(NumberDead, NumberAlive) ~ CollectionYear * Day5 Intensity + Day2 Intensity + Subgroup + (1|Isolate)

Table S3.14. Summary of GLME with binomial distribution for estimating predicted probability of mortality with shedding intensity data. Residual degrees of freedom = 112. Reference level for subgroup predictor is MN. Model structure is given at the bottom of the table.

Fixed effect	**Estimate**	**SE**	**z-value**
(Intercept)	0.83140	0.68921	1.206
Collection Year	0.09382	0.05484	1.711
Day5 Intensity	-0.01081	0.21008	-0.051
Collection Year* Day5 Intensity	-0.01732	0.01750	-0.990

cbind(NumberDead, NumberAlive) ~ Collection Year * Day5 Intensity + (1|Isolate)

CHAPTER 4: Quantifying viral transmission rate over the course of IHNV infection in rainbow trout (*Oncorhynchus mykiss*)

ABSTRACT

Infectious hematopoietic necrosis virus (IHNV) represents a resource-rich system for exploring the viral dynamics of shedding and transmission. This chapter explores how shedding fitness at the individual level directly translates to transmission to new hosts. Generally shedding quantity has been considered the most accurate proxy of transmission potential and theorized to be a good metric for viral fitness overall, but few studies have empirically measured transmission. Evolutionary trends identified thus far in the IHNV-rainbow trout host system include increased virulence and variable shedding intensity and durations. Whether transmission success correlates with one or more of these virulence and shedding traits is unknown. Using juvenile rainbow trout hosts and two isolates, which represent old and new IHNV strains as well as low and high virulence phenotypes, this chapter examines how shedding is associated with transmission. This was achieved using a novel method of paired cohabitation at discrete time points over one week following host infection. Results demonstrated a reduction in infectiousness of shed virus over the course of host infection. Additionally, shedding intensity was not a strong predictor for transmission success. This study underscores the importance of considering not only replication and shedding success for viruses but also temporal nuances in transmission dynamics.

INTRODUCTION

Transmission throughout a population, typically represented by the theoretical metric R_0, is the ultimate measure of viral fitness. Persistence of pathogens and their associated disease risk hinges on how readily the pathogen can move through populations. A prevalent assumption in epidemiological research is that viral shedding is a good proxy for transmission (1). This assumption is more accurately framed as transmission potential, since quantification of viral shedding via molecular methods such as quantitative PCR typically lacks the ability to identify whether shed virions are viable to infect and replicate in subsequent hosts. This is a common challenge across host-pathogen systems, and studies frequently lack the opportunity to examine transmission beyond shedding. Validation of the assumption that viral shedding is an accurate proxy for transmission is thus warranted, through direct measurement of the associations between shedding rate, shedding duration, and transmission success. This also makes it possible to determine how these associations change over the course of infection; that is, whether the infectivity of virus shed early in the infection differs from that shed later in the infection.

Various relationships between viral transmission, virulence, and shedding fitness have been proposed. The virulence-transmission tradeoff theory puts forth that host virulence via pathogen replication and shedding is a necessary consequence of pathogen transmission pathways, but the strength and variability of this relationship has been difficult to ascertain (2, 3). Evolution in the short term and translation to long term transmission dynamics has been explored theoretically (4, 5). Transmission dynamics in relation to pathogen shedding remains poorly understood. Empirical inquiry is needed to explore the base question of what the relationship is between the amount of virus shed and the associated transmission. Furthermore, how does infection dose and transmission efficacy vary across genetically distinct strains of virus and the time since initial host infection?

Past studies in the infectious hematopoietic necrosis virus (IHNV) system have yielded considerable insights into the variety of fitness phenotypes that have impacted the trout farming industry from the time of disease emergence. IHNV continues to pose immense disease challenges to salmonid aquaculture. Virulence of IHNV has been steadily increasing among isolates dominant on the farm landscape since emergence in the rainbow trout host (*Oncorhynchus mykiss*) (Chapter 1). This relationship has been demonstrated along multiple branches of the M-genogroup associated with the trout host, indicating a consistent exacerbated disease risk in farm settings (Chapter 3). To some degree, shedding phenotypes also appear to be under selection in the IHNV system. While not as ubiquitous as the shift in virulence type, shedding intensity and duration phenotypes are changing for IHNV (Chapters 2, 3). Intensity measured across multiple days during the peak shedding periods for selected M-genogroup isolates indicated a decrease in time (Chapter 2), but a follow-up study with more extensive representation across collection years identified mixed trends across M subgroups (Chapter 3). Variation in the post-peak shedding period suggested that clearance rate and shedding duration may provide evolutionary space for viral isolates to adapt (Chapters 2, 3). A transmission model found a correlation between low virulence IHNV types and higher transmission, but persistence of low-virulence phenotypes depended on fish culling practices enacted in farm settings (6). Whether or not real transmission correlates with shedding metrics, either as mean values over the shedding period or at discrete time points, is unknown. Evaluating transmission among currently circulating isolates of IHNV is particularly pertinent to commercial aquaculture since the practice of sterilizing eggs in hatcheries and farms functionally precludes vertical transmission in the system and forces IHNV to rely on horizontal transmission for persistence.

IHNV transmission studies have explored allowing uninfected fish and infected fish to share water to elicit horizontal transmission in serial passage experiments (7). The introduction of a single infected fish to naïve groups of cohabitating fish has also been tested, to emulate introduction of an infected individual into a new population, but this method is complicated by

relatively low shedding rates produced by single infected donors as well as individual host variability (8). Using a balanced design of infected hosts and naïve recipients, as well as repeatedly and non-destructively measuring transmission from individual fish, would eliminate some of the variability encountered by these designs.

In this study, we aim to measure transmission success over the course of infection and determine how it is associated with quantity of virus shed as measured by quantitative PCR. Building upon procedures developed by previous examiners in the IHNV system, here we present a novel method for measuring transmission rate of IHNV using a donor: recipient *in vivo* design (7, 8). Understanding the relationships of shedding, recovery, and transmission is not only critical for modeling IHNV epidemiology for the benefit of trout aquaculture, but also provides a rare opportunity to dissect viral fitness into discrete quantifiable traits. There is a strong case for managing pathogen transmission in farms and collating data relevant to guiding virulence evolution in both agriculture and public health (4, 9, 10). If critical stages of transmission or mechanisms of transmission could be identified, new tools or methods might be identified for improved disease management in commercial aquaculture, salmonid conservation efforts, and other systems.

METHODS

1. Virus and Host

Virus isolates were selected to represent a high virulence and a low virulence phenotype, as well as old and new isolates from the M-genogroup of IHNV (Table 4.1). Previous work identified the isolate Ht134-17 to be highly virulent in juvenile rainbow trout hosts. Ht134-17 belongs to a more recently emerged subgroup of IHNV (Chapter 1 data). The same study identified the isolate HaVT-74 as a strain with low virulence by comparison. HaVT-74 is representative of

IHNV virulence phenotypes shortly after its host jump to rainbow trout (Chapter 1 data). Isolates were obtained from the USGS IHNV archive and stored in MEM-10 at -80°C until use as previously described (Chapter 1).

Rainbow trout (*Oncorhynchus mykiss*) were obtained from Trout Lodge and raised from eggs to a mean size of 2.2 grams on UV-irradiated flow-through water held at 15°C at the Virginia Institute of Marine Science (Gloucester Point, VA) as previously described (Chapter 1-2). The fish were split into two categories, donors and recipients. Donor fish were marked by clipping the adipose fin under anesthesia (0.0001% MS-222, pH 7.0) and allowed to recover for three weeks prior to in vivo challenge**.** All animals were handled in accordance with William & Mary IACUC protocols (IACUC-2021-07-02-15072-arwargo).

2. *In vivo experiment: a novel cohabitation design*

To measure transmission, a cohabitation assay was used. Initially, two groups of 25 donor fish per treatment were exposed to virus (200000 PFU/mL) by immersing them in a 6L tank in a 1L volume of static water with aeration for one hour, then washed for one hour with high flow (750mL/min), as previously described (Chapter 1-2). A Mock treatment included 5 donor fish dosed only with the diluent used for virus inoculant, Minimum Essential Media with 10% fetal bovine serum. After the one-hour wash, the donor fish were separated into individual 0.8L tanks (static, aerated) containing one naïve recipient per tank (hereafter termed “T1” to represent the first timepoint). The donor and recipient fish were allowed to comingle for 47 hours, then a water sample was taken from each tank to determine the shed load from the donor fish, the functional exposure dose for the recipient fish. The recipient fish was subsequently transferred to a new tank. This process was repeated with a new recipient fish 4 and 6 days post-exposure using the same donor fish (“T2” for the second timepoint and “T3” for

the third timepoint, respectively). As such, transmission from the same donor fish was measured at 3 independent time points: 2, 4, and 6 days post initial exposure to virus.

For each recipient fish, after the cohabitation period and transfer to a new tank the fish received a 1hr flush (200mL/min, or approximately 15 water exchanges) to eliminate any donor virus that might have been transferred with the recipient, then held static for three days (with aeration). Water samples were taken on the third day after its separation to determine whether recipient fish began shedding (indicating a transmission event occurred between donor and recipient). After cohabitation, the donor fish tanks were also flushed to eliminate virus for one hour (>200mL/min) before the next cohabitation time period. On each sample day, a 750mL water sample was taken and stored at -80°C until quantification.

3. *Virus quantification*

RNA was extracted consistently with previous chapters, according to protocol described previously (11). Extracted RNA was reverse transcribed and quantified via 1-step digital qPCR on a QIAcuity 4 (QIAGEN) with the following master mix reagents per 8uL extracted sample: 3.25uL 4x Probe Master Mix, 0.13uL 100x RT Master Mix, 0.234uL Forward Primer (50μMol), 0.234uL Reverse Primer (50μMol), 0.26uL Probe (10μMol), and 0.892uL nuclease-free water. All samples were loaded using QIAcuity dPCR Nanoplates (8.5K partitions, 96-well). The primers and probe correspond to the IHNV N-gene as previously described (12). Cycling parameters were as follows: 50°C for 40 minutes (reverse transcription), 95°C for 2 minutes, followed by 50 cycles of 95°C for 5 seconds (denaturing), and 60°C for 30 seconds (annealing and extension). Imaging conditions used exposure durations of 800ms (Green channel) and 500ms (Yellow channel) with Gain 6. Output was processed according to manufacturer's instructions with a minimum threshold value of 60 RFU. All samples were visually inspected for image quality before fluorescence measurements were used in analysis.

4. Statistical analysis

Analyses were conducted in R (version 3.4.2) and RStudio (13, 14). To analyze the probability of transmission over the three cohabitation timepoints, a generalized linear model (GLM) approach was used with transmission event status (binomial; 0 = no transmission or 1 = successful transmission) as the response and predictors of timepoint (continuous) and viral isolate (categorical). To assess how transmission success varied with the quantity of virus shed by the donor (exposure dose for recipient) during the first timepoint which constituted peak shedding, a generalized linear mixed effects model (GLME) approach was used (14). Here the response variable was again transmission event status (binomial) and the predictors included viral isolate (categorical) and donor shed quantity (continuous) as fixed effects, and donor (repeated measure unit) as a random effect. Donor shed quantity was normalized with a $\log_{10}(x)$ transformation. Model selection was based on a ΔAICc threshold of 2, as previously described (chapters 1-2).

RESULTS

Nearly all donor fish shed during timepoint T1 and the proportion of positive donors declined at each subsequent timepoint (Figure 4.1, raw data). No viral shedding was detected in mock pairs at any timepoint (data not shown). Donor fish in the HaVT-74 treatment, which represented low-virulence, old M virus, shed more during T1, but no shedding differences were present between the isolates during T2 or T3 (Figure 4.2, Table S4.1). Of the original 50 donor:recipient pairs per treatment, only 1 pair in the HaVT-74 treatment had a transmission event at T3 whereas 5 pairs in the newer isolate Ht134-17 treatment had transmission events (Figure 4.3, raw data).

The generalized linear model analysis indicated that the probability of transmission declined steadily, such that each timepoint was 0.30 times less likely to result in a transmission event relative to the previous timepoint (Figure 4.4, Tables S4.1-S4.2). Since this analysis included only data from donors shedding detectable virus, this result is reflective of reduced probability of transmission for a given donor fish. In other words, donors actively shedding virus exhibited decreased infectiousness over the measured time points. However, the probability of transmission was not found to significantly differ between the viral isolates, regardless of time point, despite suggestive trends that the HaVT-74 isolate produced more transmission events at T1 and T2 than Ht134-17, and vice versa at T3 (Figure 4.3, Table S4.3). It should be noted that four alternative models were within $\Delta AICc < 2$ of the best fit model (Table S4.2). Three of the models indicated a timepoint effect as described, three indicated a difference between virus isolates, and one indicated an interaction between virus isolate and timepoint. Models that included a random effect of donor would not converge and were not considered further.

The analysis of the relationship between donor fish shedding quantity and transmission success indicated no relationship between the quantity of virus shed and probability of transmission (Figure 4.5). The overall transmission probability was predicted at 38.4% across shedding dosages of 2.0-4.7 log copies/mL, the detected range of donor shedding at T1 (Figure 4.5). The model did not indicate a difference in relative infectiousness as a function of shedding quantity, or between the viral isolates, despite a suggestive trend that the newer isolate Ht134-17 remained infectious over a longer duration (Figures 4.2-4.3). The experimental design allowed for calculation of the amount of virus shed needed to infect 50% of fish (ID_{50}). ID_{50} did not vary significantly between time point or virus isolate and was estimated to range between 9 - 376 viral RNA copies/mL (Figure 4.6).

DISCUSSION

This chapter explored how isolate transmission success varied over one week following exposure between an old and new representative virus, as well as a low virulence and high virulence phenotype for IHNV. Generally, transmission success decreased through time, loosely correlating with the number of donor fish shedding, but did not demonstrate a strong relationship with exposure dose for recipient fish. There was a suggestive trend that the more recently emerged, high virulence-typed isolate corresponded had greater shedding and transmission success in the later infection period, but this was not statistically resolved.

Previous studies in this and other systems indicate that viral shedding is an accurate proxy for transmission (7, 15, 16). In the IHNV system there has also been evidence of higher virulence and shedding correlating with in-host viral replication (17, 18). Here, although the probability of transmission and quantity of virus shed decreased over the course of infection, there was no observed association between transmission and shedding (Figures 4.2, 4.4, 4.5). Furthermore, it did not appear to be associated with viral isolate virulence or collection, as previously described (Chapters 1-2). This finding agrees with a previous study that investigated infectivity of IHNV in the context of serial displacements of IHNV genotypes in steelhead (anadromous *O. mykiss*) populations from a field landscape, where transmission was not correlated with virulence or emergence time (19).

A caveat of this study is the examination of only two genotypes from a diverse phylogenetic tree. As explored in Chapter 3, IHNV inhabits a wide range of phenotypes across the M-genogroup, and the shedding phenotype displayed by the two examined here may not be representative of all isolates. Hernandez et al. began to compare infectivity across the IHNV tree in Chinook salmon (*O. tshawytscha*) by comparing representative viruses from the U, M, and L-genogroups which have all been detected in Chinook hosts (20, 21). While virulence among the genogroups varied significantly, infectivity did not, except between two host populations with differing life histories (21). Recent advances in the field have demonstrated that

population-level differences in exposure may significantly influence epidemiological dynamics (22–24). Host population factors were beyond the scope of the present study.

The role of individual variability both in shedding donor hosts and among susceptible recipients is notable since almost no relationship was identified among donor shedding quantity (exposure dose) and transmission success. Host to host variation in susceptibility may thus be playing a larger role in driving transmission success than the quantity of virus shed into the environment. Individual host susceptibility has been shown to strongly influence transmission rates in other systems, sometimes even more than density-driven contact rates (24, 25). Genetics and immunological factors also undoubtedly influence transmission dynamics but were also beyond the scope of this study. Thus far, infectivity of IHNV does not appear to vary on the same scale that virulence or shedding phenotypes do.

Our study indicates that the relationship between virus shedding quantity and transmission is weak at the individual fish level. Despite this, we did observe that IHNV is infectious at extremely low shedding titers, with ID_{50} values ranging as low as 10 viral RNA copies/mL, with the cohabitation assay used. This is in line with studies from the field, which have observed epidemics, when viral titers detected in the environment are low (26–30). As such, even low titers of virus have been predicted to be epidemiologically relevant for densely congregating salmonids (31).

Viral shedding is posited to be associated with virulence and is selected on in tandem with transmission success, resulting in an evolutionary balance between transmission success by viral shedding and duration over the host recovery period (tradeoff theory). Infectiousness as a function of shedding over the recovery period is a current issue not only for IHNV but also understanding viral epidemiology in agriculture and public health at large. There is evidence from studies in several different host types including rabies, Ebolavirus and HIV, and butterfly parasites, that high virulence may correlate with high transmission rates (37–41). However, there are also multiple contemporary examples that have demonstrated that variation in

virulence does not always correlate with variation in transmission strategies, especially where artificial modulation of the pathogen transmission pathway occurs (1). Ascertaining whether there are commonalities in shedding and transmission dynamics could directly inform the mechanisms behind viral transmission.

While it is unclear from this study whether shedding quantity or shedding duration is a weightier factor for IHNV transmission, the possibility of adapted shedding durations is important to consider in disease management practices. A 2017 community study of human influenza virus demonstrated that isolates that shed over an extended duration were more successful in maintaining transmission through time relative to isolates with a shorter shedding duration (42). This differential transmission fitness also resulted in reduced influenza virulence, adding to the growing body of work that demonstrates how shifts in shedding kinetics may also have implications for virulence evolution and long-term viral prevalence (16, 42, 43). These dynamics are particularly useful to consider in systems where host populations experience high density and evolution may subsequently occur in a condensed time frame due to elevated host contact rate. Such examples include myxomatosis, IHNV, and influenza, all case studies in which hosts congregate with extremely high turnover (through rapid reproduction, stocking, or social behavior patterns, respectively). Viral evolution and diversity in these systems suggest that sustained transmission success via prolonged shedding can constitute high evolutionary fitness in settings where dense populations facilitate horizontal transmission pathways.

In summary, examining transmission dynamics and possible variation is crucial for understanding evolutionary fitness over time. Particularly for host-pathogen systems which are highly managed, being able to anticipate which mechanisms may facilitate pathogen success is vital to safeguarding human and environmental health. This chapter, alongside previous findings, highlights that shedding intensity is not necessarily the most informative metric for assessing disease risk, and that transmission success and shedding duration are highly nuanced. The later infection period following peak shedding is worth investigating further in the

IHNV system. A more subtle evolutionary strategy focused on prolonged shedding may be the most important part of ensuring long term viral persistence in commercial trout farms. Whether this is the strategy for IHNV may require expanded assessment of transmission success of multiple viral isolates at various timepoints. Future work may consider incorporating a broader range of viral genotypes as well as host factors to fully understand both the relationship of IHNV transmission fitness and evolutionary fitness, as well as the evolutionary trajectory in trout farms and other heavily managed agricultural systems.

References

1. A. R. Wargo, G. Kurath, Viral fitness: Definitions, measurement, and current insights. *Current Opinion in Virology* **2**, 538–545 (2012).

2. S. L. Messenger, I. J. Molineux, J. J. Bull, Virulence evolution in a virus obeys a trade-off. *Proceedings of the Royal Society of London - Biological Sciences* **266**, 397–404 (1999).

3. J. J. Bull, A. S. Lauring, Theory and Empiricism in Virulence Evolution. *PLOS Pathogens* **10**, e1004387 (2014).

4. D. Ebert, J. J. Bull, Challenging the trade-off model for the evolution of virulence: Is virulence management feasible? *Trends in Microbiology* **11**, 15–20 (2003).

5. B. R. Levin, J. J. Bull, Short-sighted evolution and the virulence of pathogenic microorganisms. *Trends in Microbiology* **2**, 76–81 (1994).

6. A. R. Wargo, G. Kurath, R. J. Scott, B. Kerr, Virus shedding kinetics and unconventional virulence tradeoffs. *PLOS Pathogens* **17**, e1009528 (2021).

7. J. Doumayrou, M. Gray Ryan, A. R. Wargo, Method for serial passage of infectious hematopoietic necrosis virus (IHNV) in rainbow trout. *Diseases of Aquatic Organisms* **134**, 223–236 (2019).

8. H. Ogut, P. W. Reno, Early kinetics of infectious hematopoietic necrosis virus (IHNV) infection in rainbow trout. *Journal of Aquatic Animal Health* **16**, 152–160 (2004).

9. K. E. Atkins, *et al.*, Vaccination and reduced cohort duration can drive virulence evolution: Marek's disease virus and industrialized agriculture. *Evolution* **67**, 851–860 (2013).

10. R. Fan, S. A. H. Geritz, Virulence management: Closing the feedback loop between healthcare interventions and virulence evolution. *Journal of Theoretical Biology* **531**, 110900 (2021).

11. A. R. Wargo, K. A. Garver, G. Kurath, Virulence correlates with fitness in vivo for two M group genotypes of Infectious hematopoietic necrosis virus (IHNV). *Virology* **404**, 51–58 (2010).

12. M. K. Purcell, *et al.*, Universal reverse-transcriptase real-time PCR for infectious hematopoietic necrosis virus (IHNV). *Diseases of Aquatic Organisms* **106**, 103–115 (2013).

13. Posit team, RStudio: Integrated Development Environment for R. (2024). Deposited 2024.

14. R Core Team, R: A Language and Environment for Statistical Computing. (2023).

15. D. Bates, M. Mächler, B. Bolker, S. Walker, Fitting Linear Mixed-Effects Models Using {lme4}. *Journal of Statistical Software* **67**, 1–48 (2015).

16. V. S. Cooper, *et al.*, Timing of transmission and the evolution of virulence of an insect virus. *Proceedings of the Royal Society B: Biological Sciences* **269**, 1161–1165 (2002).

17. L. L. H. Lau, *et al.*, Viral Shedding and Clinical Illness in Naturally Acquired Influenza Virus Infections. *The Journal of Infectious Diseases* **201**, 1509–1516 (2010).

18. D. J. Páez, D. McKenney, M. K. Purcell, K. A. Naish, G. Kurath, Variation in within-host replication kinetics among virus genotypes provides evidence of specialist and generalist infection strategies across three salmonid host species. *Virus Evolution* **8**, 1–12 (2022).

19. M. M. D. Peñaranda, A. R. Wargo, G. Kurath, In vivo fitness correlates with host-specific virulence of Infectious hematopoietic necrosis virus (IHNV) in sockeye salmon and rainbow trout. *Virology* **417**, 312–319 (2011).

20. R. Breyta, D. Mckenney, T. Tesfaye, K. Ono, G. Kurath, Increasing virulence, but not infectivity, associated with serially emergent virus strains of a fish rhabdovirus. *Virus Evolution* **2**, 1–14 (2016).

21. D. G. Hernandez, M. K. Purcell, C. S. Friedman, G. Kurath, Susceptibility of ocean- and stream-type Chinook salmon to isolates of the L, U, and M genogroups of infectious hematopoietic necrosis virus (IHNV). *Diseases of Aquatic Organisms* **121**, 15–28 (2016).

22. D. G. Hernandez, W. Brown, K. A. Naish, G. Kurath, Virulence and infectivity of UC, MD, and L strains of infectious hematopoietic necrosis virus (IHNV) in four populations of Columbia River Basin chinook salmon. *Viruses* **13** (2021).

23. D. M. Hawley, *et al.*, Prior exposure to pathogens augments host heterogeneity in susceptibility and has key epidemiological consequences. [Preprint] (2024). Available at: https://www.biorxiv.org/content/10.1101/2024.03.05.583455v3 [Accessed 2 July 2024].

24. K. E. Langwig, *et al.*, Limited available evidence supports theoretical predictions of reduced vaccine efficacy at higher exposure dose. *Nature Scientific Reports* **9** (2019).

25. K. E. Langwig, *et al.*, Vaccine effects on heterogeneity in susceptibility and implications for population health management. *mBio* **8** (2017).

26. J. L. Brunner, L. Beaty, A. Guitard, D. Russell, Heterogeneities in the infection process drive ranavirus transmission. *Ecology* **98**, 576–582 (2017).

27. P. F. B. Ferguson, R. Breyta, I. Brito, G. Kurath, S. L. LaDeau, An epidemiological model of virus transmission in salmonid fishes of the Columbia River Basin. *Ecological Modelling* **377**, 1–15 (2018).

28. P. K. Hershberger, *et al.*, Factors controlling the early stages of viral haemorrhagic septicaemia epizootics: low exposure levels, virus amplification and fish-to-fish transmission. *Journal of Fish Diseases* **34**, 893–899 (2011).

29. J. Jarungsriapisit, *et al.*, Relationship between viral dose and outcome of infection in Atlantic salmon, Salmo salar L., post-smolts bath-challenged with salmonid alphavirus subtype 3. *Veterinary Research* **47**, 102 (2016).

30. S. E. Lapatra, J. S. Rohovec, J. L. Fryer, Detection of Infectious Hematopoietic Necrosis Virus in Fish Mucus. *Fish Pathology* **24**, 197–202 (1989).

31. D. G. McKenney, G. Kurath, A. R. Wargo, Characterization of infectious dose and lethal dose of two strains of infectious hematopoietic necrosis virus (IHNV). *Virus Research* **214**, 80–89 (2016).

32. K. A. Garver, *et al.*, Estimation of parameters influencing waterborne transmission of infectious hematopoietic necrosis virus (IHNV) in atlantic salmon (Salmo salar). *PLoS ONE* **8** (2013).

33. S. Alizon, A. Hurford, N. Mideo, M. Van Baalen, Virulence evolution and the trade-off hypothesis: History, current state of affairs and the future. *Journal of Evolutionary Biology* **22**, 245–259 (2009).

34. S. Alizon, Y. Michalakis, Adaptive virulence evolution: The good old fitness-based approach. *Trends in Ecology and Evolution* **30**, 248–254 (2015).

35. S. Alizon, M. van Baalen, Emergence of a Convex Trade-Off between Transmission and Virulence. *The American Naturalist* **165**, E155–E167 (2005).

36. M. A. Acevedo, F. P. Dillemuth, A. J. Flick, M. J. Faldyn, B. D. Elderd, Virulence-driven trade-offs in disease transmission: A meta-analysis*. *Evolution* **73**, 636–647 (2019).

37. R. Singh, *et al.*, Rabies – epidemiology, pathogenesis, public health concerns and advances in diagnosis and control: a comprehensive review. *https://doi.org/10.1080/01652176.2017.1343516* **37**, 212–251 (2017).

38. C. Fraser, *et al.*, Virulence and pathogenesis of HIV-1 infection: An evolutionary perspective. *Science* **343** (2014).

39. P. Vetter, *et al.*, Ebola Virus Shedding and Transmission: Review of Current Evidence. *J Infect Dis.* **214**, S177–S184 (2016).

40. J. C. De Roode, A. J. Yates, S. Altizer, Virulence-transmission trade-offs and population divergence in virulence in a naturally occurring butterfly parasite. *Proceedings of the National Academy of Sciences of the United States of America* **105**, 7489–7494 (2008).

41. J. Doumayrou, A. Avellan, R. Froissart, Y. Michalakis, An experimental test of the transmission-virulence trade-off hypothesis in a plant virus. *Evolution* **67**, 486 (2012).

42. D. K. M. Ip, *et al.*, Viral Shedding and Transmission Potential of Asymptomatic and Paucisymptomatic Influenza Virus Infections in the Community. *Clinical Infectious Diseases* **64**, 736–742 (2017).

43. A. E. Fleming-Davies, G. Dwyer, Phenotypic variation in overwinter environmental transmission of a baculovirus and the cost of virulence. *American Naturalist* **186**, 797–806 (2015).

Table 4.1. Virus included in this study and background information. Information includes: genotype name, location of original field collection, year of collection, species from which the sample was taken, relative virulence (chapter 1), IHNV genetic clade, and specific G-gene sequence (43).

Genotype	Collection Location	Collection Year	Species of Isolation	Relative virulence	Genogroup	Sequence type
HaVT-74	Hagerman Valley, ID	1974	O. mykiss	low	M	mG400M
Ht134-17	Hagerman Valley, ID	2017	O. mykiss	high	M	mG335M

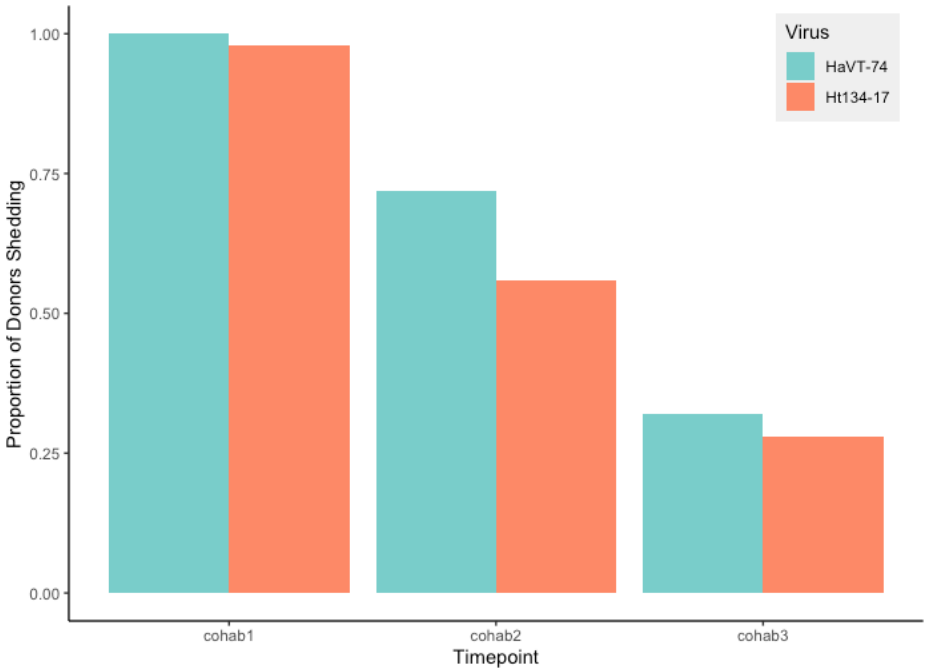

Figure 4.1. Proportion of positive donors over time for each isolate (blue = HaVT-74; orange = Ht134-17). 50 donors were included for each isolate.

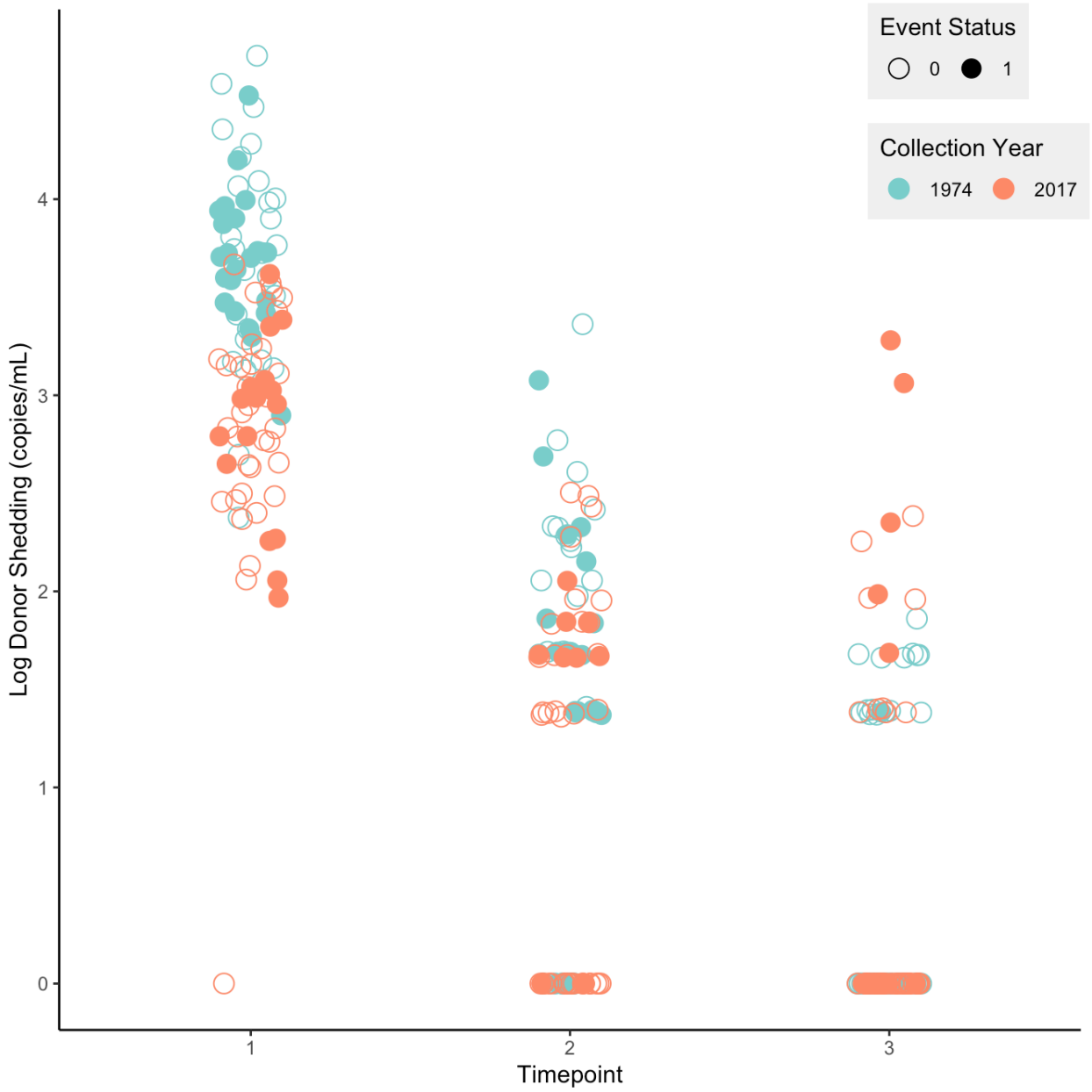

Figure 4.2. Quantity of virus shed by donors (raw data, $\log_{10}$(copies/mL +1)), color coded by isolate (blue = HaVT-74; orange = Ht134-17). Each point represents an individual donor at each time point. Shape of point indicates whether or not a transmission event occurred at that time point (i.e. whether or not the recipient fish tested positive after being exposed to the donor), where open circles represent no transmission event and filled circles represent a successful transmission event. Points at y=0 indicate donors who did not shed. Points are jittered along the axis for easier visualization across the three timepoints.

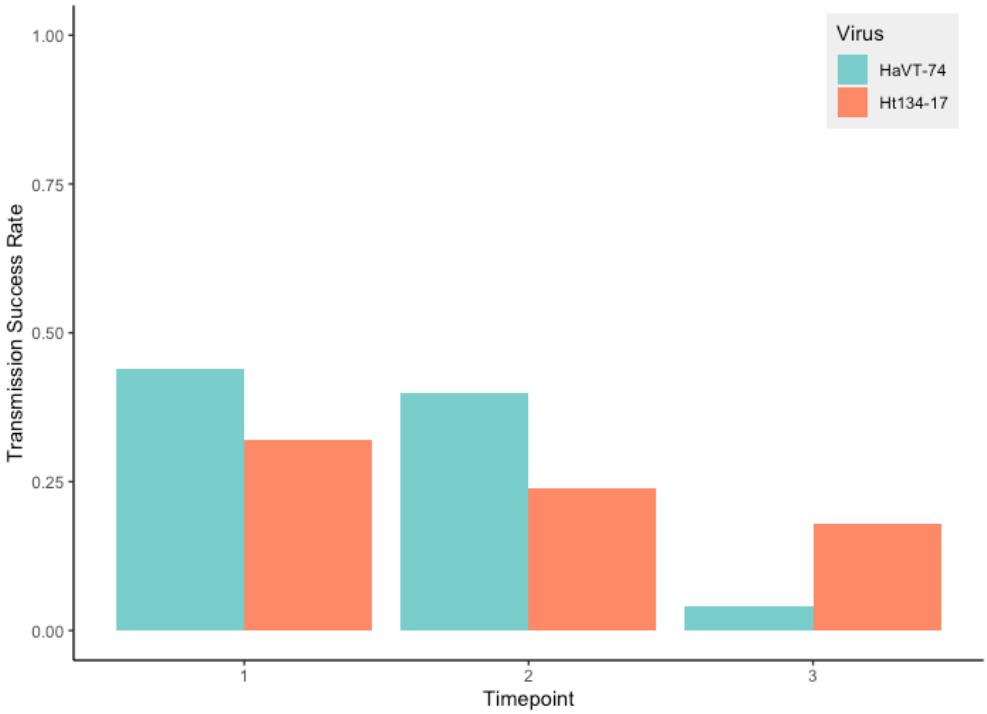

Figure 4.3. Transmission success rate, calculated as proportion of successful transmission events from all donor:recipient pairs at each timepoint, color coded by isolate (blue = HaVT-74; orange = Ht134-17; raw data). Data was dropped from one donor which never shed over the course of the experiment.

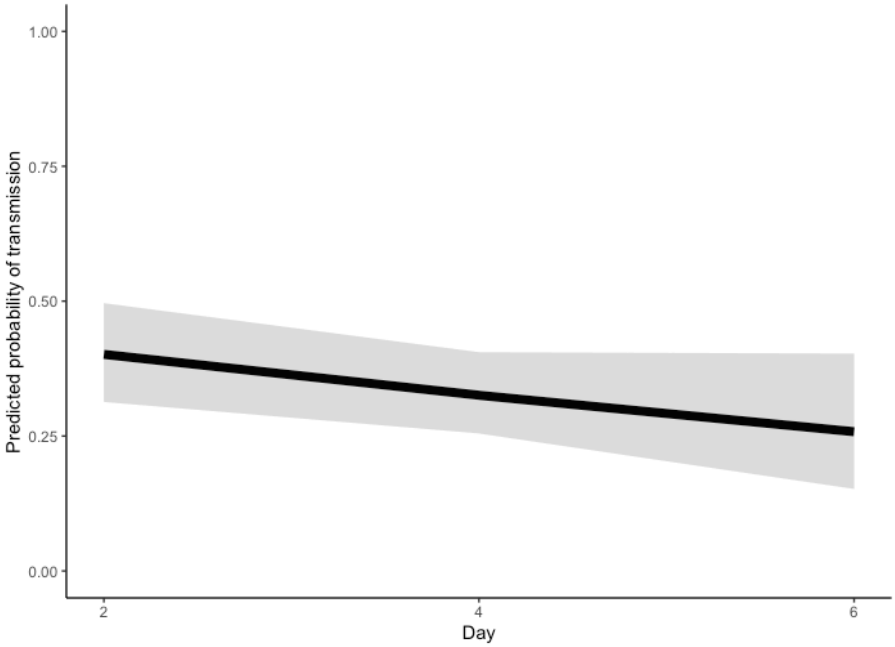

Figure 4.4. Predicted probability of transmission from positive donors infected on Day 0, from AICc-selected GLM model. Data from donors that did not shed were dropped. Isolate as a predictor dropped out of the model so a single trendline with 95% confidence intervals applies to all data. Days 2, 4, 6 correspond to Timepoints 1, 2, 3 respectively. See Table S4.2 for model selection table and Table S4.3 for parameter estimates.

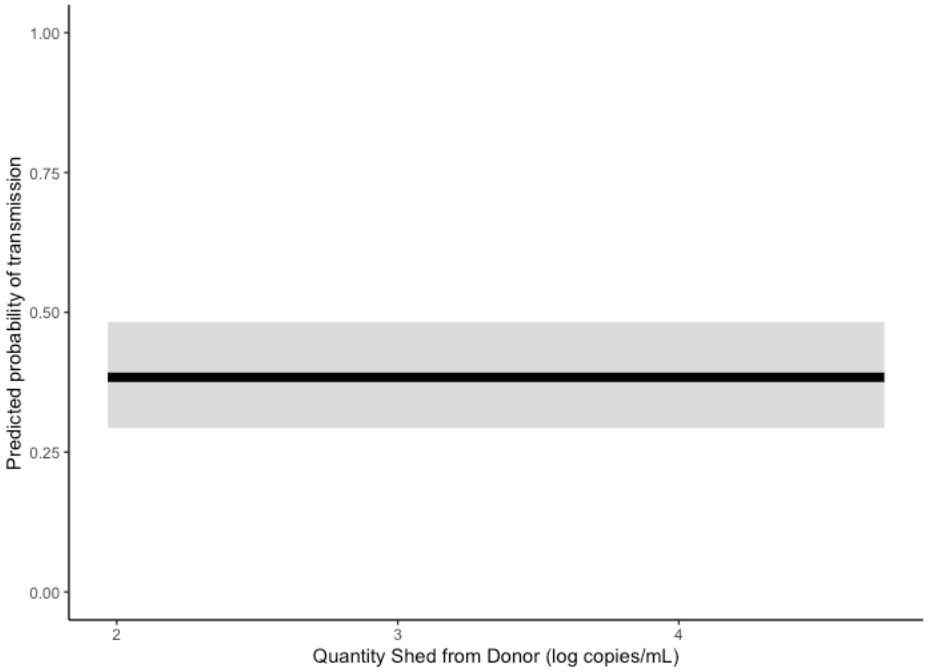

Figure 4.5. Predicted probability of transmission over quantity of virus shed from donors, from AICc-selected GLME model. Isolate and Quantity predictors both dropped out of the model so a single trendline at the intercept value with 95% confidence intervals applies to all data. The x-axis of log-transformed quantity spans the range of detected viral shedding from donor fish at T1. See Table S4.4 for model selection table and Table S4.5 for parameter estimates.

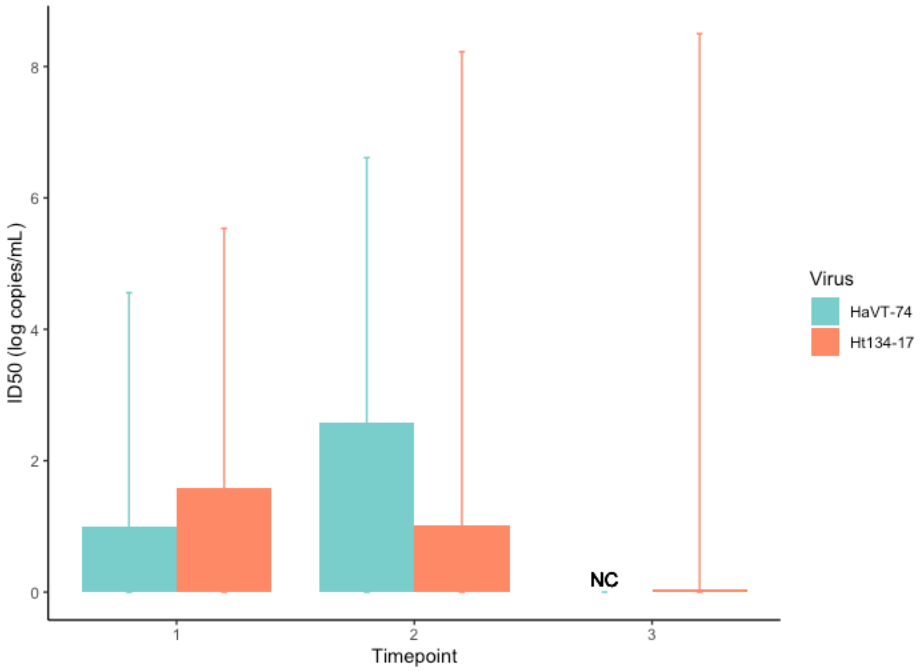

Figure 4.6. Predicted infectious dose (ID_{50}) modeled using data from positive donors (blue = HaVT-74; orange = Ht134-17). Lower 95% confidence intervals based on predicted data overlapped zero and are not displayed. Note that data was extremely limited at the T3 timepoint. ID_{50} for HaVT-74 at T3 was not calculated due to insufficient data and is marked NC for "not calculated." Also, the upper confidence interval for Ht134-17 at T3 is artificially shortened for ease of visualization and far exceeds the values of other confidence intervals. See Table S4.6 for estimates.

Supplemental materials

Table S4.1. Differences in shed virus quantities from positive donors between Timepoint (cohab) and Isolate treatment combinations. The comparisons were performed with a two-way ANOVA [LogDonorShed ~ Timepoint * Virus] and level difference estimates were obtained with a post-hoc Tukey's HSD test. Levels were considered significantly different if $p < 0.05$. Virus quantity was normalized with a $\log_{10}(x)$ transformation before analysis.

Comparison					
Combination 1	Combination 2	Mean difference	lower 95% CI	upper 95% CI	Adjusted pval
cohab2:HaVT-74	cohab1:HaVT-74	-1.7101	-1.9961	-1.4242	0.0000
cohab3:HaVT-74	cohab1:HaVT-74	-2.1654	-2.5412	-1.7897	0.0000
cohab1:Ht134-17	cohab1:HaVT-74	-0.8025	-1.0655	-0.5396	0.0000
cohab2:Ht134-17	cohab1:HaVT-74	-1.9137	-2.2261	-1.6012	0.0000
cohab3:Ht134-17	cohab1:HaVT-74	-1.6961	-2.0916	-1.3006	0.0000
cohab3:HaVT-74	cohab2:HaVT-74	-0.4553	-0.8483	-0.0622	0.0130
cohab1:Ht134-17	cohab2:HaVT-74	0.9076	0.6205	1.1948	0.0000
cohab2:Ht134-17	cohab2:HaVT-74	-0.2035	-0.5365	0.1295	0.4944
cohab3:Ht134-17	cohab2:HaVT-74	0.0140	-0.3980	0.4261	1.0000
cohab1:Ht134-17	cohab3:HaVT-74	1.3629	0.9862	1.7396	0.0000
cohab2:Ht134-17	cohab3:HaVT-74	0.2518	-0.1609	0.6645	0.4963
cohab3:Ht134-17	cohab3:HaVT-74	0.4693	-0.0094	0.9481	0.0582
cohab2:Ht134-17	cohab1:Ht134-17	-1.1111	-1.4247	-0.7976	0.0000
cohab3:Ht134-17	cohab1:Ht134-17	-0.8936	-1.2900	-0.4971	0.0000
cohab3:Ht134-17	cohab2:Ht134-17	0.2176	-0.2133	0.6484	0.6937

Table S4.2. GLM model selection table generated with dredge() for probability of transmission from positive donors. Candidate models are listed in order of lowest AICc value. Model 1 is the best fit model reported in Results.

Model	Intercept	Timepoint	Virus	Cohab* Virus	df	log Likelihood	AICc	ΔAICc	AICc weight
1	-0.0712028	-0.328315			2	-123.57	251.21	0.00	0.2541
2	-0.6007739				1	-124.80	251.62	0.41	0.2072
3	0.12359218	-0.341534	+		3	-122.80	251.73	0.52	0.1962
4	0.58145133	-0.627652	+	+	4	-121.77	251.75	0.54	0.1938
5	-0.4382549		+		2	-124.11	252.28	1.07	0.1487

Table S4.3. Best fit GLM for probability of transmission from positive donors as identified by AICc. Residual degrees of freedom were 190.

	Estimate	SE	Z value
Intercept	-0.0712	0.3701	-0.192
Timepoint	-0.3283	0.2131	-1.541
Event.status ~ Timepoint			

Table S4.4. GLME model selection table generated with dredge() for probability of transmission from positive donors at T1 in relation to donor shed quantity. Candidate models are listed in order of lowest AICc value. Model 1 is the best fit model reported in Results.

Model	Intercept	Quantity	Virus	Quantity* Virus	df	logLik	AICc	delta	weight
1	-0.4733				2	-65.93	135.98	0.00	0.42
2	-0.2412		+		3	-65.25	136.75	0.78	0.28
3	-0.9805	0.1538			3	-65.82	137.90	1.92	0.16

Table S4.5. Best fit GLME for probability of transmission success in relation to donor shed quantity. The best fit model is the null model. Residual degrees of freedom = 97.

	Estimate	SE	Z value
Intercept	-0.4733	0.2067	-2.29
Event.status ~ 1 + (1|Donor)			

Table S4.6. Predicted ID50 estimates based on the GLME model [Event.status ~ LogDonorShed + (1|Donor)]. Estimated ID50 represents the log(infectious dose) at which the probability of infection is 50% for the respective treatment. Due to insufficient data for HaVT-74 at Timepoint 3, no meaningful ID50 could be calculated and values are marked NC for "not calculated."

Virus	Timepoint	Estimate	Std.Error	Z value	ID50	SE	lower 95% CI	upper 95% CI
HaVT-74	1	0.012	0.5995	0.02	0.99	1.82	-2.58	4.56
HaVT-74	2	-0.946	0.722	-1.31	2.58	2.06	-1.46	6.61
HaVT-74	3	-22.47	296.12	-0.08	NC	NC	NC	NC
Ht134-17	1	-0.465	0.699	-0.66	1.59	2.01	-2.35	5.54
Ht134-17	2	-0.011	1.303	-0.01	1.01	3.68	-6.20	8.22
Ht134-17	3	3.187	3.632	0.88	0.04	37.79	-74.03	74.12

SUMMARY

Over four chapters, this dissertation has quantified virulence, shedding, and transmission phenotypes for the viral pathogen IHNV. Additionally, the trajectories of viral virulence and shedding fitness evolution have been described across four genetic subgroups which represent five decades of evolution.

To summarize, six independent studies within chapter 1 indicated that emergent IHNV isolates rapidly gained virulence after a host jump from sockeye salmon into rainbow trout. Following the host jump, M-genogroup isolates developed increased virulence. The results contrast with classical evolution theory which predicts virus virulence will attenuate following a host jump but are in line with other studies in the system and join a growing body of epidemiological work that demonstrate diverse possible viral evolution trajectories.

In Chapter 2, the fifteen viral isolates utilized in Chapter 1 were typed for shedding fitness at two different temperatures. Recent isolate collection year was positively correlated with increased peak shedding, later peak days, and longer shedding durations. Virulence analysis identified a possible relationship between higher peak shedding loads and greater probability of death, offering a possible link between these traits. The analyses did not conclusively support or eliminate the possibility of a temperature adaptation for IHNV in the novel host. At the genogroup level, M isolates resulted in higher prevalence, greater shedding intensity and total quantity, and higher mortality than U isolates, consistent with past studies that have compared representative high and low virulence types of IHNV.

In Chapter 3, the selection of IHNV isolates was expanded to 40 genetically distinct strains which spanned collections from 1972-2017 and four subgroups of the M-genogroup. Shedding phenotypes across subgroups were shown to vary in the later period of infection, where increasing virulence correlated with shedding intensity on an individual host scale but not the genogroup level scale. The relationships uncovered in Chapter 2 (increased peak and post peak shedding), were diminished at the subgroup level. Rather than shedding intensity, shedding duration and clearance rate of the virus may be key to evolutionary fitness. The current study adds empirical evidence that the relationship of virulence, shedding, and transmission is complex.

Chapter 4 sought to relate shedding fitness to transmission fitness by developing a novel cohabitation method. In line with shedding frequency and intensity, transmission success decreased with time since viral exposure. Interestingly, transmission success did not seem to correlate with shed quantity and infectious dose appeared not to vary across timepoints. Together the results of Chapters 3 and 4 suggest that later shedding and transmission appears to be key to viral fitness. Shedding intensity and transmission success does not vary significantly early in the host recovery period, but a qualitative comparison between old and new isolates suggested that infectivity of virions may vary between isolates.

The results offered by Chapters 2, 3, and 4 could point to a recovery tradeoff consistent with evolutionary trends classically demonstrated by myxomatosis in European rabbits introduced to Australia. Specifically, those myxomavirus strains that were most successful in the field held a fitness advantage not in high virulence but in shedding duration and longer host recovery. A similar relationship between host recovery, shedding duration, and evolutionary fitness might explain the results for IHNV shown here. Transmission success is lower overall for the high virulence, newer isolate. How then does this virus make a living? Transmission perhaps does not need to be common if infection is rampant enough in dense host populations to sustain long low-level transmission.

In modern commercial trout aquaculture, it is possible that the cost of virulence associated with intense shedding may be too great to sustain ever higher levels of host shedding, and instead a long term, steady transmission strategy may constitute a more fit phenotype like Ht134-17. In contrast, HaVT-74, which was collected in 1974 and continues to

exhibit one of the lowest virulence phenotypes, sheds considerably more. In Chapter 4, not only did 100% of donors shed during the first timepoint, but the low-virulence isolate also yielded the highest 9% of donor intensity measures, all during the first timepoint. If the evolutionary trends of the M-genogroup can be summarized by these representative isolates, IHNV would seem to have transitioned from an acutely shedding virus with moderate early transmission success to a less intense but prolonged shedding phenotype with low levels of transmission success throughout the shedding duration. Virulence may constitute the cost of extended shedding and transmission, resulting in host death in cases of very high shedding, but the mechanism for the consistent evolved increased virulence across IHNV M-genogroup remains unclear. Heterogeneity in individual hosts was apparent in all studies, and should be considered alongside results as future studies in the system continue to deepen our understanding of viral evolution and the story of IHNV in rainbow trout and other salmonid hosts.

The emergence and evolution of viral pathogens in aquaculture and agriculture is likely to become more threatening as the human population continues to extract natural resources. Higher incidence and intensity of marine pathogens has been documented in multiple phyla across the globe and are predicted to become more dramatic with the added effects of climate change. Similarly, zoonotic disease along wild-managed corridors adjacent to human populations is increasingly concerning given the higher potential for spillover, spillback, and host jumps, which may all incur catastrophic damage to host populations. Virulence, shedding, and transmission dynamics may shift according to changing climate factors, introductions and range expansions, and other opportunities for adaptation. High throughput, high density farming is a major tenet of modern food production systems, but the long term consequences of imperfect disease management must be weighed against the benefits of food production efficiency in the short term. Beyond economic importance, aquatic viruses should remain a vibrant research focus as marine and coastal systems sustain the majority of ecological productivity and biodiversity. Management of these systems should be approached thoughtfully and deliberately, holding paramount the intersection of environmental, animal, and human health.